

Early and Post Transition Metal Complexes as a Single or Combined Components in the Ethylene and Isoprene Polymerization

LUCIANO GOMES FURLAN

Tese de Doutorado



PORTO ALEGRE, SETEMBRO DE 2005.



EXAMINING COMMISSION

- Osvaldo de Lázaro Casagrande Jr. (mastermind) - Professor at the Federal University of Rio Grande do Sul, Chemistry Institute, Porto Alegre, Rio Grande do Sul, Brazil

- Jean-François Carpentier (mastermind) - Professor at the Rennes 1 University, Chemistry Institute, Rennes, France.

- Adriane Simanke - Braskem Petrochemical Company S.A, Triunfo, Brazil;

- Benedito dos Santos Lima Neto - Professor at the State University of São Paulo, Chemistry Institute of São Carlos , São Paulo, Brazil.

- Michèle Oberson de Souza - Professor at the Federal University of Rio Grande do Sul, Chemistry Institute, Porto Alegre, Rio Grande do Sul, Brazil

GRATEFULNESS

To Andréia especially for affection, dedication and for understanding the absent moments.

To my parents, Tania e Laudeli, because without them nothing would be possible

To my grandparents Modesto, Cenira and Maria; to all my family for the incentive.

To the Prof. Osvaldo Casagrande Jr. for the excellent orientation and the opportunity. For the friendship and dedication in all moments.

To the Prof. Jean-François Carpentier for the excellent reception in his laboratory, for orientation, opinions and questions.

To the Prof. Roberto Fernando de Souza and Prof. Jairton Dupont for the support.

To all my fellows from the K-208B laboratory, Marcelo, Fernando, Fabio Mota, Adriana, Fabio Kunrath, Elton and Maria Cristina for the friendship.

To my fellows from the K102, K106 and K110 for the assistance.

To my fellows of UMR 6509 laboratory and Chemistry Institute of Rennes;. To Nouredinne, Christophe, Bing and Abder for the good friendship in my permanence in France.

To Estima and Mello family by the incentive.

To my fellows of Tribo do Sol for the companionship, especially Conceição.

To my fellows of Rosario's football, because sport is health.

To CAPES for the support.

To the UFRGS Chemistry Institute.

To everybody who has contributed in some way for the development of this work.

SCIENTIFIC PRODUCTION ORIGINATING OF THIS THESIS

1. COMPLETE PAPERS ORIGINATING FROM OF THAT THESIS

(1) Furlan, L. G.; Kunrath, F. A.; Mauler, R. S., Souza, R. F.; Casagrande, O. L.;

“Linear low density polyethylene (LLDPE) from ethylene using $\text{Tp}^{\text{Ms}}\text{NiCl}$ ($\text{Tp}^{\text{Ms}} =$ hydridotris(3-mesitylpyrazol-1-yl)) and Cp_2ZrCl_2 as a tandem catalyst system”

Journal of Molecular Catalysis A: Chemical **2004**,214, 207–211.

(2) Furlan, L. G.; Casagrande, O. L.

“Dual Catalyst System Composed by Nickel and Vanadium Complexes Containing Nitrogen Ligands for Ethylene Polymerization”.

Journal of Brazilian Chemical Society, **2005** (accepted for publication)

2. COMPLETE WORKS PUBLISHED IN SCIENTIFIC EVENTS

(1) Luciano G. Furlan, Fabio A. Kunrath, Raquel S. Mauler, Roberto F. de Souza e Osvaldo L. Casagrande Jr.; *Produção de Polietileno Ramificado Utilizando Combinação de Catalisadores*, In 11º Congresso Brasileiro de Catálise e 1º Congresso de Catálise do Mercosul, 2001, Bento Gonçalves-RS

(2) Luciano G. Furlan, Roberto F. de Souza e Osvaldo L. Casagrande Jr; *Formação de Blendas de Polietileno Utilizando combinações de Precursores Catalíticos de Níquel (II) E Vanádio (V)*, In 12º Congresso Brasileiro de Catálise, 2003, Angra dos Reis, RJ.

(3) Luciano Gomes Furlan, Noureddine Ajellal, Jean-François Carpentier e Osvaldo L. Casagrande Jr; *Estudo da Polimerização do Isopreno Utilizando o Precursor Catalítico $[(\text{Alil})_2\text{NdCl}(\text{MgCl}_2)_2\cdot(\text{THF})_4]$* , In XIX Simposio Iberoamericano de Catálisis, 2004, Mérida, Yucatán, México.

GENERAL INDEX

EXAMINING COMMISSION.....	I
GRATEFULNESS.....	II
SCIENTIFIC PRODUCTION ORIGINATING OF THIS THESIS.....	III
FIGURE INDEX.....	VIII
TABLE INDEX.....	XI
ABBREVIATIONS.....	XII
ABSTRACT.....	XV
RÉSUMÉ.....	XVI
CHAPTER 1. INTRODUCTION.....	1
CHAPTER 2. BIBLIOGRAFIC REVIEW.....	2
2.1. GENERAL CONSIDERATIONS.....	2
2.2. NON-METALLOCENE CATALYSTS APPLIED IN DIFFERENT POLYMERIZATION PROCESSES.....	6
2.2.1. Binary Catalyst Systems.....	6
2.2.1.1. Application of Catalytic mixtures in Polyethylene Synthesis.....	7
2.2.1.2. Production of Polymer Blends Using Binary Catalyst Systems.....	8
2.2.1.3. Tandem Catalysis.....	12
2.3. POLYISOPRENE.....	22
2.3.1. Historical Background.....	23
2.3.2. Applications of Polyisoprene.....	24

2.3.3. Polymer Properties.....	26
2.3.4. Lanthanide Catalysts for Isoprene Polymerization.....	26
CHAPTER 3. OBJECTIVES.....	32
CHAPTER 4. EXPERIMENTAL PART.....	33
4.1. GENERAL PROCEDURES.....	33
4.2. COMPLEXES SYNTHESIS.....	34
4.3. POLYMERIZATION PROCEDURES.....	35
4.3.1. Production of Polymer Blends Using Binary Catalyst Systems.....	35
4.3.2. Tandem Catalyst System.....	36
4.3.3. Isoprene polymerization.....	37
4.4. POLYMERS CHARACTERIZATIONS.....	38
CHAPTER 5. RESULTS AND DISCUSSION.....	40
5.1. DUAL CATALYST SYSTEM COMPOSED BY NICKEL AND VANADIUM COMPLEXES CONTAINING NITROGEN LIGANDS FOR ETHYLENE POLYMERIZATION.....	40
5.1.1. Influence of experimental parameters in the activity.....	40
5.1.2. Influence of x_{Ni} and polymerization temperature on the polymer properties.....	45
5.2. LINEAR LOW DENSITY POLYETHYLENE (LLDPE) FROM ETHYLENE USING $Tp^{Ms}NiCl$ (Tp^{Ms} = hydridotris(3-mesitylpyrazol-1-yl) AND Cp_2ZrCl_2 AS A TANDEM CATALYST SYSTEM.....	52
5.2.1. The influence of x_{Ni} and temperature on copolymer properties.....	54
5.3. SYNTHESIS AND CHARACTERIZATION OF $M(allyl)_2Cl(MgCl_2)_2.(THF)_4$ (M = Nd, Y and La) AND THEIR USE IN ISOPRENE POLYMERIZATION.....	58
5.3.1. $M(allyl)_2Cl(MgCl_2)_2.(THF)_4$ (M= Nd, Y and La) complexes characterization	

by by ^1H and ^{13}C NMR spectroscopy and elementary analysis.....	58
5.3.2. Isoprene polymerization using Lanthanide systems composed by $\text{Nd}(\text{allyl})_2\text{Cl}(\text{MgCl}_2)_2 \cdot (\text{THF})_4$ / MAO and the effect of polymerization parameters in polyisoprene properties.....	60
5.3.3. Influence of cocatalyst using group 3 metals complexes $\text{M}(\text{allyl})_2\text{Cl}(\text{MgCl}_2)_2 \cdot (\text{THF})_4$ ($\text{M} = \text{Nd}, \text{Y}$ and La) in isoprene polymerization and their effect on polyisoprene properties.....	67
5.3.4. Addition of Borate based cocatalysts in isoprene polymerization using Lanthanide catalysts composed by $\text{Ln}(\text{allyl})_2\text{Cl}(\text{MgCl}_2)_2 \cdot (\text{THF})_4$ ($\text{Ln} = \text{Nd}$ and La) and your effect on polyisoprene properties.....	72
5.3.5. Production of <i>Cis/Trans</i> polyisoprene blends using combination of group 3 metals composed by $\text{M}(\text{allyl})_2\text{Cl}(\text{MgCl}_2)_2 \cdot (\text{THF})_4$ ($\text{M} = \text{Y}$ and La) activated by TiBA and the effect of Yttrium Molar Fraction (x_Y) on polyisoprene properties.....	79
CHAPTER 6. CONCLUSIONS.....	82
CHAPTER 7. BIBLIOGRAPHIC REFERENCES.....	84

FIGURE INDEX

Figure 1. Numbers of publications on non-metallocene olefin polymerization catalyst systems appearing in the academic literature: (a) by year between 1990 and 2001, and (b) by periodic group for the 4-year periods 1994-1997 and 1998-2001.....	5
Figure 2. General processes for ethylene polymerization using a homogeneous binary system.....	8
Figure 3. Ni-Diimine (a) and zirconocene (b) Complexes applied in reactor blends	9
Figure 4. Iron complex utilized for blends formation.....	10
Figure 5. Simple Tandem process.....	12
Figure 6. Low Density Polyethylene (LDPE), High-density Polyethylene (HDPE) and Low Linear Density Polyethylene (LLDPE).....	13
Figure 7. Tandem synthesis of LLDPE by two catalytic systems using only ethylene as monomer.....	14
Figure 8. NiP [^] O complexes for applied in ethylene oligomerization.....	15
Figure 9. Iron complex for ethylene oligomerization.....	16
Figure 10. More controlled LLDPE synthesis by action of CGC catalysts.....	16
Figure 11. Tandem action of Ti (1) and Zr (2) catalysts.....	17
Figure 12. Chromium-(SNS) complex employed in 1-hexene synthesis.....	18
Figure 13. LLDPE synthesis using Borate systems of Ti and Ni catalysts.....	19
Figure 14. Tandem synthesis of LLDPE by action of three catalysts.....	20
Figure 15. Tandem system by mononuclear (B ₁) and binuclear activators (B ₂) with Zr and Ti catalysts.....	21

Figure 16. Possible microstructures of polyisoprene.....	22
Figure 17. Polymerization of Isoprene by LnI_2 and $\text{LnI}_2(\text{THF})_x$	29
Figure 18. Polymerization of Isoprene by Ternary and Binary Lanthanide Catalytic Systems.....	30
Figure 19. Neodymium complex ($\text{Ln} = \text{Nd}$) used for isoprene polymerization.....	30
Figure 20. Pyrex glass reactor (1.0 L) used for reactor blends production.....	36
Figure 21. Double walled glass reactor (120 mL) used for Tandem synthesis of LLDPE.....	37
Figure 22. $\text{NiCl}_2(\alpha\text{-diimine})$ (1) and $\{\text{TpMs}^*\}\text{V}(\text{Ntbu})\text{Cl}_2$ (2) structures.....	40
Figure 23. Effect of the polymerization temperature on the activity varying x_{Ni} for the polymerization reactions performed in hexane	43
Figure 24. Influence of the polymerization temperature on the activity varying x_{Ni} for the polymerization reactions performed in toluene	44
Figure 25. DSC curves of the PE blends produced at 0 °C in Hexane.....	46
Figure 26. DSC curves of the PE blends produced at 0 °C in Toluene.....	46
Figure 27. Dependence of melting temperature (T_m) with x_{Ni} for ethylene polymerization in Toluene.....	48
Figure 28. SEM micrographs of BPE/HDPE blends crio-fractured surfaces produced at 30°C in hexane: (a) $x_{\text{Ni}} = 0.25$ (x 2000); (b) $x_{\text{Ni}} = 0.25$ (x 2000) after etched with o-xylene.....	50
Figure 29. SEM micrographs of BPE/HDPE blends crio-fractured surfaces produced at 50°C in hexane: (a) $x_{\text{Ni}} = 0.25$; (b) $x_{\text{Ni}} = 0.25$ after etched with o-xylene.....	51
Figure 30. $\{\text{Tp}^{\text{Ms}}\}\text{NiCl}$ (1) and Cp_2ZrCl_2 (2) complexes used in Tandem process.....	52

Figure 31. Plausible tandem catalytic mechanism to produce copolymer from ethylene using a combination of 1 and 2.....	54
Figure 32. DSC curves of the polymers varying x_{Ni} ; Polymerization reactions performed at 0 °C, $[Al]/[M] = 200$, and using a mixture MAO/TMA (1:1) as activator.....	55
Figure 33. Melting point and branching content as a function of x_{Ni} of the copolymers; Polymerization reactions performed at 0 °C, $[Al]/[M] = 200$, and using a mixture MAO/TMA (1:1) as activator.....	56
Figure 34. ^{13}C NMR spectra of copolymers obtained varying x_{Ni}	57
Figure 35. 1H NMR spectrum (C_6D_6) of $La(allyl)_2Cl(MgCl_2)_2(THF)_4$ catalyst.....	59
Figure 36. 1H NMR spectrum (C_6D_6) of $Y(allyl)_2Cl(MgCl_2)_2(THF)_4$ catalyst.....	59
Figure 37. 1H NMR spectrum (C_6D_6) of $Y(allyl)_2Cl(MgCl_2)_2(THF)_4$ catalyst.....	60
Figure 38. Influence of polymerization time in the Yield and molecular weight (M_n) on isoprene polymerization using $Nd(allyl)_2Cl(MgCl_2)_2.(THF)_4 / MAO$	63
Figure 39. Typical GPC chromatogram (THF, 25 °C) of polyisoprene produced by $Nd(allyl)_2Cl(MgCl_2)_2(THF)_4/MAO$	64
Figure 40. Influence Ratio I_p/Nd on the molecular weight (M_n) in isoprene polymerization using $Nd(allyl)_2Cl(MgCl_2)_2.(THF)_4 / MAO$	65
Figure 41. Typical 1H NMR spectrum ($CDCl_3$) of polyisoprene produced by $Nd(allyl)_2Cl(MgCl_2)_2(THF)_4/MAO$; Indications of hidrogens of <i>cis</i> -1,4-form (1,67ppm), <i>trans</i> -1,4-form (1.57ppm) and 3,4-form (4.70 ppm).....	66
Figure 42. Typical ^{13}C NMR spectrum ($CDCl_3$) of PI produced by $Nd(allyl)_2Cl(MgCl_2)_2(THF)_4/MAO$; Indications of C_2 (135.2 ppm), C_3 (125.0 ppm), C_1 (32.19 ppm), C_5 (26.37 ppm) and C_4 (23.42 pm).....	67

Figure 43. Influence of lanthanide on polymer yield using group 3 metal complexes	71
M(allyl) ₂ Cl(MgCl ₂) ₂ .(THF) ₄ (M = Nd, Y and La).....	
Figure 44. Influence of cocatalyst type on polymer molecular weight using group 3 metal complexes composed by M(allyl) ₂ Cl(MgCl ₂) ₂ .(THF) ₄ (M = Nd, Y and La).....	72
Figure 45. Effect of B ₁ content employing the system TMA/Nd (Allyl) ₂ Cl (MgCl ₂) ₂ .(THF) ₄	75
Figure 46. Influence of Ratio Ip/Nd on the Yield and molecular weight (Mn) of polyisoprene produced by TMA/ Nd(allyl) ₂ Cl(MgCl ₂) ₂ .(THF) ₄ / B ₁ using Al/Nd/B ₁ = 30/1/3.....	76
Figure 47. Effect of amount of B ₁ in molecular weight distribution employing the system TMA / La (allyl) ₂ Cl (MgCl ₂) ₂ .(THF) ₄ (Al/La = 30/1) in isoprene polymerization.....	77
Figure 48. Effect of B ₂ content in molecular weight distribution employing the system TIBA / Nd (Allyl) ₂ Cl (MgCl ₂) ₂ .(THF) ₄ /B ₂ (Al/Nd =30/1) in isoprene polymerisation.....	78
Figure 49. Influence of Yttrium Molar Fraction (x _Y) in stereoregularity of polyisoprene produced by M(allyl) ₂ Cl(MgCl ₂) ₂ .(THF) ₄ / TiBA (M = Y and La) combinations.....	81

TABLE INDEX

Table 1. Consumption of Synthetic Polyisoprene.....	25
Table 2. Ethylene polymerizations using homogeneous binary catalyst system composed of $[\text{NiCl}_2(\alpha\text{-diimine})]$ (1) and $[\text{Tp}^{\text{Ms}^*}\text{VCl}_2(\text{N}^t\text{Bu})]$ (2) in hexane under atmospheric ethylene pressure.....	41
Table 3. Ethylene polymerization using homogeneous binary catalyst system composed of $[\text{NiCl}_2(\alpha\text{-diimine})]$ (1) and $\text{Tp}^{\text{Ms}^*}\text{VCl}_2(\text{N}^t\text{Bu})]$ (2) in toluene under atmospheric ethylene pressure.....	42
Table 4. Results of ethylene polymerization using a combination of $\{\text{Tp}^{\text{Ms}}\}\text{NiCl}$ (1) and Cp_2ZrCl_2 (2).....	53
Table 5. Results of Isoprene polymerizations using $\text{Nd}(\text{allyl})_2\text{Cl}(\text{MgCl}_2)_2\cdot(\text{THF})_4 / \text{MAO}$	62
Table 6. Results of Isoprene polymerizations using $\text{M}(\text{allyl})_2\text{Cl}(\text{MgCl}_2)_2\cdot(\text{THF})_4$ complexes with different alkylaluminum cocatalysts.....	68
Table 7. Effect of Borate adition in isoprene polymerisation ^a using $\text{Ln}(\text{allyl})_2\text{Cl}(\text{MgCl}_2)_2\cdot(\text{THF})_4$ complexes ($\text{Ln} = \text{Nd}$ and La).....	73
Table 8. Isoprene polymerization reactions using combinations of $\text{Y}(\text{allyl})_2\text{Cl}(\text{MgCl}_2)_2\cdot(\text{THF})_4$ and $\text{La}(\text{allyl})_2\text{Cl}(\text{MgCl}_2)_2\cdot(\text{THF})_4$ actived by TiBA.....	79

ABBREVIATIONS

BPE = branched polyethylene

CGC = Constrained Geometry Catalysts

Cp* = pentamethylcyclopentadienyl

Cp = cyclopentadienyl

dme = dimethoxyethane

DSC = differential scanning calorimetry

EPDM = Ethylene Propylene Diene Monomer

Et = ethyl

GPC = gel permeation chromatography

HPDE = high-density polyethylene

Ind = indenyl

¹Pr = isopropyl

IR = stereoregular polyisoprene

La = Lanthanum

LCB = long-chain branching

LDPE = low density polyethylene

LLDPE = linear low density polyethylene

Ln = lanthanide metal

M = metal

MAO = methylaluminoxane

MFI = melt flow index

MMAO = modified– methylaluminoxane

Mn = Number average molecular weight

M_w = Weight average molecular weight
M_wD or M_w/M_n = molecular weight distribution
Nd = Neodimium
NMR = Nuclear Magnetic Resonance
O-iPr = isopropoxide
PE = polyethylene
Ph = phenyl
PI = Polyisoprene
PI = polyisoprene
Pz = pyrazol, pyrazolyl
R= alkyl group
Rac = racemic
SBR = styrene butadiene rubber
SEM = Scanning electron microscopy
SHOP = Shell Higher Olefin Process
Sm = samarocene
t-Bu = terc-butyl
TEA =Trimethylaluminum
THF = tetrahydrofurane
TiBA = triisobuthylaluminum.
T_m = melting temperature
TMA = trimethylaluminum
TMED = N, N, N',N',-tetramethyl-ethylenediamine
TMS = trimethylsilane
Tp = tris(pyrazolyl)borate ligand

$Tp^{Ms} = HB(3\text{-mesityl(pyrazolyl)-1-yl})_3$

$Tp^{Ms*} = HB(3\text{-mesityl(pyrazolyl)-1-yl})_2(5\text{-mesityl(pyrazolyl)-1-yl})$

Wt = weight

X = halide

x_i = mole fraction

Y = Yttrium

ZN = Ziegler-Natta

χ = cristallinity percentage

ABSTRACT

In this work is reported, in a first step, the effect of different experimental parameters and their relation with polymer properties using the homogeneous binary catalyst system composed by $\text{Ni}(\alpha\text{-diimine})\text{Cl}_2$ ($\alpha\text{-diimine}$ = 1,4-bis(2,6-diisopropylphenyl)-acenaphthenediimine) and $\{\text{TpMs}^*\}\text{V}(\text{Ntbu})\text{Cl}_2$ (TpMs^* = hydridobis(3-mesitylpyrazol-1-yl)(5-mesitylpyrazol-1-yl)) activated with MAO. This complexes combination produces, in a single reactor, polyethylene blends with different and controlled properties dependent on the polymerization temperature, solvent and Nickel molar fraction (x_{Ni}).

In second, the control of linear low density polyethylene (LLDPE) production was possible, using a combination of catalyst precursors $\{\text{Tp}^{\text{Ms}}\}\text{NiCl}$ (Tp^{Ms} = hydridotris(3-mesitylpyrazol-1-yl)) and Cp_2ZrCl_2 , activated with MAO/TMA, as Tandem catalytic system. The catalytic activities as well as the polymer properties are dependent on x_{Ni} . Polyethylene with different Mw and controlled branches is produced only with ethylene monomer.

Last, the application group 3 metals catalysts based, $\text{M}(\text{allyl})_2\text{Cl}(\text{MgCl}_2)_2 \cdot 4\text{THF}$ (M = Nd, La and Y), in isoprene polymerization with different cocatalysts systems and experimental parameters is reported. High yields and polyisoprene with good and controlled properties were produced. The metal center, cocatalysts and the experimental parameters are determinant for the polymers properties and their control. High conversions in *cis*-1,4- or *trans*-1,4-polyisoprene were obtained and the polymer microstructure depending of cocatalyst and metal type. Combinations of Y and La precursors were effective systems for the *cis/trans*-polyisoprene blends production, and the control of *cis-trans*-1,4-microstructures by Yttrium molar fraction (x_{Y}) variation was possible.

RÉSUMÉ

Il est décrit dans la première partie de ce document l'effet de différents paramètres expérimentaux et leurs relations avec les propriétés du polymère produit par un système binaire homogène composé des précurseurs catalytiques $\text{Ni}(\alpha\text{-diimine})\text{Cl}_2$ ($\alpha\text{-diimine} = 1,4\text{-bis}(2,6\text{-diisopropylphényl})\text{-acenaphthènediimine}$) et $\{\text{TpMs}^*\}\text{V}(\text{Ntbu})\text{Cl}_2$ ($\text{TpMs}^* = \text{hydridobis}(3\text{-mesithylpyrazol-1-yl})(5\text{-mesithylpyrazol-1-yl})$) associés à l'agent activateur méthylaluminoxane (MAO), les réactions de polymérisation étant conduites dans un seul réacteur. La variation de la relation entre les deux précurseurs catalytiques, exprimée en fraction molaire x_{Ni} , ainsi que la température de réaction provoquent la formation de différentes matières polymériques et modifient les valeurs de productivités ainsi que les propriétés physico-chimique des polymères.

Dans la deuxième partie du document, il est montré que l'utilisation de différents mélanges de précurseurs catalytiques $\{\text{Tp}^{\text{Ms}}\}\text{NiCl}$ ($\text{Tp}^{\text{Ms}} = \text{hydridotris}(3\text{-mésithylpyrazol-1-yl})$) et Cp_2ZrCl_2 , activés par un mélange MAO/TMA (1 :1) (TMA = triméthylalumine), ce qui constitue un système catalytique *Tandem*, qui permet de contrôler la production de polyéthylène linéaire de basse densité (LLDPE). Les activités catalytiques ainsi que les propriétés du polymère dépendent de la valeur de x_{Ni} . La production de polyéthylène avec différents Mw ainsi que le degré de ramification (par incorporation de buteno-1) est contrôlée, en utilisant seulement l'éthylène comme monomère.

La dernière partie de ce document décrit l'étude de la synthèse des complexes du groupe 3, $\text{M}(\text{allyl})_2\text{Cl}(\text{MgCl}_2)_2 \cdot 4\text{THF}$ ($\text{M} = \text{Nd}, \text{La}$ et Y), et leur réactivité dans la réaction de polymérisation de l'isoprène utilisant différents cocatalyseurs et variant les paramètres expérimentaux. De hauts rendements ont été obtenus ainsi que le contrôle des propriétés du polyisoprène. Ont été atteintes de hautes conversions en *cis*-1,4- et *trans*-1,4-polyisoprène

et concernant ce polymère, il a été montré que sa microstructure dépend de la nature du cocatalyseur et du centre métallique. Les combinaisons de Y et La forment des systèmes catalytiques efficaces pour les formation du *cis/trans*-polyisoprène. Dans ce cas, la microstructure des polymères dépend de la porportion de Y ce qui permet de controler la quantité de *cis-trans*-1,4 polyisoprène.

1. INTRODUCTION

Polymer materials are very significant in world economy and absolutely necessary for our daily life; therefore, it is of extreme needs to understand their chemistry and synthetic processes, based in catalytic process.

Catalysis is the key to many chemical transformations and extremely necessary for the polymers synthesis, and for that it becomes very important to investigate effect in these products properties. An immense variety of materials, whether it is a synthetic fiber, plastic resin, or elastomer are made with a catalytic process for our benefit.

Since the first generation of Ziegler-Natta catalysts in the 1950s, the field of polymerization catalysis has experienced a phenomenal activity in the last decades, with many academic and industrial research laboratories engaging varied technological innovations for controlled synthesis of polymer products. The new structural variations at the level of the molecular architecture lead to a constant evolution of the materials properties.

The control of the polymer properties is a very useful tool because it makes possible to adapt the material to the use purpose with earnings in performance. This strategy becomes extremely advantageous, allowing developing products of better quality, and this way to benefit our lives. For that, they are necessary technological innovations to supply the great competition in all the segments. In the same context, this work has the objective of studying some catalytic systems for the best control of polymer properties.

2. BIBLIOGRAFIC REVIEW

2.1. GENERAL CONSIDERATIONS

Since the 1950s, four generations of Ziegler-Natta catalysts were developed allowing a better control of polyolefin molecular structure during polymerization, with polymers of broad molecular weight distribution (MwD). In the ZN-type catalysts, which are heterogeneous, the active metal center occupies a position on the crystal surface. Polymerization at the active site is influenced by the electronic and steric environment of the crystal lattice. Because the active centers can occupy a wide variety of lattice sites, they tend to give products with a broad MwD and also, for example, non-homogeneous comonomer distribution in olefin copolymers.

It was necessary therefore to create a new type of catalyst, the metallocenes, which proved to be a homogenous system capable of polymerizing olefins. But the first systems using them were found to have low activity. It was not until 1980, when they were put together with a methylaluminoxane cocatalyst (MAO), that their full potential was realized. Their big advantage over the Ziegler-Natta systems is that olefin polymerization proceeds through only one reactive site (*Single Site Catalysts*). The polymerization continues in a far more controllable fashion, leading to polymers with narrow range of molecular weight and, more importantly, predictable and desirable properties.

The seeds of this activity are traceable to advances in Group 4 metallocene systems and their related half-sandwich titanium amide (*Constrained Geometry Catalysts* - (CGC)) catalysts during the 1980s¹. During that period, studies on Group 4 metallocenes afforded much needed insight into the nature of the active species, and the possibilities for controlling the nature of the polyolefin products were most elegantly demonstrated by the capacity of metallocene structures to polymerize propylene with high *iso*- or *syndiotactic* control².

Changes to the ligand skeleton provided access to more unusual materials with good properties. Contemporaneously, metallocenes systems were shown to possess an unparalleled capacity to incorporate longer chain R-olefin comonomers with the same degree of incorporation over the entire molecular weight range of the polyolefin product¹.

However, this technology reached high production levels. The patenting of new metallocene catalysts hit a peak in 1999, with 295 new metallocenes out of a total of 572 new catalysts for polyolefins³. Since that time, the number of new metallocenes has fallen, becoming necessary the creation of new classes of catalytic systems. So polymer chemists have started searching for new types of single site catalysts.

A lot of research is now being directed at other types of chemical that can produce polyolefins with the desired properties. During the first half of the 1990s, interest grew in developing new generation “non-metallocene” catalysts.⁴ It was a discovery in this time that had a great impact on researchers in the polyolefin catalysis field. Although some earlier work on nickel catalyst systems of the type employed in the Shell Higher Olefin Process (SHOP) had revealed the potential for late transition metals to polymerize ethylene⁵, it was the discovery of highly active (α -diimine) nickel catalysts capable of polymerizing ethylene to either linear or highly branched polyethylene (PE), depending on the ligand backbone and reaction conditions, that dramatically demonstrated the possibilities for expanding metals beyond the first half of the transition series. This offered the commercially attractive possibility of being able to incorporate polar comonomers into polyolefin materials, to give modified surface properties at low levels of comonomer incorporation, and change the bulk properties of the polyolefin at higher levels of incorporation and other interesting properties.

This and other works could clearly be built upon to explore uncharted areas of the transition series and, more generally, the periodic table. The potential for this approach was soon to be realized with the discovery in the late 1990s of highly active ethylene

polymerization catalysts based on iron, a metal with no previous track record in olefin polymerization⁶.

Another significant development has been the introduction of systems capable of catalyzing the living polymerization of olefinic monomers⁷. The absence of chain-transfer or chain-termination processes allows access to polyolefinic materials with very narrow molecular weight distributions (typically <1.1), block copolymers, and polymers with novel topologies of the field seemed appropriate.

These and other examples evidence the evolution of non-metallocene systems and their growing wide use. To have an idea of the proportion of this growth, Figure 1a shows the increase in the number of publications by year over the past decade, while Figure 1b gives the number of publications by Group for the 4-year periods 1994-1997 and 1998-2001. Notable are the increased number of publications for the Group 8 and Group 10 metals. The number of publications on the Group 10 metals for the period 1998-2001 substantially surpassing those for the Group 4 metals over the previous 4-year period. These data evidence that this area has been attracting a lot attention of the researchers in the last years.

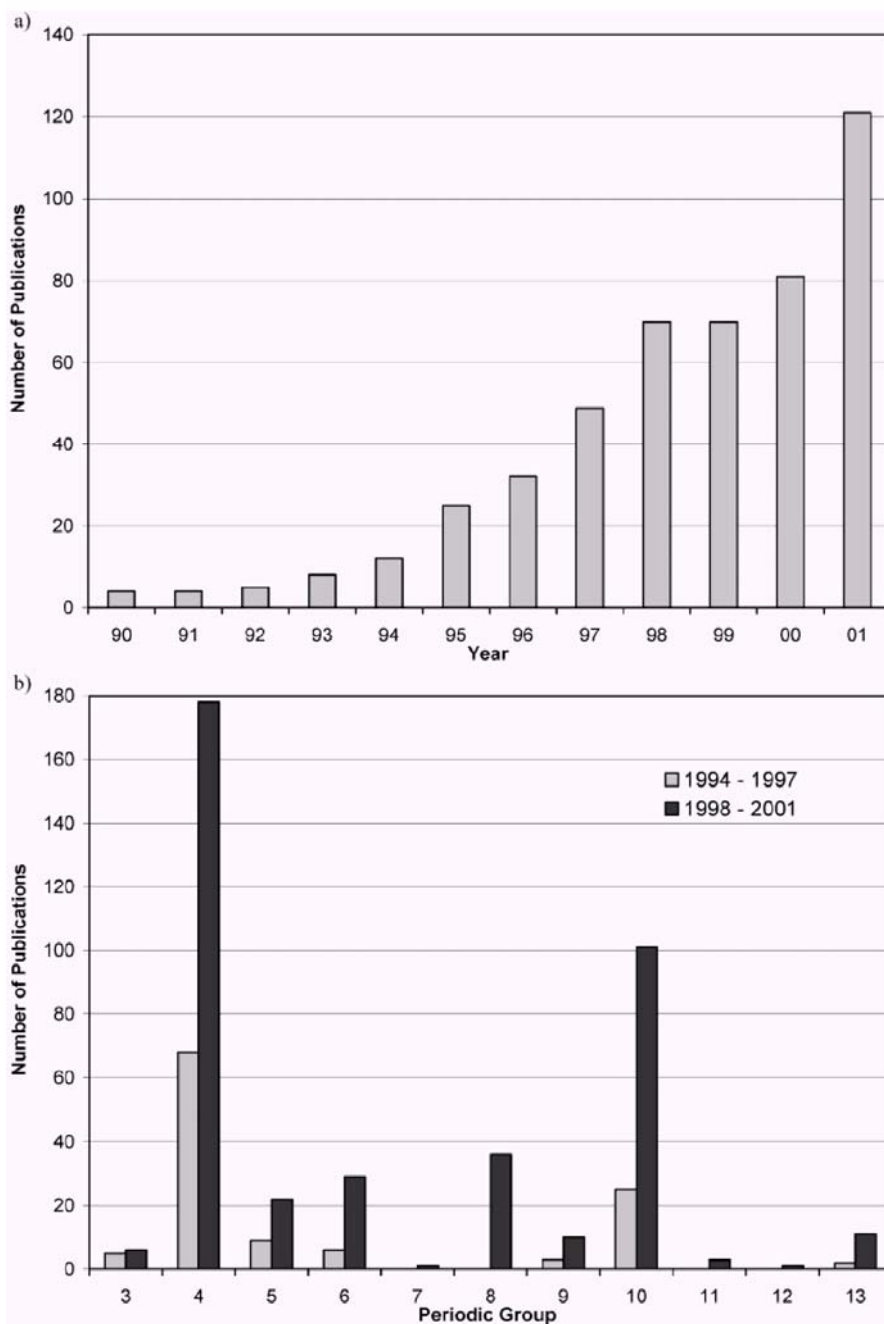


Figure 1. Numbers of publications on non-metallocene olefin polymerization catalyst systems appearing in the academic literature: (a) by year between 1990 and 2001, and (b) by periodic group for the 4-year periods 1994-1997 and 1998- 2001^{4,8}.

2.2. NON-METALLOCENE CATALYSTS APPLIED IN DIFFERENT POLYMERIZATION PROCESSES.

2.2.1. Binary Catalyst Systems

New polyolefinic materials constitute a cobblestone for the development of better performance materials with numerous industrial applications. In polymer processing and applications, molecular-weight (Mw) and molecular-weight distribution (MwD or Mw/Mn) represent basic characteristics, which serve as major determinants of polymer properties.

Molecular weight largely relates to the mechanical properties, while molecular weight distribution is responsible for rheological properties. Although high molecular weight polyethylene has superior physical properties, it is difficult to process. On the other hand, an increase in molecular weight distribution tends to improve the flow behavior at high shear rate, which is important for blow molding and extrusion techniques. For resolution of these problems, several methods for controlling Mw and MwD are available:

(i) The first involves the physical blending of polymers with different Mw. This widely used solution faces problems of energy consumption, operational costs and miscibility limitations.

(ii) The second method involves the use of a series of reactors (multi-stage reactors), each one run under different polymerization reaction conditions. This method inasmuch used at pilot plant level has been revealed as expensive, cumbersome and time-consuming.

(iii) The third method utilizes the variation of operation conditions, such as temperature, comonomer concentration, and hydrogen pressure (non-steady-state polymerization), in a single reactor during polymerization.⁹ This process is effective for laboratory-scale reactors, but is unlikely to be applied to the production of commodity polyolefins.

(iv) Finally, the fourth method consists of combining two or more types of catalysts to produce polymers with different and controlled Mw and MwD in a single reactor. The advantage of this latter method, which is capable of producing more easily polymers with good properties by using just a single polymerization process, have received considerable attention by industrial laboratories as can be seen by the number of new patents¹¹ issued in recent years.

2.2.1.1. Application of Catalytic mixtures in Polyethylene Synthesis.

Several homogeneous binary systems have been utilized in ethylene polymerization as an alternative to control the polymer properties. Two main polymerization processes are utilized using a combination of homogeneous catalysts (Figure 2).

In the process 1, the catalysts precursors polymerize ethylene independently generating different polyethylenes (Polymer Blends) during the polymerization reaction in a typical reactor blending procedure. In process 2, one catalyst of the binary system produces 1-alkenes *in situ* and the other one polymerizes ethylene and incorporates the 1-alkene in the growing chain. That process is called “Tandem Catalysis”.

Several factors must be considered for coupling the activity of multiple catalysts, the primary and most obvious condition being compatibility, there should be no interference between the catalytic species and decomposition or unwanted side reactions. The activity of catalysts is very important, the proportion between the species are fundamental for optimization (the catalysts should have similar activities). Another factor of extreme importance is the selectivity of the systems; should be used catalysts with high selectivity that minimize the sub product formation.

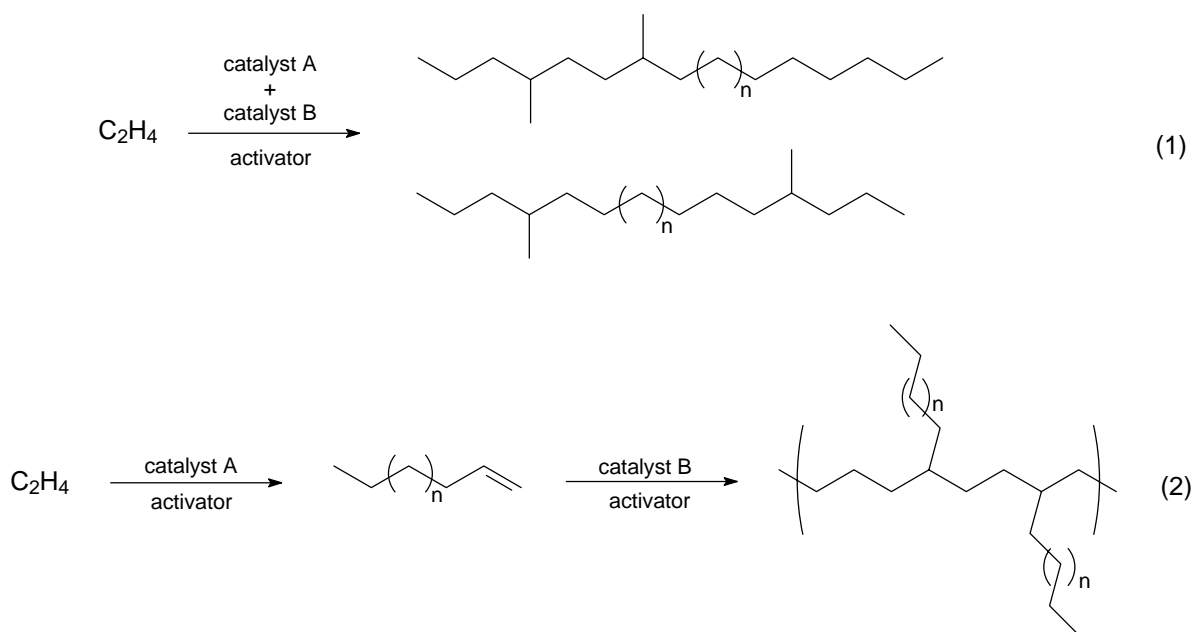


Figure 2. General processes for ethylene polymerization using a homogeneous binary system.

2.2.1.2 Production of Polymer Blends Using Binary Catalyst Systems

The generation of polymer blends *in situ* with two or more catalysts is possible and simple process. In a single operation, catalytic combinations polymerize ethylene generating different polyethylene types, not obtained by use of single catalyst. During the polymerization reaction, can afford PE blends with interesting chemical and physical properties.

One of the first reports related to the production of polyolefins, PE with broad MwDs are produced, using a homogeneous binary system consisting in metallocene catalysts, such as Cp_2TiPh_2 and $\text{Cp}_2^*\text{ZrCl}_2$ ($\text{Cp}^* = \text{C}_5\text{Me}_5$). Activated with methylaluminoxane (MAO) this system generated bimodal PEs with MwDs ranging from 5.4 to 7.8¹⁰. After this, various compositions of homogeneous binary systems have been created, by using of new compounds, to produce branched and linear polyethylenes¹¹.

Mw control using the different soluble catalysts $\text{rac-Et}(\text{Ind})_2\text{ZrCl}_2$, Cp_2ZrCl_2 , $\text{Ind}_2\text{ZrCl}_2$ and Cp_2HfCl_2 in the presence of MAO demonstrated broad monomodal or bimodal MwDs. The polymer properties are dependent of the system composition¹².

Combination of different Hf molar fraction (x_{Hf}) using $\text{rac-Et(Ind)}_2\text{ZrCl}_2$ with $\text{rac-Et(Ind)}_2\text{HfCl}_2$ ($X_{\text{Hf}} = 0.95$), in the presence of MAO, afforded PEs with bimodal MwD, where each catalyst produced its own polymer independently. The productivity changed drastically with temperature (20 to 70°C) and this behavior was reflected in the MwDs of the polymerization products¹³.

A mixture of metallocene compounds $\text{rac-Et(Ind)}_2\text{ZrCl}_2$, Cp_2ZrCl_2 , Cp_2HfCl_2 and Cp_2TiCl_2 produced ethylene homopolymer just as they would independently, suggesting that the chemical nature of the active sites is not affected by interactions between the different site-types present in the polymerization mixture. The authors demonstrated how variability in catalyst activity translates into variability in MwD when mixing soluble catalysts for polymerization¹⁴.

Polymerizations using late-transition metal catalysts bearing nitrogen ligands, combined with metallocene compounds, produce branched and linear polyethylenes¹⁵. The type of metallocene compound influences the polymer properties. The use of $\text{Ni}(\alpha\text{-diimine})\text{Cl}_2$ catalyst in combination with $\text{Me}_2\text{C}(\text{Cp})(\text{Fl})\text{ZrCl}_2$; Fl = fluorenyl) (figure 3b) produces reactor blends with densities varying from 0.91 to 0.93 $\text{g}\cdot\text{mL}^{-1}$ and viscosity-average molecular weights in the range $2.0 - 2.46 \times 10^5 \text{ g}\cdot\text{mol}^{-1}$.

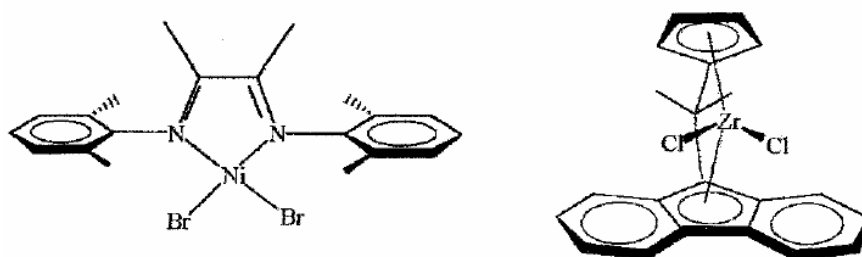


Figure 3. Ni-Diimine (a) and zirconocene (b) Complexes applied in reactor blends

A binary system involving two late-transition metal catalysts, LFeCl_2 (L = 2,6-diacetylpyridinebis(2,6-diisopropylanil), figure 4, and complex $\text{Ni}(\alpha\text{-Diimine})$, figure 3a, produces reactor blends with different properties related to the polyethylenes produced by the

catalysts separately. The combination of this system with MAO (60°C, toluene, $P_{\text{ethylene}} = 10$ atm, $x_{\text{Ti}} = 0.55$) produces PE with a viscosity-average molecular weight of 3.66×10^4 g.mol⁻¹ and 8 branches/1000 backbone chain carbon atoms. In all cases, no interactions between the metal centers have been reported¹⁵.

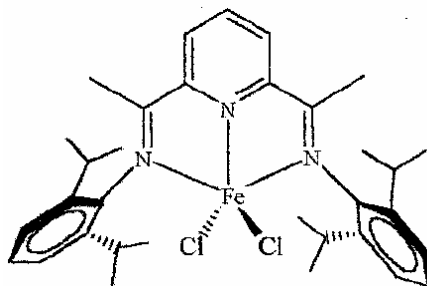


Figure 4. Iron complex utilized for blends formation.

Efforts to control the degree of long-chain branching (LCB) and the MwD of the polyethylene obtained¹⁶ using a binary system consisting of $[(\eta^5\text{-C}_5\text{Me}_4)\text{SiMe}_2(\eta^1\text{-NCMe}_3)]\text{TiMe}_2$ (CGC-Ti with CGC = *constrained-geometry catalyst*) and *rac*-Et(Ind)₂ZrCl₂ in the presence of MAO and B(C₆F₅)₃ as cocatalysts. The number of long-chain branches (LCB) per 10000 carbon atoms depends on the mole fraction of CGC-Ti (x_{Ti}) in the binary system. As x_{Ti} increased the degree of branching increased as well attaining a maximum for $x_{\text{Ti}} = 0.50$ (4.21 branches per 10 000).

The combination of early and late-transition metal complexes containing nitrogen ligands, Ni(α -diimine)Cl₂, which is known as being active for the production of branched polyethylene, and Tp^{Ms*}TiCl₃ (Tp^{Ms*} = hydridobis(3-mesitylpyrazol-1-yl)(5-mesitylpyrazol-1-yl)), that has been described as being active in the production of linear high-molecular weight polyethylene, was applied to ethylene polymerization using MAO as the cocatalyst¹⁷. Ethylene polymerization reactions carried out at 30°C in toluene and under atmospheric ethylene pressure showed a nonlinear correlation between x_{Ni} and productivity, which

suggests the occurrence of a synergistic effect between the Ni and Ti catalysts, generating a catalytic system more active than systems where the catalytic precursors work independently.

Studies of the influence of the molar ratio between the catalyst precursors as well as of the temperature on the productivity and polyethylene properties were also performed using the combination of Ni(α -diimine) type catalyst and *rac*-ethylenebis(IndH₄)ZrCl₂ (IndH₄ = 4,5,6,7-tetrahydro-1-(η^5 -indenyl)) in the presence of MAO¹⁸. Polymerizations carried out with varying x_{Zr} and temperature using constant amounts of MAO showed that the productivities are strongly dependent on these parameters. The linear correlation between productivity and x_{Zr} suggests that, in polymerization runs carried out at 0 and 50°C, the catalysts precursors work independently. At 30°C, a bell shape behavior with highest productivity for $x_{Zr} = 0.67$, show the nonlinear correlation between x_{Zr} and productivity indicates a synergistic effect between the nickel and zirconium compounds.

Combinations of Ni(α -diimine)Cl₂ (α -diimine = 1,4-bis(2,6-diisopropylphenyl)-(acenaphthenediimine) and Tp^{M_s*}TiCl₃ catalysts supported in situ on modified-methylaluminoxane (MMAO) silica (4.0 wt.-% Al/SiO₂)¹⁹ give higher activities systems. The melting temperatures (T_m) for the polyethylene blends produced at 0 °C decrease as x_{Ni} increases, indicating good compatibility between the polyethylene phases. The T_m's of the polyethylene blends were shown to depend on the order in which the catalysts were immobilized on the MMAO silica support. Analyzed by SEM (Scanning Electron Microscopy), this heterogeneous catalytic system is able to produce PE blends with an improved morphology. The spherical shape of the PE particles corresponding to that of the silica support is in accordance with the known replication effect.

2.2.1.3. Tandem Catalysis

"Tandem Catalysis"²⁰ refers to the action of multiple species, combined into one synthetic operation, to obtain products not readily obtained by a single catalyst, with minimum workup or change in conditions.

Multiple catalysts operating simultaneously could circumvent the time and yield losses associated with the isolation and purification of intermediates in multistep sequences. In a simple general example of a Tandem Catalysis cycle (Figure 5), where catalyst I transforms substrate A to give an intermediate B. B is subsequently converted to product P by catalyst II.

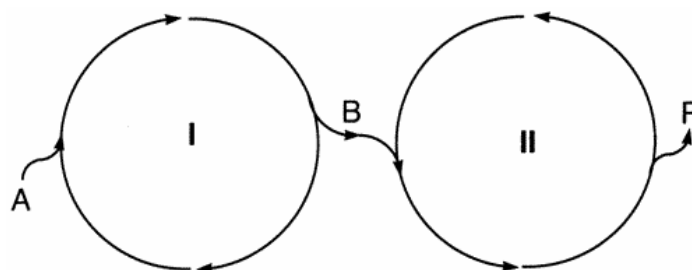


Figure 5. Simple Tandem process.

Many applications of this “new” process can be cited. Multienzymatic systems in nature, the molecular species, that are too thermally unstable for isolation, may be transformed into useful products by quickly entering a subsequent catalytic cycle prior to decomposition.

To enable this vision, chemists may choose from catalysts available from previous work on molecular, heterogeneous, and biological catalysis. Hydrogenation of a diene to a monoalkene, for example, may be a good initial reaction whereas monoalkene hydrogenation would likely not be, given the current state of alkane functionalization catalysis. In a simple example of concurrent tandem catalysis, whereby a single metal center promotes two different

catalytic cycles, alkene hydroformylation can afford alcohols by subsequent hydrogenation of the initial aldehyde product.

The polymerization of ethylene to branched polyethylene by combination of two different catalysts serves as good Tandem system example. Multiple catalyst combinations to yield polyethylene with branched structures have been examined for some time. The advantage is that the aliphatic groups can be introduced along the polymer main chain, thereby generating linear low-density polyethylene (LLDPE) (Figure 6). These pendant groups make the polymer less brittle and more easily processed than high-density polyethylene (HDPE).

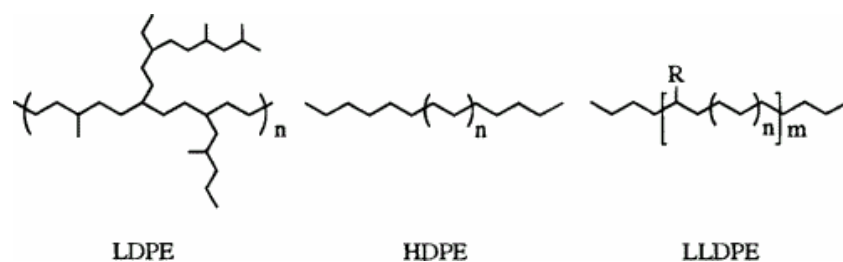


Figure 6. Low Density Polyethylene (LDPE), High-density Polyethylene (HDPE) and Low Linear Density Polyethylene (LLDPE).

In a Tandem preparation of LLDPE, one catalyst oligomerizes ethylene to R-olefins (1-alkenes) (Figure 7, cycle mediated by I). For maximum control of polymer properties, the R-olefins generated would be of a specific chain length (i.e. 1-butene, 1-hexene, 1-octene, etc.), however most oligomerization catalysts do not have such specificity and one typically must deal with a distribution of chain lengths. The second catalyst incorporates the 1-alkenes into a growing polymer chain [Figure 7, catalyst II]. This process eliminates the need to add comonomer to the ethylene polymerization reactor.

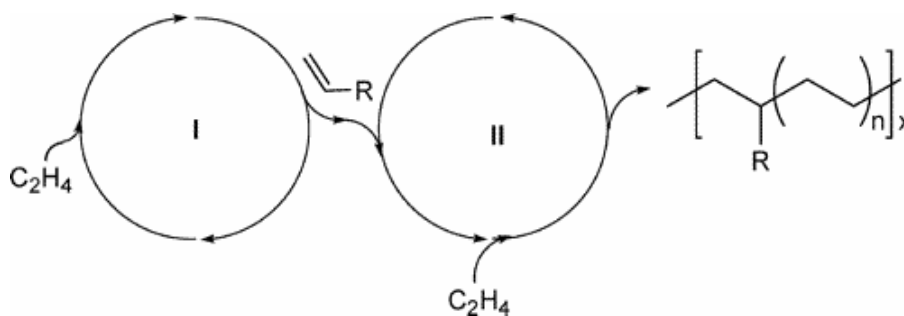


Figure 7. Tandem synthesis of LLDPE by two catalytic systems using only ethylene as monomer.

One of the earliest reports of Tandem preparation of LLDPE uses nickel and titanium based oligomerization catalysts with a different titanium polymerization site^{8b,21}. The catalysts in this combination are not perfectly balanced, and the total consumption of ethylene decreases as the concentration of the oligomerization catalyst increases. The authors attributed this drop in activity to partial poisoning of the polymerization centers and a slower insertion rate for 1-butene.

After, Phillips Petroleum patented a tandem catalyst process based on chromium compounds (such as CrO_3) deposited onto solid supports²². The reactivity of some of the chromium sites was modified by addition of pyrrole derivatives to generate oligomerization sites. The ethylene oligomers are then copolymerized with ethylene by unmodified chromium sites. In this manner, the branching content of the polymers produced could be adjusted by changing the chromium : pyrrole ratio.

Using a similar reaction strategy, a chromium (VI) oxide / silica catalyst was partially reduced by $\text{Cr}_4(\text{CH}_2\text{SiMe}_3)_8$ to produce a mixture of supported catalysts²³. The degree of branching in the polymers and distribution of the branch lengths can be altered by the $\text{Cr}_4(\text{CH}_2\text{SiMe}_3)_8$ loading.

The SHOP type phosphorus-oxygen chelated nickel ylide complexes (Figure 8, type 1) oligomerize ethylene to moderately high molecular weight R-olefins. These oligomers are

copolymerized with ethylene by using a chromium (II) / silica catalyst. Balancing the ratio of the two catalyst sites is important because at high nickel concentrations only olefins are produced. When the Cr(II) catalyst is in excess, polyethylene with long chain branches can be obtained. Similar results were obtained by the use of phosphorus-oxygen chelated nickel phosphine complexes type 2 (Figure 8) as the oligomerization site precursor²⁴.

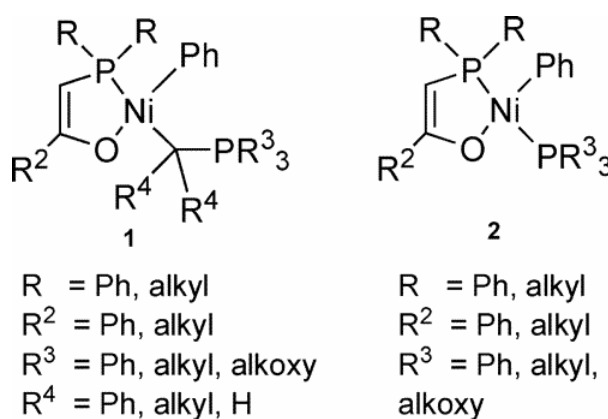


Figure 8. NiP[^]O complexes for applied in ethylene oligomerization

The advent and diversity of single site ethylene polymerization initiators has opened the opportunity of more rationally controlled tandem LLDPE production⁴.

Work performed at DuPont describes Tandem production of LLDPE²⁵. Iron Compound (Figure 9) activated with a modified methylaluminoxane (MMAO), generates ethylene oligomers²⁶. Combinations of this complex with *ansa*-zirconocenes produced moderately branched polymers²⁷. Catalysts with two fluorenyl ligands produced polymers with as much as 78 methyl groups per 1000 carbons, [Me/1000C], but did not fully incorporate the R-olefins. Similar results were attained with bis(amidinate) zirconium and titanium species. Notably, $[(\eta^5\text{-C}_5\text{Me}_4)\text{SiMe}_2(\eta^1\text{-NCMe}_3)]\text{ZrCl}_2$ gave polymer with 75 Me/1000C with negligible residual R-olefins²⁸.

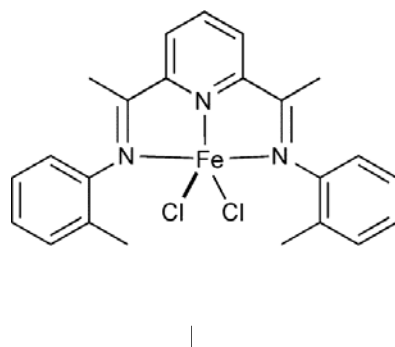


Figure 9. Iron complex for ethylene oligomerization

Compounds containing a P^oO nickel complex type 2 (Figure 8) for ethylene oligomerization and conditions were found that led to the generation of mostly 1-butene and 1-hexene. A great variety of zirconocenes, activated with MMAO, and the heterogeneous mixture MgH₂ / R-TiCl₃ / Cp₂TiCl₂ were each used as the polymerization catalyst and examined for copolymerization aptitude²⁹.

Of particular importance is the demonstration that molecules referred to as “constrained geometry catalysts” (CGC) have an excellent performance to produce LLDPE by copolymerization of R-olefins and ethylene (Figure 10)¹. Insertion into a propagating polyolefin is facilitated by the ability of CGC catalysts.

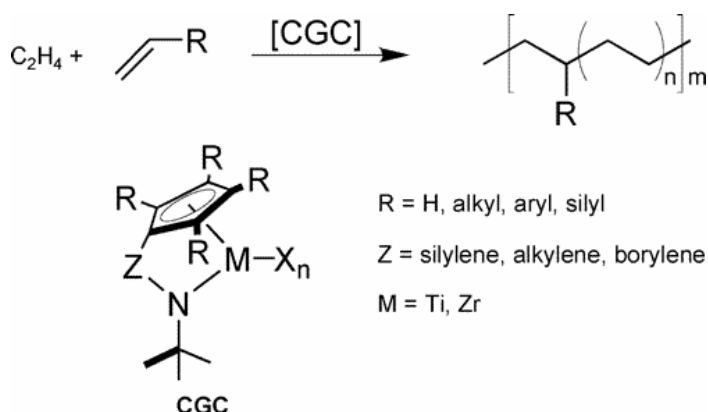


Figure 10. More controlled LLDPE synthesis by action of CGC catalysts.

Boron heterocycles as cyclopentadienyl analogues showed that activation of $(\eta^6\text{-C}_5\text{H}_5\text{B-OEt})_2\text{ZrCl}_2$, with MMAO yields a catalyst that produces a Shultz-Flory distribution of R-olefins³⁰. Its combination with $[(\eta^5\text{-C}_5\text{Me}_4)\text{SiMe}_2(\eta^1\text{-NCMe}_3)]\text{TiCl}_2$ (Figure 11) forms a well matched pair for LLDPE synthesis³¹. Considerable efforts were required to optimize polymerization conditions, so that the majority of R-olefins is incorporated into the chain and leads to monomodal molecular weight distributions. Once reaction conditions are optimized, the Zr:Ti ratio controls the melting point of the polymer products. Thus, a wide range of polymer structures, with specified properties, can be obtained simply by adjusting the ratio of components.

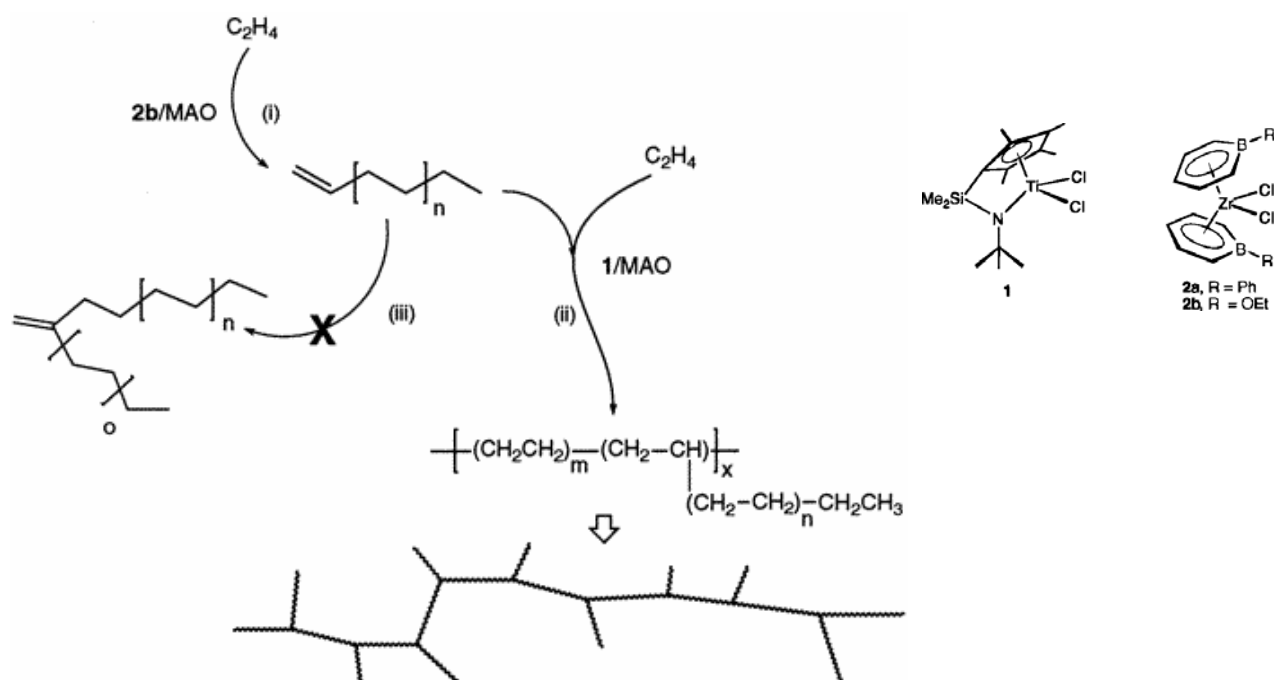


Figure 11. Tandem action of Ti (1) and Zr (2) catalysts.

Tandem systems to obtain ethylene-1-hexene copolymers recently appeared³². The *ansa*-metallocene-based system $(\eta^5\text{-C}_5\text{H}_4\text{CMe}_2\text{C}_6\text{H}_5)\text{TiCl}_3/\text{MMAO}$ trimerize ethylene to 1-hexene. The CGC system $[(\eta^5\text{-C}_5\text{Me}_4)\text{SiMe}_2(\eta^1\text{-NtBu})]\text{TiCl}_2 / \text{MMAO}$ copolymerize ethylene with the *in situ* produced 1-hexene to poly(ethylene-co-1-hexene). By changing the catalyst

ratio and reaction conditions, a series of copolymer grades with different 1-hexene fractions and high purity were effectively produced.

Action of highly selective aluminoxane-activated bis(2-decylthioethyl)amine, CrCl_3 complex (Figure 12) for the synthesis of 1-hexene in tandem with a number of metallocene catalysts is evaluated. Copolymers of 1-hexene and ethylene are produced with significant selectivity toward 1-hexene as comonomer. The selectivity of 1-hexene incorporation by different metallocene catalysts follows the trend in the order $[\text{Me}_2\text{Si}(2\text{-Me-Ind})_2]\text{ZrCl}_2 > [\text{Me}_2\text{Si}(2,3,4,5\text{-Me-Cp})(t\text{-Bu-N})]\text{TiCl}_2 > \text{Cp}_2\text{ZrCl}_2$. The highly selective nature of the ethylene trimerization catalyst employed in this study suggests that industrial application of tandem catalysis is becoming increasingly viable since it approaches conventional 1-hexene LLDPE in terms of polymer microstructure control³³.

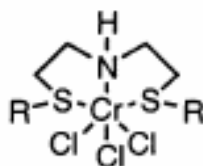


Figure 12. Chromium-(SNS) complex employed in 1-hexene synthesis.

Action of a heterogeneous (in fact supported) ethylene polymerization catalyst and a homogeneous ethylene oligomerization catalyst was also recently reported. Namely, a MAO-preactivated CGC site $[(\eta^5\text{-C}_5\text{Me}_4)\text{SiMe}_2(\eta^1\text{-NR})]\text{TiCl}_2$ ($\text{R} = \text{Me}$ or $t\text{Bu}$), supported on pyridylethylsilane-modified silica, and a homogeneous dibromo nickel catalysts, having a pyridyl-2,6-diisopropylphenylimine ligand in the presence of MMAO, gave polyethylenes with long-chain branches ($M_w = 15,000\text{-}50,000$)³⁴.

The effect of cocatalyst is very important for activities and selectivities. These studies are motivated by the poorly defined structures of aluminoxanes and by the fact that the ratio

of aluminoxanes to transition metal influences the rates of ethylene consumption. For example, addition of $B(C_6F_5)_3$ to $[(\eta^5-C_5Me_4)SiMe_2(\eta^1-NCMe_3)]TiMe_2$ gives $\{[(\eta^5-C_5Me_4)SiMe_2(\eta^1-NCMe_3)]TiMe\} \{MeB(C_6F_5)_3\}$ (Figure 13). The combination of NiP[^]O complex in reaction with $B(C_6F_5)_3$, and under specific reaction conditions, produces 1-butene exclusively. Combination of borate based systems of Ti and Ni (Figure 13) give high molecular weight branched polymers, which incorporate the vast majority of the R-olefins produced by Ti catalyst. Examination of the polymer structure, using ^{13}C NMR spectroscopy, showed a linear relationship between the degree of branching in the polymer and the Ti:Zr ratio in the tandem pair.

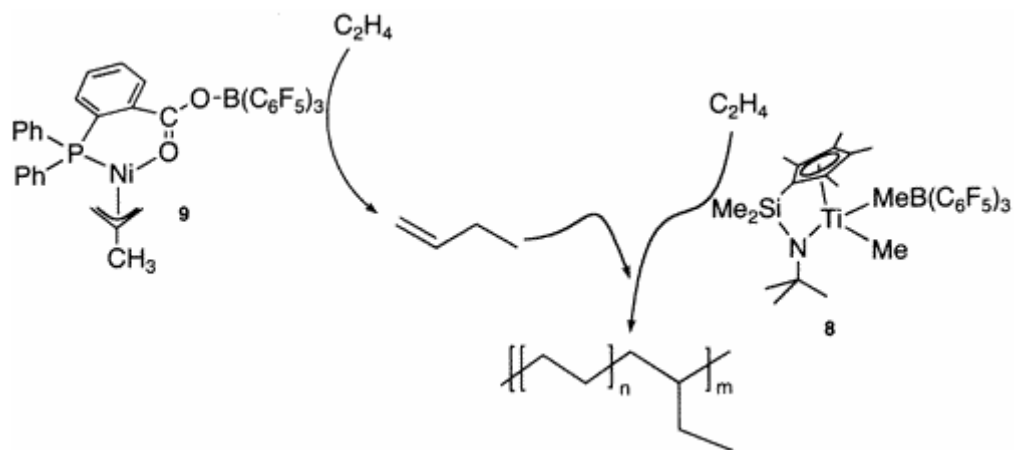


Figure 13. LLDPE synthesis using Borate systems of Ti and Ni catalysts.

It is possible to find conditions so that three active sites can be coordinated to provide a branched polyethylene structure unattainable by Tandem action of two active sites (Figure 14).

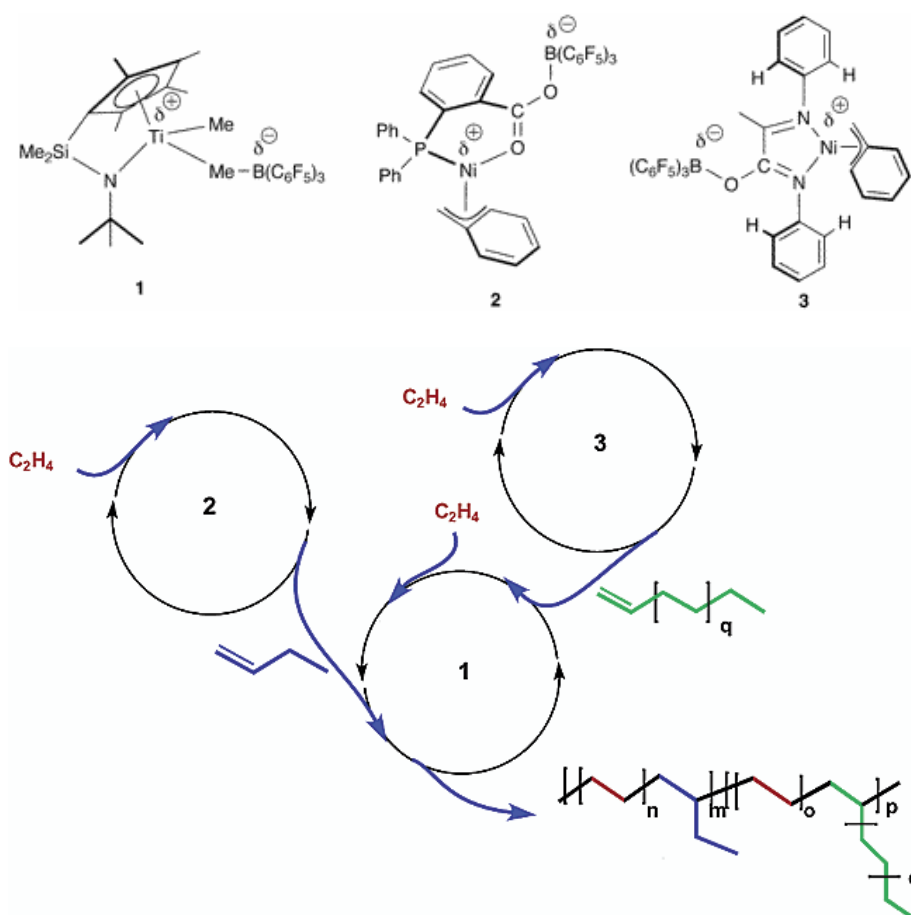


Figure 14. Tandem synthesis of LLDPE by action of three catalysts.

In figure 14, compound **3** generates a Schultz-Flory distribution of 1-alkenes under conditions where **2** generate 1-butene. A coordinated action of **1**, **2** and **3** provides PE with varying ratios of ethyl branches and longer branches³⁵. Optimization of the reaction conditions to obtain a polymer product with a monomodal molecular weight distribution proved difficult for a variety of reasons. Different 1-alkenes also display different insertion rates, depending on size. At the moment when ethylene enters, the reaction cycle the titanium site produces strictly linear polymer. With increasing reaction time the concentration of 1-alkenes produced by **1**/ C_2H_4 and **3**/ C_2H_4 increases and 1-alkenes begin to incorporate into the growing polymer chain at Ti, until a steady state is reached. By using high-throughput parallel reactor technology and computer control of reaction conditions, the optimization of process can be made.

The type of cocatalyst can modify the polymer properties, e.g. by the use of the binuclear activator $[\text{Ph}_3\text{C}]_2[1,4\text{-}\{\text{B}(\text{C}_6\text{F}_5)_3\}_2\text{C}_6\text{F}_4]$ (B_2) and mononuclear $[\text{Ph}_3\text{C}][\text{B}(\text{C}_6\text{F}_5)_4]$ (B_1) in Figure 15³⁶. The precursor for the oligomerization catalyst $(\eta^5\text{-3-ethylindenyl})\text{Me}_2\text{Si}(\eta^1\text{-NtBu})\text{ZrMe}_2$ (Zr), and $(\eta^5\text{-C}_5\text{Me}_4)\text{Me}_2\text{Si}(\eta^1\text{-NtBu})\text{TiMe}_2$ (Ti) gave rise to the sites responsible for incorporating the oligomers into a growing polyethylene chain. Under stoichiometrically appropriate ratios of Zr:Ti, use of B_2 gave rise to polymer products that have narrower molecular weight distributions than those obtained using the monofunctional activator $[\text{Ph}_3\text{C}][\text{B}(\text{C}_6\text{F}_5)_4]$. In this particular example, the binuclear activator B_2 increases the efficiency of processes by generating the R-olefin in close proximity to the Ti site, where incorporation into the larger polymer structure takes place. These results show that the activator dramatically increases the efficiency of homogeneous hetero bimetallic olefin enchainment processes for LLDPE synthesis.

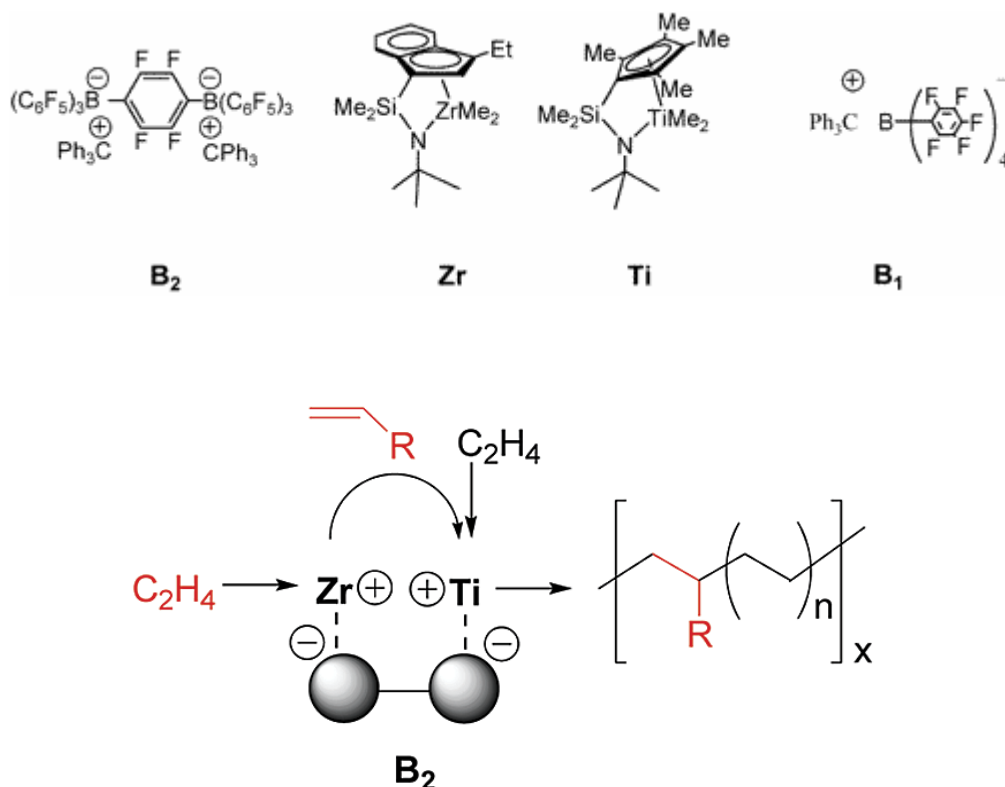


Figure 15. Tandem system by mononuclear (B_1) and binuclear activators (B_2) with Zr and Ti catalysts³⁶.

2.3. POLYISOPRENE

Modern synthetic polyisoprene is designed to be similar to natural rubber in structure and properties. Although it still demonstrates lower green strength, slower cure rates, lower hot tear and lower aged properties than its natural counterpart, synthetic polyisoprene exceeds the natural types in consistency of product, cure rate, processing, and purity. In addition, it is superior in mixing, extrusion, molding, and calendering processes. To approach these performances, it is necessary to convert isoprene stereospecifically in a *cis*-1,4- microstructure (Figure 16).

In recent years, many attempts were made to synthesize materials with such properties. The development of polyisoprene (PI) chemistry is important since there is only a limited supply of natural rubber in the world. This material can be considered a strategic commodity; therefore, new alternatives for PI synthesis can be applied.

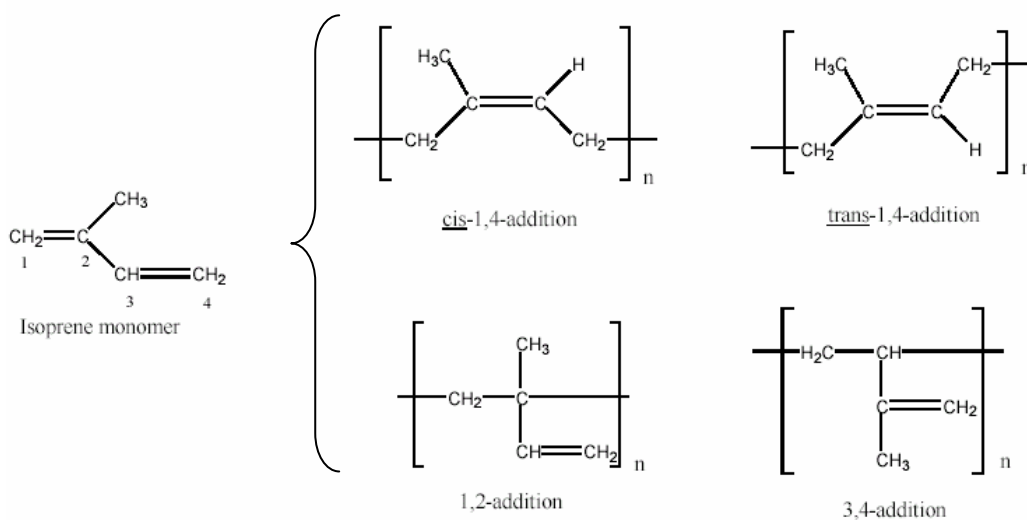


Figure 16. Possible microstructures of polyisoprene.

Whereas *cis*-polyisoprene polymerization has been to a large extent more studied, *trans*-specific polymerization of isoprene has seen a renewed interest⁵⁰. Occurring naturally as gutta-percha rubber, this form appears well suited for the elaboration of high-performance

tires^{37,38}. The *cis* form is soft and flexible because the chains do not pack well and the overall polymer is mainly amorphous. The *trans* form is hard because the *trans* chains pack well together, able to crystallize due to regular structure. In this context, one blend that involves different *cis/trans*-1,4-polyisoprene contents can provide improvements in polymer properties, as the processability and mechanical properties³⁹.

2.3.1. Historical Background

The successful synthesis of stereoregular polyisoprene (IR) fulfilled a goal sought by polymer chemists for nearly a century. Researchers knew that isoprene was the building block for natural rubber, and through the years, many attempts were made to synthesize materials with similar properties.

Initially, the resulting polymers failed to exhibit some of the desired aspects of natural rubber because of differences in microstructure, which plays an important role in PI physical properties. The polymer chains in the early syntheses contained mixtures of all possible molecular configurations joined together in a random fashion. Specifically, they lacked the very high *cis*-1,4 structure of the natural rubber backbone that gives the ability to undergo strain crystallization.

In the mid 1950s, researchers discovered and developed new types of catalyst systems that could selectively join together monomer units in a well-ordered fashion. Shortly after Karl Ziegler's breakthroughs in catalyst systems for the polymerization of ethylene, similar catalysts were developed for the use with isoprene. These "stereospecific" catalysts allowed the production of a nearly pure *cis*-1,4 structure, and in doing so, the production of a synthetic natural rubber.

Initial commercialization of a stereoregular, low *cis*-1,4-IR (90% to 92%) was realized in 1960 by Shell Chemical Company with the introduction of Shell Isoprene Rubber, produced with an alkyl lithium catalyst (Li-IR). However, the *cis*-1,4 content of Li-IR was insufficient to achieve the important crystallization properties of natural rubber.

In 1962, Goodyear introduced NATSYN^(TM), a Ziegler-Natta (titanium-aluminum) catalyzed IR (Ti-IR) with a *cis*-1,4 content of 98.5%. Goodrich-Gulf introduced another Ti-IR polymer about three years later, but subsequently withdrew it from the market in 1978. The manufacture of high *cis* IR has been undertaken elsewhere, primarily in Russia and Japan.

In addition to the *cis*-1,4 configuration, several other IR microstructures have been reported. A high *trans*-1,4 structure was produced by Polysar, and is now being produced by Kuraray. This polymer has significant room temperature crystallinity and is a synthetic analog of the naturally occurring Balata. A Li-IR with increased 3,4 structure can be prepared by adding polar modifiers to the alkyl lithium catalyst system. However, the higher *cis*-1,4 configuration most closely mirrors the properties of natural rubber and is the most important commercially.

Lanthanide based systems have been developed a while ago and are currently commercially used by Japan Synthetic Rubber (JSR), Enichem.

2.3.2. Applications of Polyisoprene

Currently synthetic PI is being used in a wide variety of industries in applications requiring low water swell, high gum tensile strength, good resilience, high hot tensile, and good tack. Gum compounds based on synthetic polyisoprene are being used in rubber bands, cut thread, baby bottle nipples, and extruded hose. Black loaded compounds find use in tires, motor mounts, pipe gaskets, shock absorber bushings and many other molded and mechanical

goods. Mineral filled systems find applications in footwear, sponge and sporting goods. In addition, recent concerns about allergic reactions to proteins present in natural rubber have prompted increased usage of the more pure synthetic polyisoprene in some applications.

Consumption of synthetic polyisoprene stabilized in the early 1990's was limited by manufacturing capacity and monomer availability. Recent increases in capacity, concerns about the stability of the price of natural rubber, and the mandate to move away from natural rubber in certain applications provide avenues for future growth in the industry. Table 1 shows the consumption history of synthetic polyisoprene over the past forty years.

Typical raw polymer and vulcanized properties of polyisoprene are similar to values obtained for natural rubber. Natural rubber and synthetic polyisoprene both exhibit good inherent tack, high compounded gum tensile, good hysteresis, and good hot tensile properties.

The very specific nature of synthetic PI provides a number of factors that differentiate it from natural rubber. There is minimal variance in physical properties lot to lot. Polymerization conditions are narrowly controlled to assure that the polymer is highly stereospecific. There is a low level of non-polymer constituents as compared to natural rubber.

Table 1. Consumption of Synthetic PI

	(1,000 Metric Tons)								
	1965	1970	1975	1980	1985	1990	1995	2000	2005
North America	41	81	67	66	47	56	62	78	78
World ^a	80	165	196	222	129	143	137	147	154

^a World consumption excludes Eastern Europe

2.3.3. Polymer Properties

Synthetic PI exhibits greater compatibility than natural rubber in blends with solution SBR and EPDM. The uniformity is a factor where the desire for consistent quality is paramount, as is increasingly the case in many industries with an emphasis on precise dimensional control in processing.

Because of the lower raw polymer viscosity, part or the entire breakdown step normally used for natural rubber should be eliminated. Synthetic PI compounds at the same plasticity of natural rubber will have less die swell because of having less nerve. Also, at the same plasticity, the synthetic polymer will have significantly faster extrusion rates.

Synthetic PI compounds can be adapted for curing in any conventional molding operation whether it is compression, transfer, or injection. The material is especially well suited for injection molded compounds. Because of its uniform cure rate, exact time/temperature press cycles can be established with assurance that all pieces will be uniformly cured. In addition, the Mooney of synthetic polyisoprene reduces injection pressures and times with a resultant increase in output.

2.3.4. Lanthanide Catalysts for Isoprene Polymerization

A great industrial development for polyisoprene production made significant advances on catalysis in recent years. New catalyst systems have been developed, some of which have a high activity and stereospecificity. Because of the permanent search for new-generation polymerization catalysts, there is considerable interest in developing the catalytic chemistry of group 3 metals, especially the rare earth metals. The area developed faster and faster in the late 1980s with the discovery of the high potential of these compounds as very active catalysts for polymerization. So far, organolanthanide chemistry has been dominated mainly by

metallocene complexes containing cyclopentadienyl ligands,⁴⁰ and cyclopentadienyl-free organolanthanide compounds have been more seldom. These lanthanide-based systems have remarkable polymerization abilities towards other monomers, such as dienes and styrenics⁴¹.

In some examples of isoprene polymerizations using group 3 metals, especially lanthanides, binary lanthanide catalysts (Ln = Nd, Pr and Gd) composed of tetrahydrofuran adducts of lanthanide chlorides and triethylaluminum (TEA) in hydrocarbon solvents which stereospecifically polymerize butadiene and isoprene are described. The catalyst composed of NdCl₃.2THF with TEA can be used to produce polyisoprene 96% *cis*-1,4 units, respectively, with good activity (95% of conversion) in heptane solution at 50 °C⁴².

Conventional neodymium systems are usually prepared by reacting a neodymium carboxylate with AlEt₂Cl (or other halide donors such as AlEtCl₂, AlBr₃, Alkyl halides), which leads to the formation of neodymium halide, and then adding of triisobutylaluminum (TiBA). Several variants to this system have been proposed, generally based on the use of NdCl₃ complexes with donors. In all these systems, the percentage of Nd active in the polymerization reactions is 6-8%, due to poor alkylation of Nd compound and the formed polymers have broad MwD⁴³.

The effects of the usual polymerization conditions, such as polymerization temperature, solvent, and Al:Ln molar ratio, etc., on the stereoregularity and molecular weight of polyisoprene as well as the catalytic activity in isoprene polymerization are reported with a (β-CH₃-π-allyl)₂LnCl₅Mg₂.TMED(Ln)/ Aluminum cocatalyst (Ln= Nd, Ce, and La, TMED = N, N, N',N',-tetramethyl-ethylenediamine, Aluminum cocatalyst = TiBA, TEA and TMA) catalyst⁴⁴. The metal type is determinant for the yield, the order of reactivity is Nd>Ce>La. When the cocatalyst type is changed, the order of yield were TiBA> TEA> TMA. Furthermore, TMA was capable of forming higher *cis*-1,4-polymer (83%). The stereoregularity was also influenced significantly by various solvents, the *cis* content for n-

hexane reaches 75%. Decreases of *cis* content were observed when toluene (47 %), o-xilene (51%) and chlorobenzene (54%) were used in Ce catalyst polymerizations. The stereoregularity is sensitive with different polymerization temperatures and/or polymerization times (49 – 75% of *cis*-content).

Anionic samarocene(III)bis(allyl) complexes such as $[(\text{Me}_2\text{C})_2(\text{C}_5\text{H}_4)_2\text{Sm}(\text{C}_3\text{H}_5)_2]\text{Li}(\text{dme})$ (dme = dimethoxyethane) are reported to initiate *trans*-1,4 polymerization of isoprene through dissociation of LiC_3H_5 ⁴⁵.

The neodymium iso-propoxide $[\text{Nd}(\text{O}i\text{-Pr})_3]$ catalyst activated by modified methylaluminoxane (MMAO) provide polymers with high molecular weight ($M_n \approx 10^5$), in heptane solution, with narrow molecular weight distribution ($M_w/M_n \approx 1.1\text{--}2.0$) and mainly *cis*-1,4 structure (82–93%). The polymer yield increased with increasing $[\text{Al}]/[\text{Nd}]$ ratio (50–300 mole ratio) and polymerization temperature (0–60°C), while the molecular weight and *cis*-1,4 content decreased. On the other hand, the same catalyst resulted in relatively low polymer yield and low molecular weight in toluene. When chlorine sources (Et_2AlCl , tBuCl , Me_3SiCl) were added, the *cis*-1,4 stereoregularity of polymer improved up to 95%, even at a high temperature of 60°C, though the polymer yield decreased.⁴⁶

Polymerization of isoprene by very simple lanthanide complexes LnI_2 ($\text{Ln} = \text{Nd}, \text{Sm}, \text{Dy}$ and Tm) and $\text{LnI}_2(\text{THF})_x$ ($\text{Ln} = \text{Sm}, \text{Tm}$) (Figure 17) without any additives or small amounts of TiBA ($\text{Al}/\text{Ln} = 10$) activators be high *cis*-1,4-polyisoprene content⁴⁷. TmI_2 , DyI_2 , NdI_2 , and SmI_2 all initiate polymerization in the presence of 10 equiv of TiBA. The additive seems to enhance the solubility of the system, and the polymerizations appear to proceed faster. The yield were also enhanced in the presence of the alkylaluminum reagent. $\text{SmI}_2(\text{THF})_x$ and $\text{TmI}_2(\text{THF})_x$ also generate polyisoprene in the presence of TiBA.

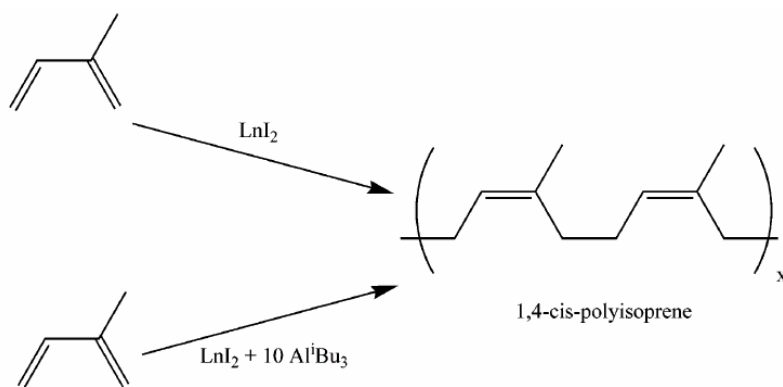


Figure 17. Polymerization of Isoprene by LnI_2 and $\text{LnI}_2(\text{THF})_x$.

Ternary and binary systems⁴⁸ (Figure 18) using lanthanide carboxylates as starting materials allow a direct evaluation of chloride and chloride-free systems to give blends of *cis*-1,4 and *trans* polyisoprene. These results are consistent with the traditional view that chloride is an essential component of the catalyst to form *cis*-1,4-polyisoprene. In the absence of chloride, the *cis* isomer can also form, but polymerization to *trans*-1,4-polyisoprene also occurs to generate a blend of isomers. The binary system is like the ternary system in which the nature of the metal, La or Nd, and the nature of the R_3Al initiator do not affect the results significantly. In addition, large excesses of R_3Al initiator are not required in the binary system. However, in the absence of chloride in the binary system, a soluble polyisoprene product is obtained which has a bimodal distribution and contains both *cis*- and *trans*-1,4-polyisoprene. This may prove to be of interest as a method to generate polymer blends *in situ*.

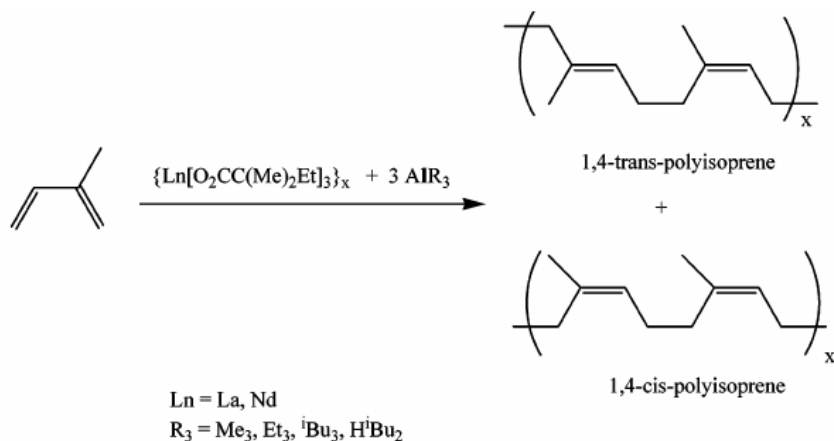


Figure 18. Polymerization of Isoprene by Ternary and Binary Lanthanide Catalytic Systems.

Catalytic investigations show that hexane-soluble neodymium complex⁴⁹ (Figure 19) polymerizes isoprene when combined with Et_2AlCl as a cocatalyst. Polymer yield and *cis*-1,4 content (by ^{13}C NMR) depend on the lanthanide-to halide ratio ($\text{Nd}/\text{Et}_2\text{AlCl}$) For the reactions using $\text{Nd}:\text{Al} = 1:1$ were obtained yield = 62% with 94% of *cis*-1,4-polyisoprene production. When increase the ratio $\text{Nd}/\text{Et}_2\text{AlCl}$ for 1/5, the yield is low (35%) but a high content of *cis*-1,4-polyisoprene (99%) was obtained.

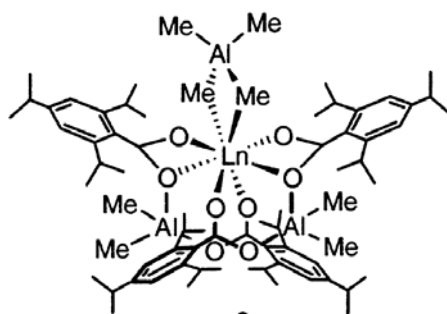


Figure 19. Neodymium complex ($\text{Ln} = \text{Nd}$) used for isoprene polymerization.

Highly stereospecific isoprene polymerization was achieved using borohydrido neodymium complexes. In combination with stoichiometric amounts of dialkylmagnesium, $\text{Nd}(\text{BH}_4)_3(\text{THF})_3$ give high activities up to 15,600 g of PIP/mol of Nd.h, *trans* stereospecific

production up to 98.5%, and molecular weights that correspond well to the monomer/catalyst ratios. The monomodal distribution is typical of a single-site character⁵⁰.

$\text{Nd}(\text{Allyl})_2\text{Cl}(\text{MgCl}_2)_2(\text{THF})_4$ catalyst were first prepared in the reaction of $\text{Mg}(\text{Allyl})\text{Cl}$ with $\text{NdCl}_3 \cdot 2\text{THF}$ ⁵¹, but the exact nature of the formed complex was not determined because only $\text{MgCl}_2 \cdot 2\text{THF}$ crystals were identified. The likely structure was defined by X-ray in the substitution of THF by tetramethylethylenediamine(tmed)⁵² to give $\text{Nd}(\text{Allyl})_2\text{Cl}(\text{MgCl}_2)_2 \cdot 2\text{tmed}$ complex. The combination of $\text{Nd}(\text{Allyl})_2\text{Cl}(\text{MgCl}_2)_2(\text{THF})_4$ with various aluminium alkyls was applied in butadiene polymerization⁵³ and the results showed larger activities than conventional heterogeneous Nd systems composed by $\text{AlEt}_2\text{Cl} \cdot \text{Nd}(\text{OCOC}_7\text{H}_{15})_3 \cdot \text{TiBA}$. The most active system was composed by MAO addition. In the combination with TMA, the activity of this system is, however, greatly enhanced by adding $\text{B}(\text{C}_6\text{F}_5)_3$ to the polymerization medium. Stirring mixtures of $\text{B}(\text{C}_6\text{F}_5)_3$ and alkylaluminum solutions generates $\text{Al}(\text{C}_6\text{F}_5)_3 \cdot \text{toluene}$, a very strong Lewis acid., by B/Al ligand exchange^{54,55}. Others activators as $[\text{Ph}_3\text{C}]^+[\text{B}(\text{C}_6\text{F}_5)_4]^-$ and $[\text{Ph}_3\text{C}]^+[\text{Al}(\text{C}_6\text{F}_5)_4]^-$ have been developed^{56,57} as effective cocatalysts for activating metallocene and related metal alkyls, thereby yielding highly efficient olefin polymerisation catalysts, which can provide greater catalytic activity and improvements in the polymer properties⁵⁸.

3. OBJECTIVES

The objectives of that thesis were the study of:

(1) The effect of different experimental parameters and their relation with polymer properties using the homogeneous binary catalyst system composed by $\text{Ni}(\alpha\text{-diimine})\text{Cl}_2$ ($\alpha\text{-diimine}$ = 1,4-bis(2,6-diisopropylphenyl)-acenaphthenediimine) and $\{\text{TpMs}^*\}\text{V}(\text{Ntbu})\text{Cl}_2$ (TpMs^* = hydridobis(3-mesitylpyrazol-1-yl)(5-mesitylpyrazol-1-yl)) activated with MAO, for different ethylene polymer blends production.

(2) The control of linear low density polyethylene (LLDPE) production using a combination of catalyst precursors $\{\text{Tp}^{\text{Ms}}\}\text{NiCl}$ (Tp^{Ms} = hydridotris(3-mesitylpyrazol-1-yl)) and Cp_2ZrCl_2 activated with MAO/TMA as Tandem catalytic system.

(3). The application of different experimental parameters using group 3 metals catalysts based, $\text{M}(\text{allyl})_2\text{Cl}(\text{MgCl}_2)_2 \cdot 4\text{THF}$ (M = Nd, La and Y), with different experimental conditions, cocatalyst systems and their effect in polyisoprene properties.

4. EXPERIMENTAL PART

4.1. GENERAL PROCEDURES

All manipulations were performed under a purified argon atmosphere using standard high vacuum Schlenk techniques or in a glovebox system. Solvents were distilled from Na/benzophenone or Na/K, stored under nitrogen and degassed thoroughly prior to use. The compounds $[\text{NiCl}_2(\alpha\text{-diimine})]$ ($\alpha\text{-diimine} = 1,4\text{-bis}(2,6\text{-diisopropylphenyl})\text{-acenaphthenediimine}$)⁵⁹, $\text{Tp}^{\text{Ms}^*}\text{VCl}_2(\text{NtBu})$ ($\text{Tp}^{\text{Ms}^*} = \text{hydridobis}(3\text{-mesitylpyrazol-1-yl})(5\text{-mesitylpyrazol-1-yl})$)⁶⁰ and $\text{Tp}^{\text{Ms}}\text{NiCl}$ ⁶¹ were synthesized following procedures described in the literature. Cp_2ZrCl_2 was purchased from Aldrich and used as received. Ethylene (polymer grade, White Martins) and argon were deoxygenated and dried by passage through columns of BTS (BASF) and activated molecular sieves (3 Å) prior to use.

MAO Witco, 5.21 wt.-% toluene solution), trimethylaluminum (TMA) (Aldrich, solution 10 wt.-% in hexane), Trimethylaluminum (TMA 2M), Triisobutylaluminum (TiBA 1M), Trimethylaluminum (TEA 1,9M) (Aldrich Chemical) and Methylaluminoxane (MAO 30 %w.t, Atofina Feluy) were used as received. Dried MAO was prepared under vacuum by evaporation of toluene solution during 6h and washed with dried pentane for remove TMA excess.

¹H NMR spectra were recorded on Bruker AC-200 spectrometer in Teflon-valved NMR tubes (for the catalyst) at room temperature. ¹H chemical shifts were determined using residual solvent resonance's and are reported vs. TMS, given in Hertz. Elemental analyses were performed by the Microanalytical Laboratory at the Institute of Chemistry of Rennes on a LECO-CHNS 932 apparatus.

4.2. COMPLEXES SYNTHESIS

The lanthanide catalysts were synthesized by procedures described in the literature⁵³. In the glovebox, MCl_3 ($M = Nd, Y$ or La) (5.12 mmol) was stirred with THF (5 mL) at room temperature for 2h. After that, (Allyl)MgCl (5.1 mL, 10.24 mmol, solution 2M in THF) was slowly added at this solution at $-20\text{ }^\circ\text{C}$. THF residual was removed under vacuum for 12h. The result is a green solid for all complexes.

Microanalyses for complexes:

$C_{22}H_{42}O_4Cl_5Mg_2Nd$: C 35.68; H 5.72; Found: C 35.70; H 5.73.

$C_{22}H_{42}O_4Cl_5Mg_2Y$: C 38.56; H 6.18; Found: C 36.55; H 5.95.

$C_{22}H_{42}O_4Cl_5Mg_2La$: C 35.93; H 5.76; Found: C 34.97; H 5.64.

1H NMR of $C_{22}H_{42}O_4Cl_5Mg_2La$:

(C_6D_6 , $20\text{ }^\circ\text{C}$, 200 MHz): 6.55 ppm (1H, Allyl₁), 5.75 ppm (1H, Allyl₂), 5.00 ppm (2H, Allyl₁), 4.20 ppm (2H, Allyl₂), 3.80 ppm (16H, THF), 3.15 ppm (2H, Allyl₁), 2.00 ppm (2H, Allyl₂), 1.35 ppm (16H, THF).

(THF- d_8): 6.80 ppm (2H, Allyl₁ e Allyl₂), 2.65 ppm (8H, Allyl₁ e Allyl₂).

1H NMR of $C_{22}H_{42}O_4Cl_5Mg_2Y$:

(C_6D_6 , $20\text{ }^\circ\text{C}$, 200 MHz): 6.80 ppm (1H, Allyl₁), 5.75 ppm (1H, Allyl₂), 5.05 ppm (2H, Allyl₁), 4.25 ppm (2H, Allyl₂), 3.85 ppm (16H, THF), 2.05 ppm (2H, Allyl₁), 1.60 ppm (2H, Allyl₂), 1.30 ppm (16H, THF). RMN 1H

(THF- d_8 , $20\text{ }^\circ\text{C}$, 200 MHz): 6.30 ppm (2H, Allyl₁ e Allyl₂), 2.95 ppm (4H, Allyl₁), 2.45 ppm (4H, Allyl₂), 3.58 ppm (16H, THF), 1.73 ppm (16H, THF)

4.3. POLYMERIZATION PROCEDURES

4.3.1. Production of Polymer Blends Using Binary Catalyst Systems

All ethylene polymerization reactions were performed in a 1.0 L Pyrex glass reactor connected to a constant temperature circulator and equipped with mechanical stirring and inlets for argon and ethylene (Figure 20). The reactor was rinsed with 300 mL of a Triisobutylaluminum (TiBA) or Trimethylaluminum (TMA) solution in hexane prior to use. Under argon atmosphere were introduced sequentially the proper amounts of solvent (toluene or hexane) and MAO solution, and then the system was saturated with ethylene. After complete saturation with ethylene at atmospheric pressure and thermal equilibration of the system, the polymerization reactions were started by adding solutions of catalysts into the reactor. The total volume of the reaction mixtures was 300 mL for all polymerizations. The polymerization reaction was stopped by the addition of 1 mL of Ethanol/HCl 1% solution. The polymer was washed with acidic ethanol, then water and ethanol and dried in a vacuum oven at 60°C for 12 h. On the basis of the results of multiple runs, we estimate the accuracy of the activities to $\pm 8\%$.



Figure 20. Pyrex glass reactor (1.0 L) used for reactor blends production.

4.3.2. Tandem Catalyst System

All polymerization reactions were performed in a double walled glass reactor (120 ml) equipped with magnetic stirring, thermocouple temperature control, and a continuous ethylene feed (1.1 atm) (Figure 21). Under an argon atmosphere, the proper amounts of toluene and MAO/TMA solution were introduced sequentially, and then the system was saturated with ethylene. After complete saturation with ethylene at atmospheric pressure and thermal equilibration of the system, the polymerization reactions were started by adding solutions of precursors. The total volume of the reaction mixtures was 60ml for all polymerizations. The polymerizations are poured with acetone, filtered and the polymer washed with acidic ethanol,

then water and ethanol, and dried in a vacuum oven at 40 °C for 12 h. On the basis of the results of multiple runs, we estimate the accuracy of the productivities to $\pm 8\%$.



Figure 21. Double walled glass reactor (120 mL) used for Tandem synthesis of LLDPE.

4.3.3. Isoprene polymerization

In the glovebox, a Schlenk flask was charged with 17 μmol of $\text{M}(\text{allyl})_2\text{Cl}$ (MgCl_2) \cdot (THF) $_4$ ($\text{M} = \text{Nd, Y and La}$) and the cocatalyst solution (MAO, TiBA, TEA, TMA or borate systems) dissolved in 5 mL of toluene. The mixture was stirred for 10 min (activation time). The polymerization is started by addition of the amount of Isoprene solution (dissolved in 3mL of hexane). The reaction was quenched by adding a solution of methanol/HCl. The polymer was washed with acetone/ethanol and dried in vacuum at 40°C for 8 hours. On the basis of the results of multiple runs, estimate the accuracy of the productivities to $\pm 8\%$.

4.4 POLYMERS CHARACTERIZATIONS

Polyethylene films were prepared in a Carver press Monarch series, model 3710 ASTM. The polymers were pre-heated for 2 min at 160 °C between the press plates without pressure and then pressed for 2 min at 3 kgf.cm⁻² at the same temperature. After this time, the pressure was released and the films were control-cooled down to room temperature at the cooling rate of 10 or 18 °C/min, or quenched in water-ice bath or liquid nitrogen. The film thickness was 0.15 mm ± 0.02.

Polymer melting temperatures (T_m) were determined on the Thermal Analysis Instruments DSC-2010 calibrated with Indium, using a heating rate of 10°C.min⁻¹ in the temperature range 40-180 °C and cooling to 40 °C at 10 °C.min⁻¹. The heating cycle was performed twice, and only the results of the second cycle are reported. The endothermic curve inflection point is the polymer melting point (T_m). The polymer crystallinity index (χ) is determined comparing the sample melting heat with a 100% crystalline PE (286.6 J/g).

The weight average molecular weight (M_w) was evaluated by gel permeation chromatography (GPC) with the waters 150CV system equipped with three columns Styragel HT3, HT4, and HT6 (103,104, and 106 Å, respectively) and a refractive index detector. Analyses were undertaken using 1,2,4-trichlorobenzene as solvent at 140 °C. The M_w was calculated using a universal calibration curve built with polystyrene standards (American Polymer Standard Corporation) and checked with polyethylene and polypropylene known samples.

The Number average molecular weight (M_n) of polyisoprene samples produced by Ln(allyl)₂Cl(MgCl₂)₂·4THF complexes (Ln = Nd and La) was evaluated by gel permeation chromatography (GPC) using a Waters 600 apparatus in THF at 20 °C calibrated with polystyrene standards.

Melt flow indexes (MFI) were determined at 190°C using a 21.6 kg standard charge.

The morphology was studied by using a Scanning Electron Microscope (JEOL JSM 5800) with 10 KV tension. The films obtained on a press are immersed in liquid nitrogen during 10 min and cryo-fractured under liquid nitrogen in two parts. One part is etched with *o*-xylene at 180 °C for dissolution of soluble branched PE. The surfaces were coated with a gold layer to make it conducting and the two parts analyzed on the microscope for comparison.

The branch content in the LLDPE samples were determined by ^{13}C NMR in a Varian Inova 300 spectrometer operating at 75MHz and at 90 °C. Samples solutions of the polymer were prepared in *o*-dichlorobenzene and benzene- d^6 (20 vol.%) in a 5mm NMR tube.

The microstructure of PI was determined by ^1H NMR in Varian Inova 200 spectrometer operating at 200MHz and at 20 °C; δ in ppm: 5.11 (s, 1H), 4.70 (d, 2H, 3,4-), 2.02 (s, 4H, $(\text{CH}_2)_n$), 1.67 (s, 3H, 1,4-*cis*), 1.57 (s, 3H, 1,4-*trans*), 3,75 (d, 2H, 3,4-).

The ^{13}C NMR analysis was determined in Varian Inova 200 spectrometer operating at 50MHz and at 20 °C 200 MHz); δ in ppm: 135.65 (S, C_2), 125.45 (S, C_3), 32.64 (S, C_1), 26.83 (S, CH_3), 23.87 (S, C_4).

Samples solutions of PI were prepared in CDCl_3 in a 5mm NMR tube.

5. RESULTS AND DISCUSSION

5.1. DUAL CATALYST SYSTEM COMPOSED BY NICKEL AND VANADIUM COMPLEXES CONTAINING NITROGEN LIGANDS FOR ETHYLENE POLYMERIZATION.

The ethylene polymerization reactions were carried out using methylaluminoxane-activated $\text{NiCl}_2(\alpha\text{-diimine})$ (**1**) and $\{\text{TpMs}^*\}\text{V}(\text{Ntbu})\text{Cl}_2$ (**2**) (figure 22) in hexane/toluene at 0, 30, and 50°C. Tables 2 and 3 show the results of polymerization runs by varying the nickel loading molar fraction (x_{Ni}) and temperature, with constant amount of MAO.

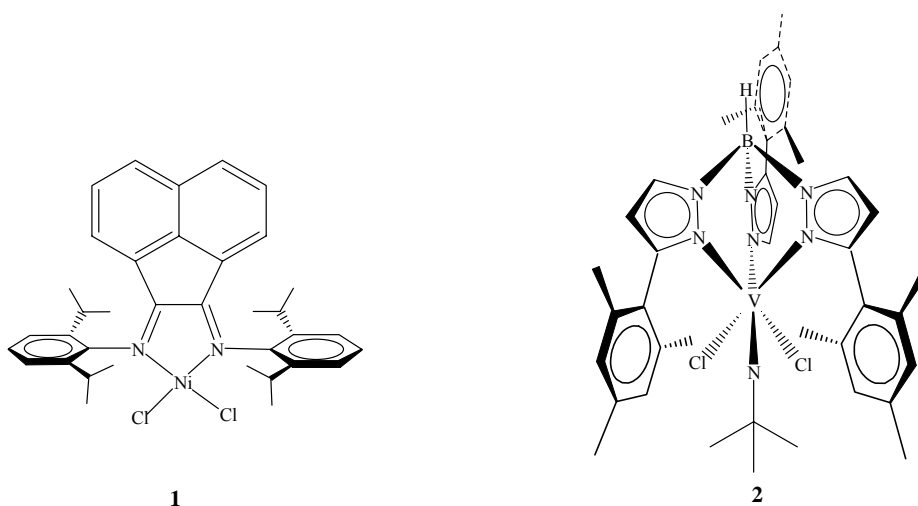


Figure 22. $\text{NiCl}_2(\alpha\text{-diimine})$ (**1**) and $\{\text{TpMs}^*\}\text{V}(\text{Ntbu})\text{Cl}_2$ (**2**) structures.

5.1.1. Influence of experimental parameters in the activity

The ethylene polymerization reactions performed employing **1** and **2** separately showed that the catalytic system **1**/MAO exhibited higher activities than **2**/MAO for all temperatures and solvents employed in the polymerization runs (Figures 23 and 24). The catalytic system **1**/MAO reached a maximum activity in toluene at 0°C (2248 kg of

PE.mol[Ni]⁻¹.h⁻¹ (entry 20) while a highest activity for system **2**/MAO was obtained in hexane at 30°C (456 kg of PE.mol[Ni]⁻¹.h⁻¹), entry 6.

Table 2. Ethylene polymerizations using homogeneous binary catalyst system composed of [NiCl₂(a-diimine)] (**1**) and [TpMs*VCl₂(NtBu)] (**2**) in hexane under atmospheric ethylene pressure.^a

Entry	Temperature (°C)	x_{Ni}^b	Yield (g)	Activity ^c	T_m^c (°C)	χ (%)	MFI ^d (g/10min)
1	0	0.00	1.07	428	144	20	< 0.001
2	0	0.25	1.84	736	142	18	< 0.001
3	0	0.50	2.22	888	135	17	0.01
4	0	0.75	2.85	1140	124	16	0.01
5	0	1.00	4.20	1680	122	14	0.02
6	30	0.00	1.14	456	144	23	< 0.001
7	30	0.25	0.72	288	139	14	0.14
8	30	0.50	0.47	188	138	5	1.79
9	30	0.75	0.84	336	135	3	0.10
10	30	1.00	2.06	824	- ^f	- ^f	13.10
11	50	0.00	1.07	428	143	29	< 0.001
12	50	0.25	0.90	360	142	20	< 0.001
13	50	0.50 ^e	0.10	204	142	25	< 0.001
			0.41		- ^f	- ^f	
14	50	0.75 ^e	0.09	180	139	17	0.18
			0.36		- ^f	- ^f	
15	50	1.00	1.37	548	- ^f	- ^f	156.00

(a) Polymerization conditions: Glass Reactor (1L); hexane = 300 mL. [Al]/[M] = 500; MAO as activator; (b) Nickel Molar fraction, $x_{Ni} = [Ni]/([Ni] + [V])$. (c) kg of PE.mol[Ni]⁻¹.h⁻¹; (d) Melt flow indexes (MFI) were determined at 190°C using a 21.6 kg standard charge; (e) The reaction showed spontaneous separation of the PE phases. (f) Amorphous PE.

Table 3. Ethylene polymerization using homogeneous binary catalyst system composed of $[\text{NiCl}_2(\alpha\text{-diimine})]$ (**1**) and $\text{Tp}^{\text{Ms}^*}\text{VCl}_2(\text{N}^t\text{Bu})$ (**2**) in toluene under atmospheric ethylene pressure.^a

Entry	Temperature (°C)	x_{Ni}^{b}	Yield (g)	Activity ^c	T_{m}^{c} (°C)	χ (%)	MFI ^d (g/10min)
16	0	0.00	0,44	176	146	27	<0.001
17	0	0.25	1,99	796	141	16	< 0.001
18	0	0.50	2,53	1012	126	12	< 0.001
19	0	0.75	5,23	2092	122	12	< 0.001
20	0	1.00	5,62	2248	117	15	< 0.001
21	30	0.00	0,85	340	143	19	< 0.001
22	30	0.25	1,04	416	141	19	< 0.001
23	30	0.50	1,48	592	135	2	0.56
24	30	0.75	2,23	892	137	4	1.82
25	30	1.00	3,73	1492	- ^e	- ^e	0.42
26	50	0.00	0,58	232	143	19	< 0.001
27	50	0.25	0,41	164	139	13	< 0.001
28	50	0.50	1,09	436	137	1	19.16
29	50	0.75	1,36	544	138	1	27.96
30	50	1.00	1,72	688	- ^e	- ^e	95.10

(a) Polymerization conditions: Glass Reactor (1L); toluene = 300 mL. $[\text{Al}]/[\text{M}] = 500$; MAO as activator; (b) Nickel Molar fraction, $x_{\text{Ni}} = [\text{Ni}]/([\text{Ni}] + [\text{V}])$. (c) kg of PE.mol $[\text{Ni}]^{-1}.\text{h}^{-1}$; (d) Melt flow indexes (MFI) were determined at 190°C using a 21.6 kg standard charge. (e) Amorphous PE.

Comparing the performance of both catalytic systems it was observed that nickel catalyst was more sensitive to temperature decreasing the activity with increasing polymerization temperature. Furthermore, the difference between the activities obtained for the systems 1/MAO and 2/MAO decreases as the polymerization temperature increases being this effect more pronounced in hexane. For instance, at 50°C this activity difference was 1.2 fold and reaches 3.9 fold at 0°C (compare entries 1 and 5, and 11 and 15).

Polymerization runs carried out when varying x_{Ni} and temperature, with constant amount of MAO, showed that the activities are strongly dependent on these parameters as can be seen in Figures 23 and 24. At low temperature (0°C) apparently the solvent does not promote any significant influence on the activity. In that case, the activities increase linearly with x_{Ni} indicating that each catalyst precursor was working independently. At higher polymerization temperatures (30 and 50°C) the influence of the solvent on the activity is more clearly presented. For the polymerization reactions performed in toluene (Figure 24, the dependence of the activity with respect to the x_{Ni} was roughly linear.

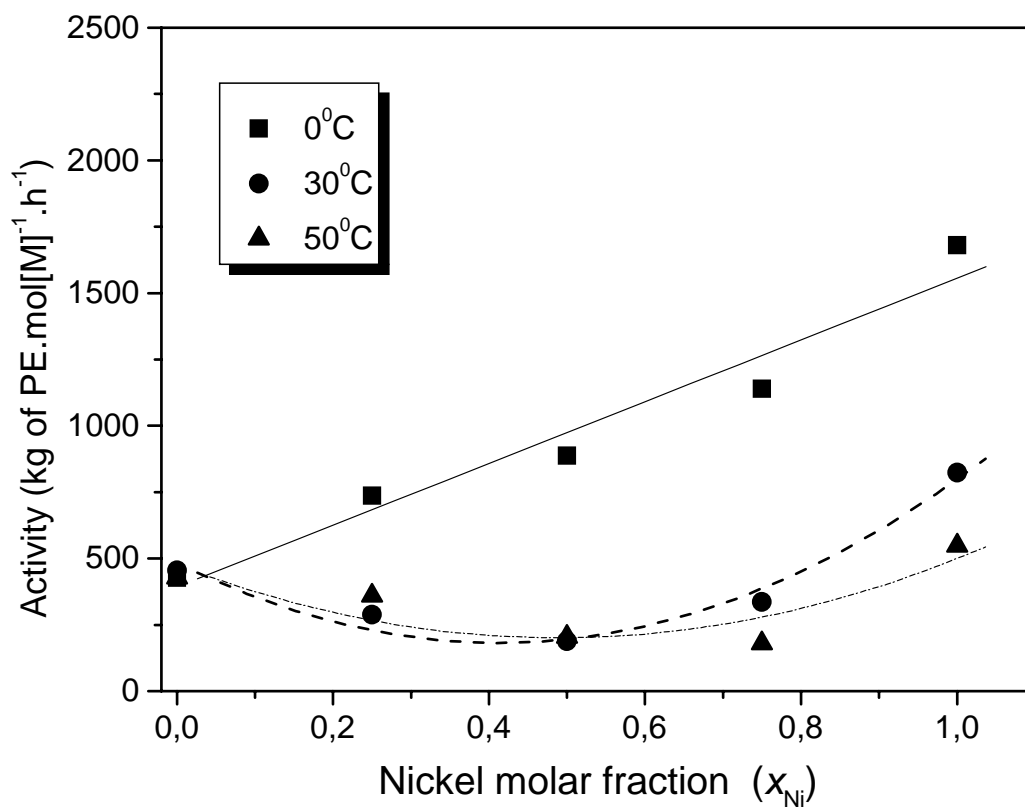


Figure 23. Influence of the polymerization temperature on the activity varying x_{Ni} for the polymerization reactions performed in hexane.

On the other hand, the use of hexane (Figure 23) instead toluene determined a clearly non-linear correlation between the nickel molar fraction ($x_{Ni} = 0.25, 0.50$ and 0.75) and the activity suggesting that the combination of **1** and **2** in this solvent can be promoting a partial deactivation of catalytic species. For instance, the activities found for $x_{Ni} = 0.50$ (30°C , 188 kg of PE.mol[Ni] $^{-1}$.h $^{-1}$; 50°C , 204 kg of PE.mol[Ni] $^{-1}$.h $^{-1}$) are 3.4 and 2.4 times respectively lower than the predicted ones (30°C , 640 kg of PE.mol[Ni] $^{-1}$.h $^{-1}$; 50°C , 488 kg of PE.mol[Ni] $^{-1}$.h $^{-1}$).

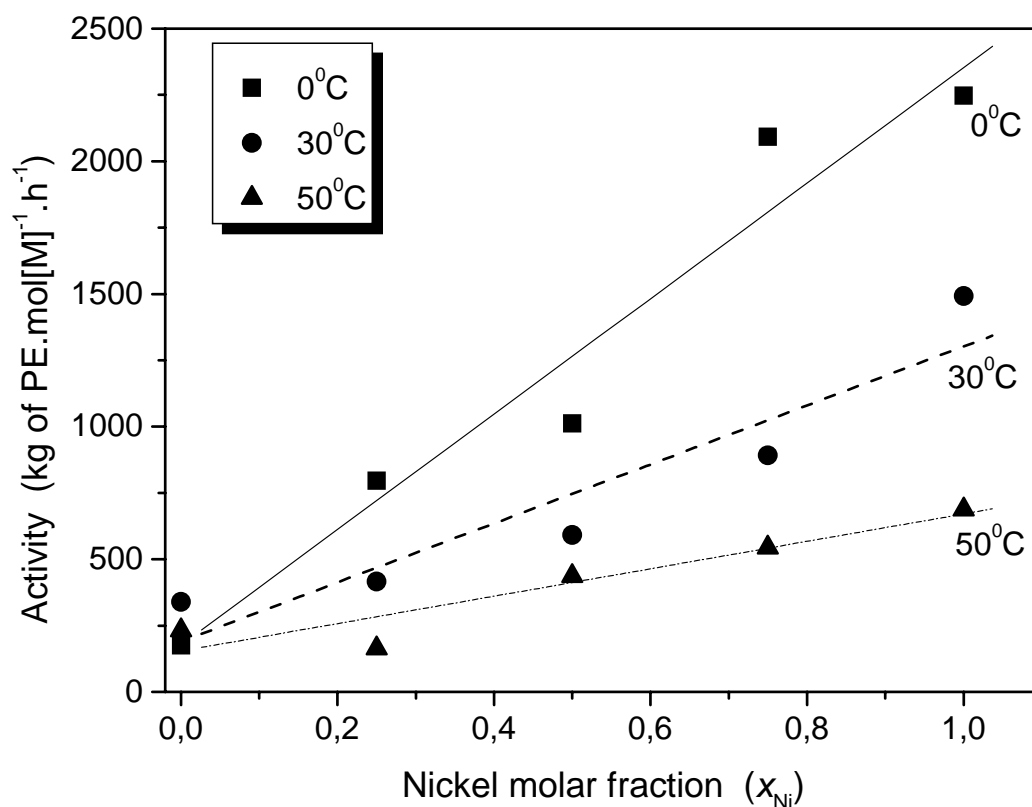


Figure 24. Effect of the polymerization temperature on the activity varying x_{Ni} for the polymerization reactions performed in toluene.

5.1.2. Influence of x_{Ni} and polymerization temperature on the polymer properties.

The influence of x_{Ni} , solvent and polymerization temperature on polyethylene microstructure have been evaluated by means of differential scanning calorimetry (DSC), and melt flow index (MFI). The results are summarized in Tables 1 and 2.

The melting temperature (T_m) of the polymers produced by **1** or **2** is not extensively affected by changing the solvent. As expected, the branched polyethylenes (BPE) produced by **1** ($x_{Ni} = 1.00$) have T_m of 118°C (toluene) and 121°C (hexane), while the high-density polyethylenes (HDPE) produced by **2** ($x_{Ni} = 0.00$) show T_m around 145°C. In contrast to the thermal behavior of the PE blends produced at 0°C using the homogeneous binary catalyst system composed by $[NiCl_2(\alpha\text{-diimine})]/[rac\text{-ethylenebis(IndH}_4\text{)ZrCl}_2]$ ¹⁸, broad single melting and crystallization peaks were observed in the PE blends produced by **1/2/MAO** catalyst system, indicating a good compatibility between the branched and high-density PE phases (Figures 25 and 26). It is significant to note that the T_m is strongly influenced at 0 °C by the nickel molar fraction, whatever the solvent used in the polymerization reaction. T_m values for the polyethylene blends produced in hexane at 0 °C varied from 122°C ($x_{Ni} = 0.75$) to 141°C ($x_{Ni} = 0.25$) (figures 25 and 26).

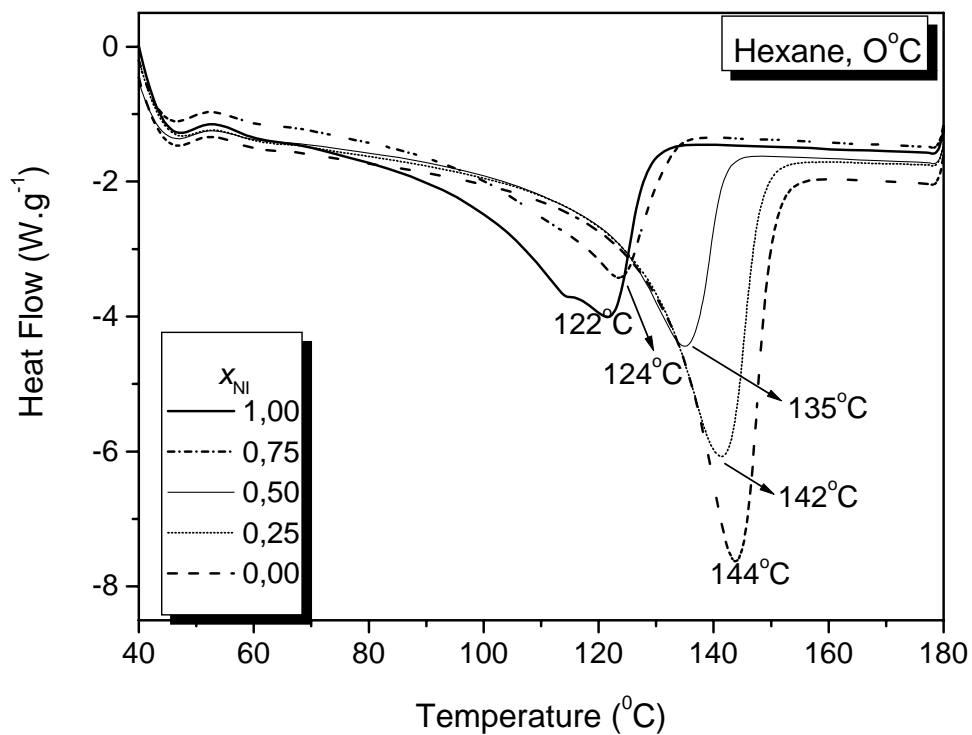


Figure 25. DSC curves of the PE blends produced at 0 °C in Hexane.

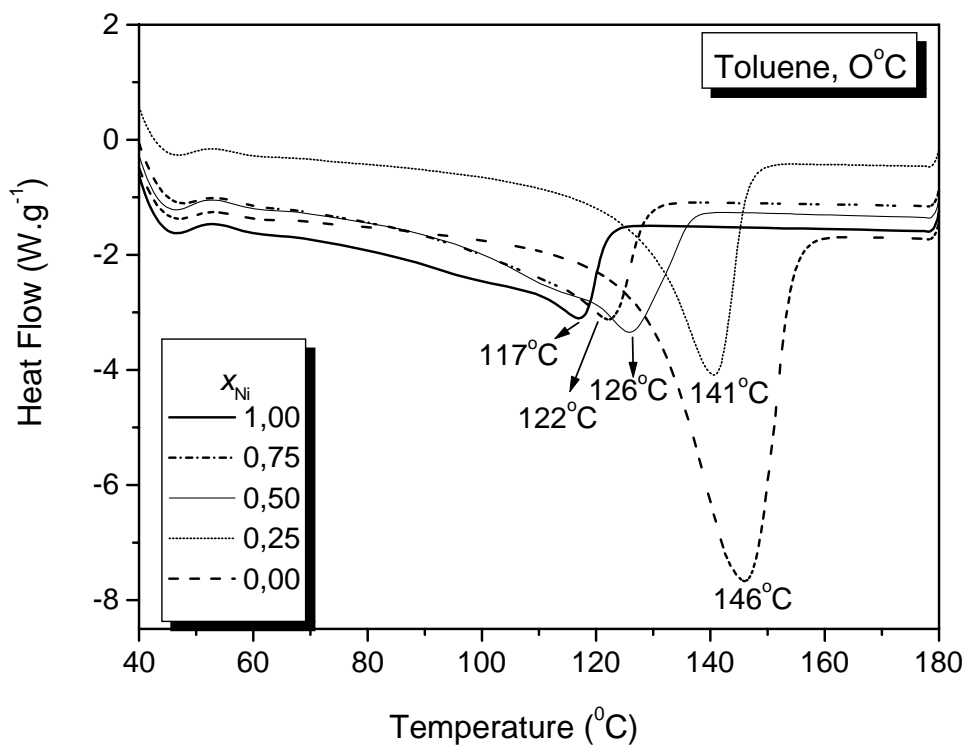


Figure 26. DSC curves of the PE blends produced at 0 °C in Toluene.

At higher polymerization temperatures (30 and 50°C) only a slight decrease of T_m was observed. At these temperatures, the polyethylenes formed by **1** are totally amorphous due to the higher branch content⁶² and apparently they do not interfere in the crystallization process of the high-density polyethylenes due to a higher level of phase segregation. This phenomenon could be better visualized in the polymerization reactions carried out in hexane at 50°C where two polymers (BPE and HDPE) separated spontaneously and thus allowed the analysis of both phases (entries 13 and 14).

Comparing the DSC results of the polymer samples produced in toluene at 0, 30, and 50°C (Figure 27), it was observed that the higher dependence of the T_m values with respect to the x_{Ni} has been noticed for the polyethylene blends produced at 0°C. This dependence decreases as the polymerization temperature increases, indicating that at 0°C the miscibility between the PE phases is more effective. It is worth noting that nickel-[α -diimine] complexes show ability to promote the displacement of the metal along the growing polymer chain so-called chain walking mechanism^{62a,63}. This process determines the number of branches in the polymer backbone and thus the extent of branching in the PE is sensitive to polymerization temperature, decreasing with decreasing polymerization temperature. At 0°C, **1** produces PE with lower degree of branching and thus, its miscibility with the PE produced by **2** is more pronounced.

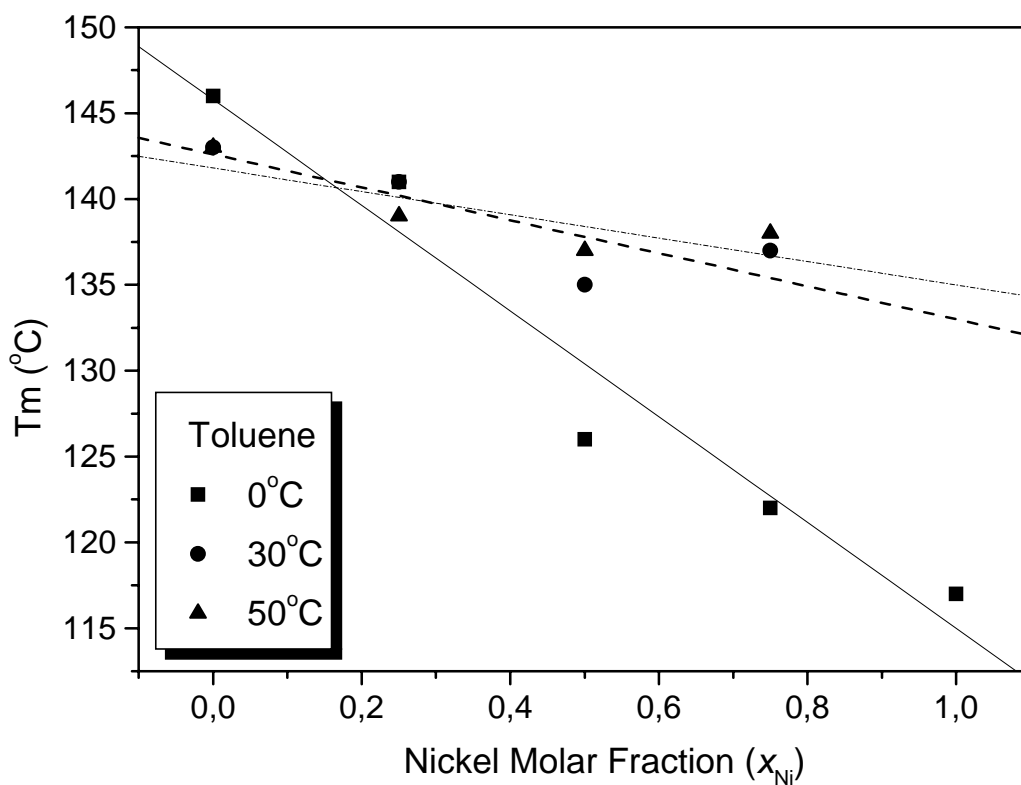
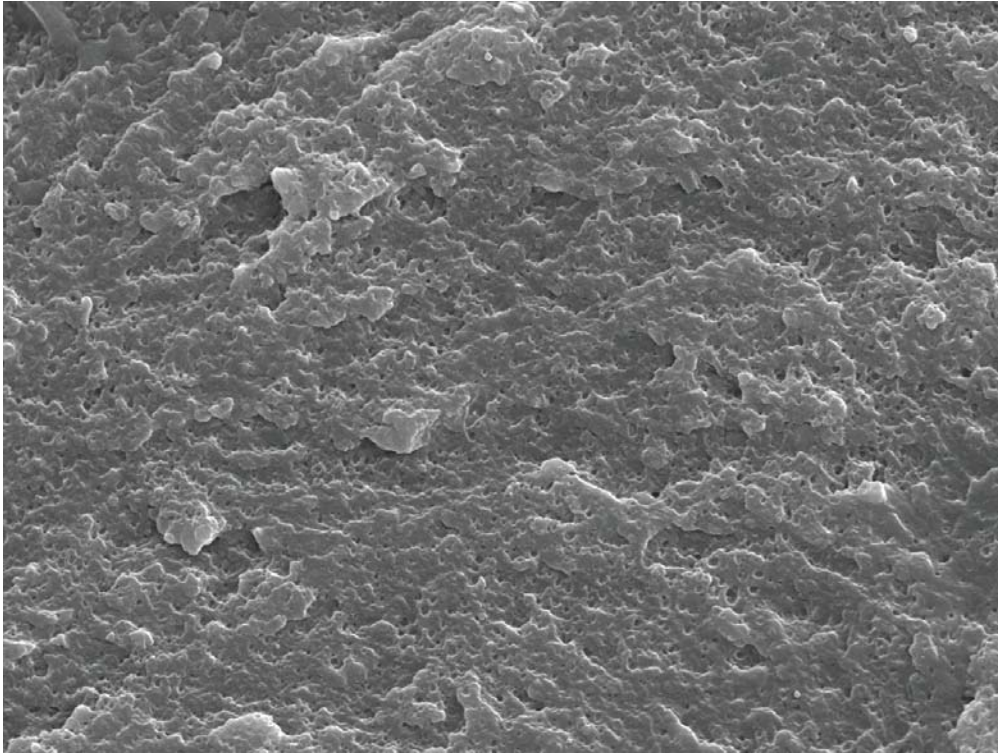


Figure 27. Dependence of melting temperature (T_m) with x_{Ni} for ethylene polymerization in Toluene

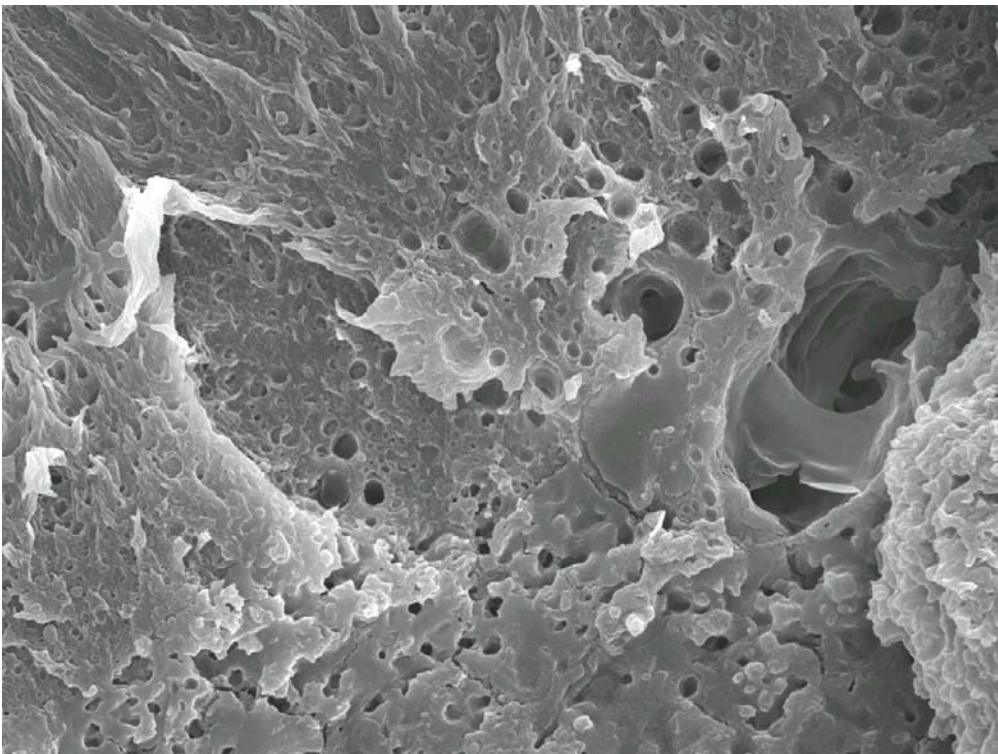
As expected, the polyethylenes produced by **1** showed higher melt flow indexes (MFI) compared to those ones obtained using **2** since catalyst **2** produces ultra-high molecular weight PE.⁶⁰ The MFI data for the polymer blends produced at 0°C indicate the formation of polymer with high molecular weight. These very low MFI values can be associated to the production of high molecular weight polyethylene by **1** at this polymerization temperature^{62b, 16, 17, 19}. In general, at higher polymerization temperatures (30 and 50°C) the MFI values increase as the x_{Ni} increases in the medium being this behavior attributed to the formation of more branched and lower molecular weight polyethylenes produced mainly by **1**.

The morphology of the polymer blends was investigated using scanning electron microscopy (SEM). SEM micrographs made on cryo-fractured surfaces of the polyethylene blend samples produced at 30 and 50°C using $x_{Ni} = 0.25$ are shown in Figures 28 and 29, respectively.

The SEM micrograph of the blend samples produced at 30°C in hexane showed two phase components (Figure 28a) well dispersed. Increasing the polymerization temperature (50°C) resulted in the production of a BPE/HDPE blend which also shows a double morphology; however, in that case, the presence of very small particles of BPE dispersed in the HDPE matrix was observed (Figure 29a). In order to evaluate the distribution of the PE phases in the matrix, cryo-fractured surfaces were etched with hot *o*-xylene and studied by SEM. Figure 28b shows the formation of big holes and defects distributed on HDPE matrix as a consequence of the extraction of the branched PE produced by **1**. The non uniform distribution of these holes and defects on the HDPE surface indicates the high incompatibility degree of these two phases components, considering mainly the large difference between the molecular weight of the PE produced by the precursors (**1** = ultra-high molecular weight PE and **2** = hyperbranched PE). The extraction of the highly branched PE from the PE blend produced at 50°C generated a "sandwich structure" (Figure 29b) similarly found for homogeneous binary catalyst system composed by $NiCl_2(\alpha\text{-diimine})$ and $Tp^{Ms*}TiCl_3$ ¹⁷.

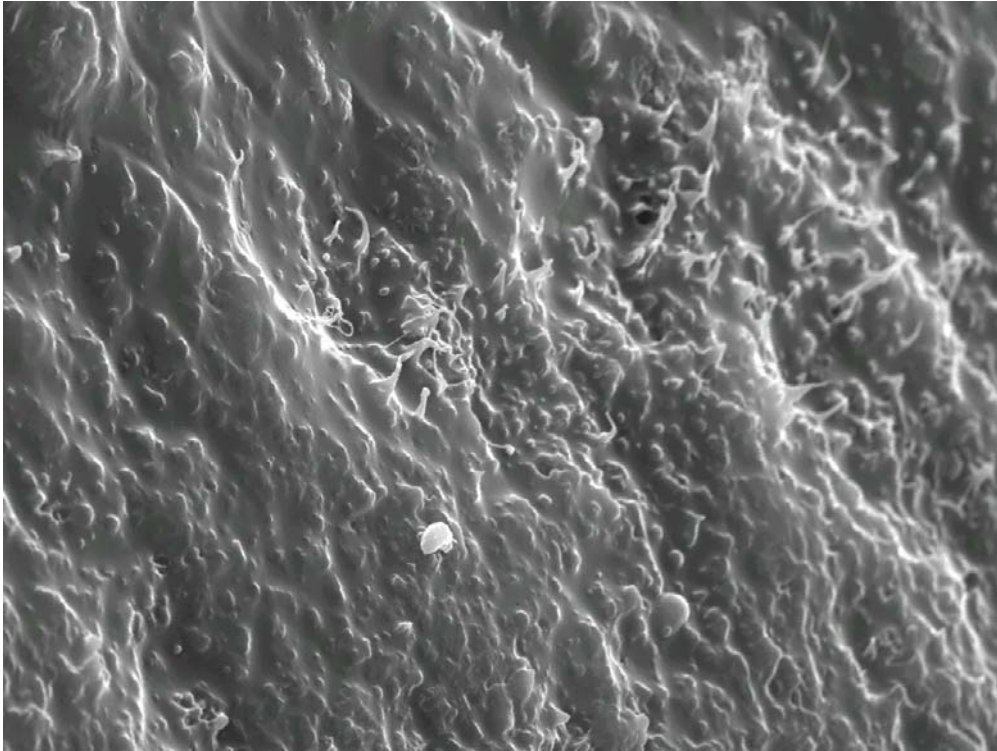


(a)

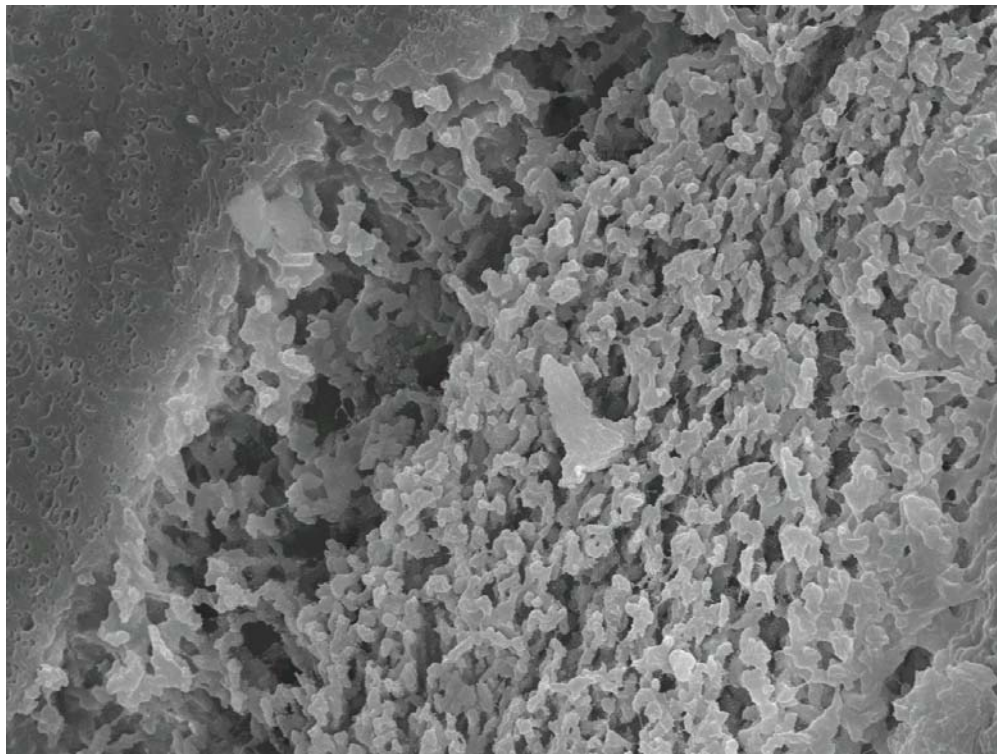


(b)

Figure 28. SEM micrographs of BPE/HDPE blends crio-fractured surfaces produced at 30°C in hexane: (a) $x_{Ni} = 0.25$ (x 2000); (b) $x_{Ni} = 0.25$ (x 2000) after etched with o-xylene.



(a)



(b)

Figure 29. SEM micrographs of BPE/HDPE blends crio-fractured surfaces produced at 50°C in hexane: (a) $x_{Ni} = 0.25$ (x 2000); (b) $x_{Ni} = 0.25$ (x 2000) after etched with o-xylene.

5.2. LINEAR LOW DENSITY POLYETHYLENE (LLDPE) FROM ETHYLENE USING $\text{Tp}^{\text{Ms}}\text{NiCl}$ (Tp^{Ms} = hydridotris(3-mesitylpyrazol-1-yl) AND Cp_2ZrCl_2 AS A TANDEM CATALYST SYSTEM

The ethylene polymerization (or oligomerization) reactions were carried out using $\{\text{Tp}^{\text{Ms}}\}\text{NiCl}$ (**1**) and Cp_2ZrCl_2 (**2**) (Figure 30) in toluene at 0 °C using a mixture of MAO/TMA (1:1) as cocatalyst (Ni precursor is more active in TMA and Zr precursor in MAO). Table 4 shows the results of polymerization runs by varying the nickel loading mole fraction (x_{Ni}).

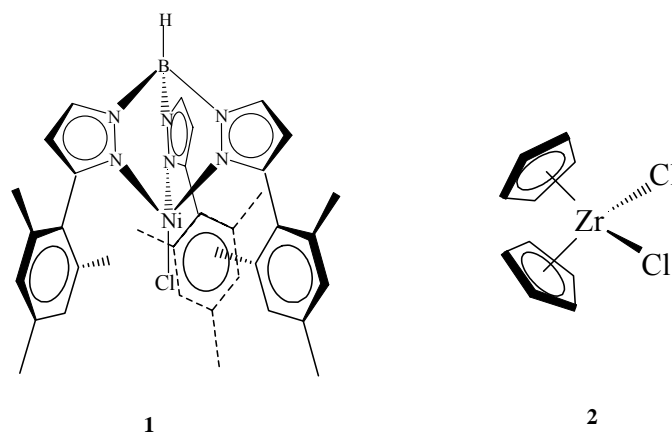


Figure 30. $\{\text{Tp}^{\text{Ms}}\}\text{NiCl}$ (**1**) and Cp_2ZrCl_2 (**2**) complexes used in Tandem process.

Previous studies⁶¹ have demonstrated that **1** shows high selectivity in 1-butene (dimers: 86%; 1-butene: 78%) with turnover frequency of $5.4 \times 10^3 \text{ h}^{-1}$ for ethylene oligomerization reactions performed in toluene at 0 °C in the presence of a mixture of MAO/TMA (1:1). Under identical polymerization conditions **2** showed turnover frequency of $7.9 \times 10^3 \text{ mol}[\text{C}_2\text{H}_4] \cdot \text{mol}[\text{Zr}]^{-1} \cdot \text{h}^{-1}$, and produced linear high density polyethylene.

In order to produce branched polyethylene, we carried out the polymerization of ethylene using the combination of **1** and **2** under identical polymerization conditions studied for the systems employing the catalysts separately. Table 4 shows the data concerning to the

performance of this catalytic system. Polymerization runs carried out varying x_{Ni} showed that the turnover frequencies are strongly dependent on this parameter, varying from 6.6×10^3 to $32.1 \times 10^3 \text{ mol}[\text{C}_2\text{H}_4].\text{mol}[\text{Zr}]^{-1}.\text{h}^{-1}$.

Table 4. Results of ethylene polymerization using a combination of $\{\text{Tp}^{\text{Ms}}\}\text{NiCl}$ (**1**) and Cp_2ZrCl_2 (**2**)^a.

Entry	x_{Ni}^{b}	Yield (g)	TOF ($\times 10^{-3}$) ^c	Tm (°C)	χ (%)	Mw ($\times 10^{-3}$)	Mw/Mn	Branching ^d		
								Ethyl	Butyl	Total
31	0.00	1.10	7.9	138	37	570	2.2	0	0	0
32	0.20	0.74	6.6	132	29	535	5.5	0	0	0
33	0.50	0.70	10.0	121	22	408	4.1	12.5	0	12.5
34	0.80	0.37	13.2	113	17	226	4.5	17.7	2.1	19.8
35	0.90	0.30	21.4	100; 109	20	312	4.3	20.0	2.6	22.6
36	0.98	0.09	32.1	98; 118; 128	7	237	4.2	23.3	3.5	26.8

(a) Polymerization conditions: Glass-reactor (120 ml), $[\text{M}] = 5 \text{ }\mu\text{mols}$, toluene = 60 ml, temperature = 0 °C, polymerization time = 1 h, $[\text{Al}]/[\text{M}] = 200$, $\text{PC}_2\text{H}_4 = 1.1 \text{ atm}$, MAO/TMA (1:1) as activator. (b) Nickel Molar Fraction, $x_{\text{Ni}} = [\text{Ni}]/([\text{Ni}] + [\text{Zr}])$; (c) Turnover Frequency (TOF) in $\text{mol}[\text{C}_2\text{H}_4].\text{mol}[\text{Zr}]^{-1}.\text{h}^{-1}$; (d) Number of branches by 1000 carbon atoms of the backbone.

Figure 31 shows a plausible tandem catalytic mechanism using a combination of **1** and **2**. The mechanism is composed by two complementary catalytic cycles characterized by ethylene dimerization, and the copolymerization process. In the first cycle, we assumed that the active species is a neutral $\text{Tp}^{\text{Ms}}\text{NiH}$ complex that promotes the production of 1-butene via β -hydrogen elimination in a similar way described by the nickel oligomerization catalysts¹⁹. Once the 1-alkene has been generated the copolymerization reaction takes place by insertion of 1-butene into the growing polyethylene chain (P) at the $\text{Cp}_2\text{Zr}(\text{P})^+$ catalytic species.

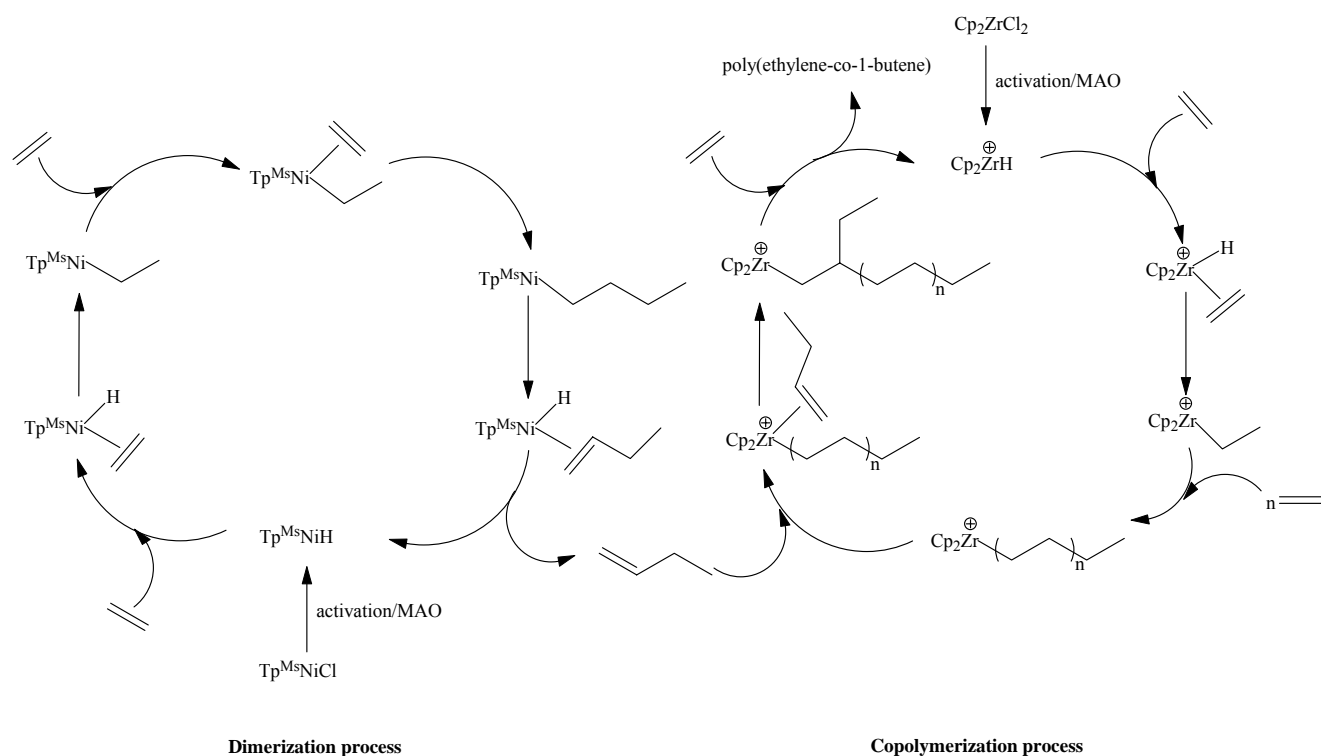


Figure 31. Plausible tandem catalytic mechanism to produce copolymer from ethylene using a combination of **1** and **2**.

5.2.1. The influence of x_{Ni} and temperature on copolymer properties

The influence of x_{Ni} and temperature on copolymer properties have been evaluated by means of differential scanning calorimetry, gel permeation chromatography and ^{13}C NMR spectroscopy. The results are summarized in Table 4.

The GPC results show that the molecular weight (Mw) of the polymers is dependent on x_{Ni} . In all cases the GPC curves displayed monomodal molecular weight distributions with polydispersities varying from 2.2 to 5.5. The homopolymer made by **2** showed molecular weight of $570 \times 10^3 \text{ g.mol}^{-1}$. On the other hand, as the x_{Ni} increases in the medium, the Mw is reduced gradually reaching a lowest value for $x_{Ni} = 0.80$ (entry 34, $226 \times 10^3 \text{ g.mol}^{-1}$). Furthermore, no significant changes on Mw were observed for higher nickel mole fraction ($x_{Ni} \geq 0.90$) as can be seen comparing entries 35–36.

The polyethylene produced using exclusively **2** showed melting temperature (T_m) of 138 °C and crystallinity of 37%. Conversely, the use of x_{Ni} as high as 0.98 (entry 36) produced copolymer with T_m of 98 °C. It should be pointed out that the presence of x_{Ni} up to 0.20 yielded copolymers with broad melting transitions, suggesting the formation of copolymers with different fractions of comonomer/short chain branches (Figure 32). In the specific case of $x_{Ni} = 0.98$, the formation of copolymer with three melting peaks was observed.

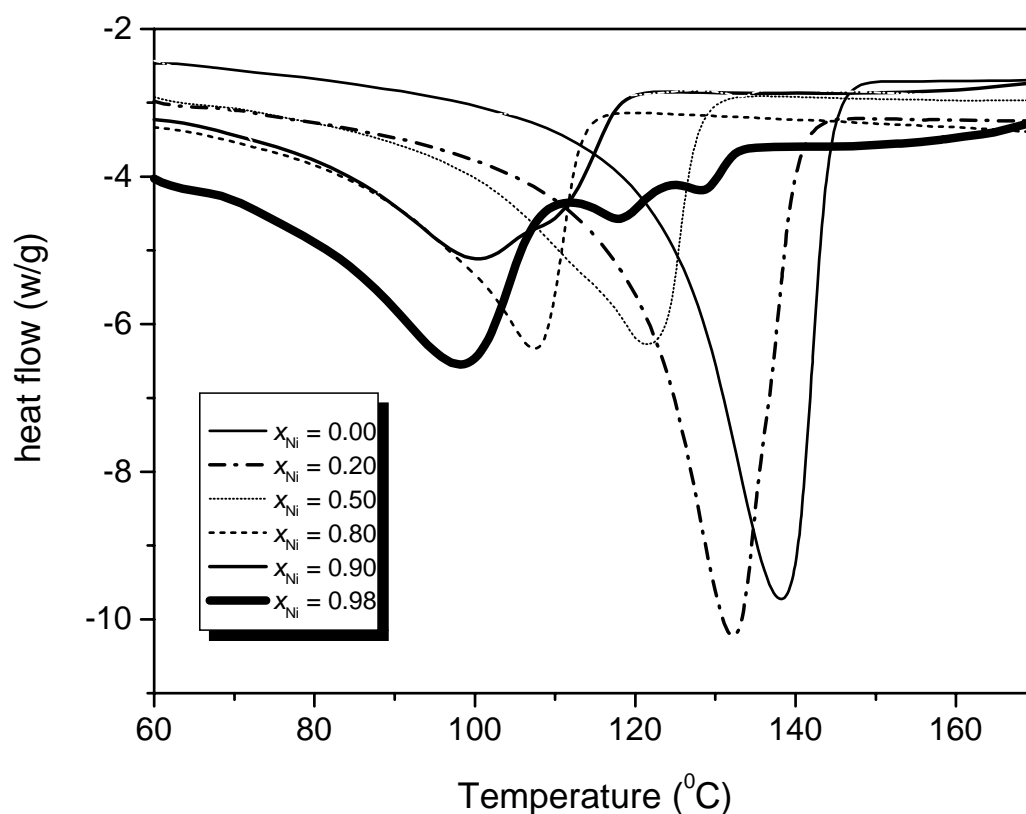


Figure 32. DSC curves of the polymers varying x_{Ni} ; Polymerization reactions performed at 0 °C, $[Al]/[M] = 200$, and using a mixture MAO/TMA (1:1) as activator.

The melting temperatures of the copolymers, obtained with increasing the nickel content, decrease almost linearly as the 1-butene and 1-hexene incorporation increases (Figure

33). It is well known that, due to short chain branches, copolymers have a lower T_m than the ethylene homopolymer⁶⁴. When the amount of short chain branches increases, the melting point decreases due to the decrease of CH_2 crystallizable segments. Crystallization of such a polymer is determined to a major extent, if not completely, by the comonomer distribution along and among the chains.

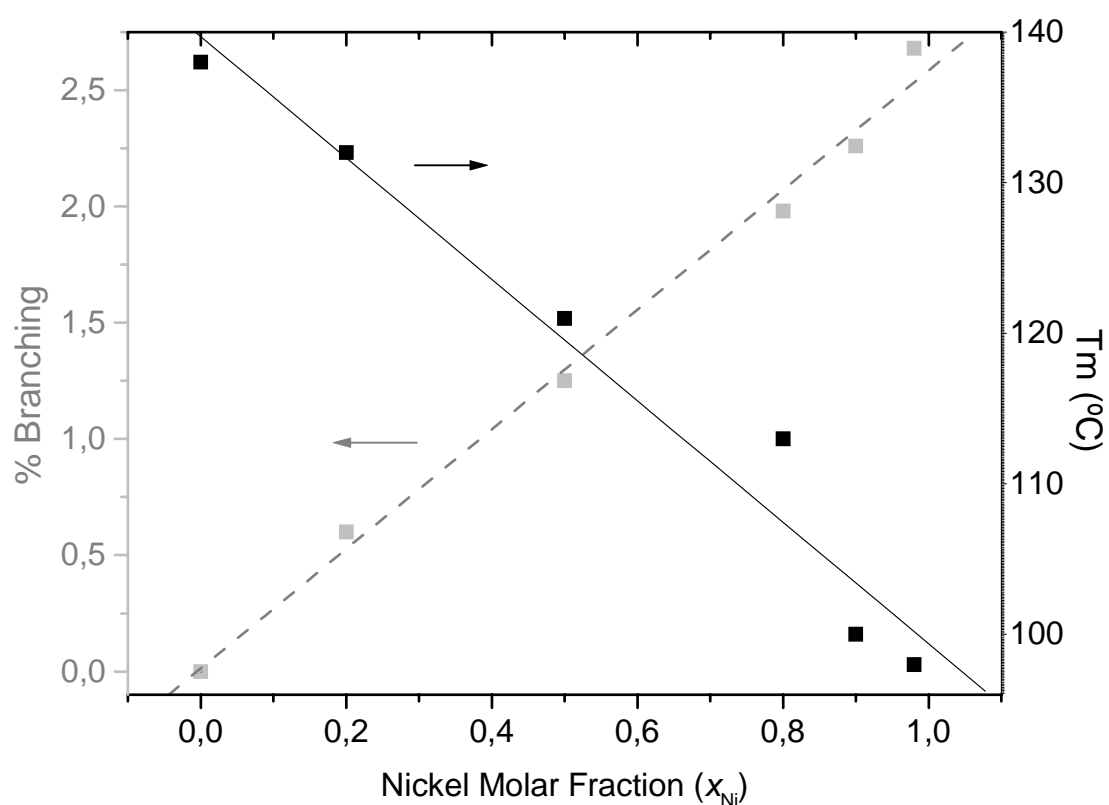


Figure 33. Melting point and branching content as a function of x_{Ni} of the copolymers; Polymerization reactions performed at 0 °C, $[\text{Al}]/[\text{M}] = 200$, and using a mixture MAO/TMA (1:1) as activator.

The ^{13}C NMR spectra of the copolymers (Figure 34) show the presence of branches due to the 1-butene and 1-hexene incorporation in the polymer chain⁶⁵. In these samples, it was observed one peak at 30.0 ppm, which is characteristic for the linear chain $(\text{CH}_2)_n$ and

peaks at 11.1, 26.5, 30.5, 33.8, and 39.4 ppm, attributed to the presence of ethyl branches, besides the incidence of much smaller signals corresponding to the butyl branches. The simplicity of polymer structure allows for the percentage of ethyl and butyl branches in the polymer to be determined and as shown in Figure 34, the percent of 1-butene/1-hexene in the polymer correlates well against the x_{Ni} . For instance, the number of branches per thousand backbone carbon atoms increases from 12.5 to 26.8 as the nickel mole fraction increases from 0.50 to 0.98.

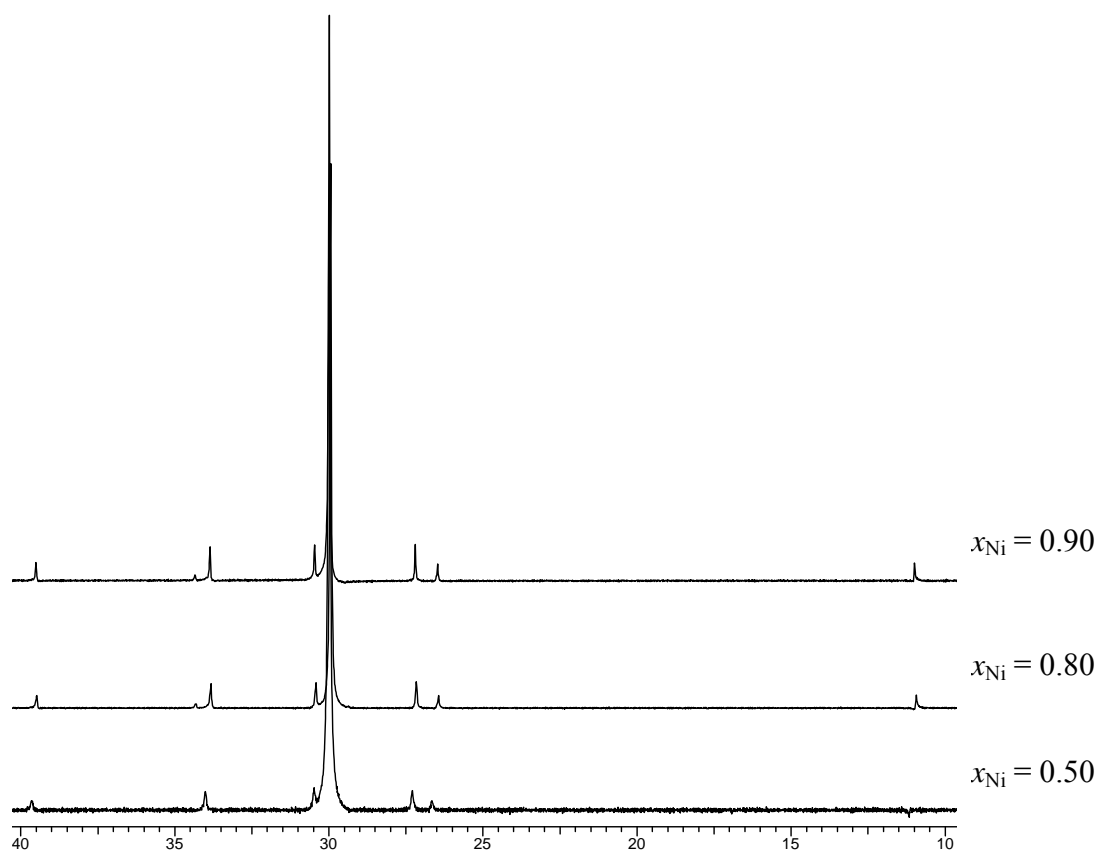


Figure 34. ^{13}C NMR spectra of copolymers obtained varying x_{Ni} .

5.3. SYNTHESIS AND CHARACTERIZATION OF $M(\text{allyl})_2\text{Cl}(\text{MgCl}_2)_2\cdot(\text{THF})_4$ ($M = \text{Nd, Y and La}$) AND THEIR USE IN ISOPRENE POLYMERIZATION

This part was developed in a co-tutele project supported by the CAPES/COFECUB program, in the laboratories of the Rennes University under orientation of Prof. Jean-François Carpentier.

5.3.1. $M(\text{allyl})_2\text{Cl}(\text{MgCl}_2)_2\cdot(\text{THF})_4$ ($M= \text{Nd, Y and La}$) complexes characterization by ^1H and ^{13}C NMR spectroscopy and elementary analysis.

The elemental analyses of $M(\text{allyl})_2\text{Cl}(\text{MgCl}_2)_2\cdot(\text{THF})_4$ ($M= \text{Nd, Y and La}$) complexes are in agreement with the formula $\text{MC}_{22}\text{H}_{42}\text{O}_4\text{Cl}_5\text{Mg}_2$. The complexes structures (see in Figure 35) are assumed as similar of literature result.⁵²

The ^1H NMR spectrum in C_6D_6 of the lanthanum complex (Figure 35) displays two sets of signals for the hydrogens of η^3 -allyl groups (Allyl_1 and Allyl_2) coordinated at metal center, the 1H centrals hydrogen's (6.53 and 5.68 ppm, respectively), the 2H terminals (4.93 ppm and 4.16 ppm, respectively) and (3.13 ppm and 2.00 ppm, respectively). The four THF molecules showed 2 different signals at 3.80 ppm (16H) and 1.39 ppm (16H).

The ^1H NMR spectrum using THF- d_8 (Figure 36) show the signals of 4THF groups coordinated in complex at 1.77 and 3.61 ppm different of solvent (3.58 and 1.73 ppm)

For the Yttrium complex (Figure 37), the ^1H NMR spectrum features two η^3 -allyl groups (Allyl_1 and Allyl_2) of centrals hydrogen's (6.80 and 5.75 ppm, respectively), the 2H terminals (5.05 ppm and 4.25 ppm, respectively) and (2.05 ppm and 1.60 ppm, respectively). The THF molecules showed 2 different signals correspondent of 4H in 3.85 ppm (16H) and 1.30 ppm (16H), respectively. The compounds are extremely air and moisture sensitive.

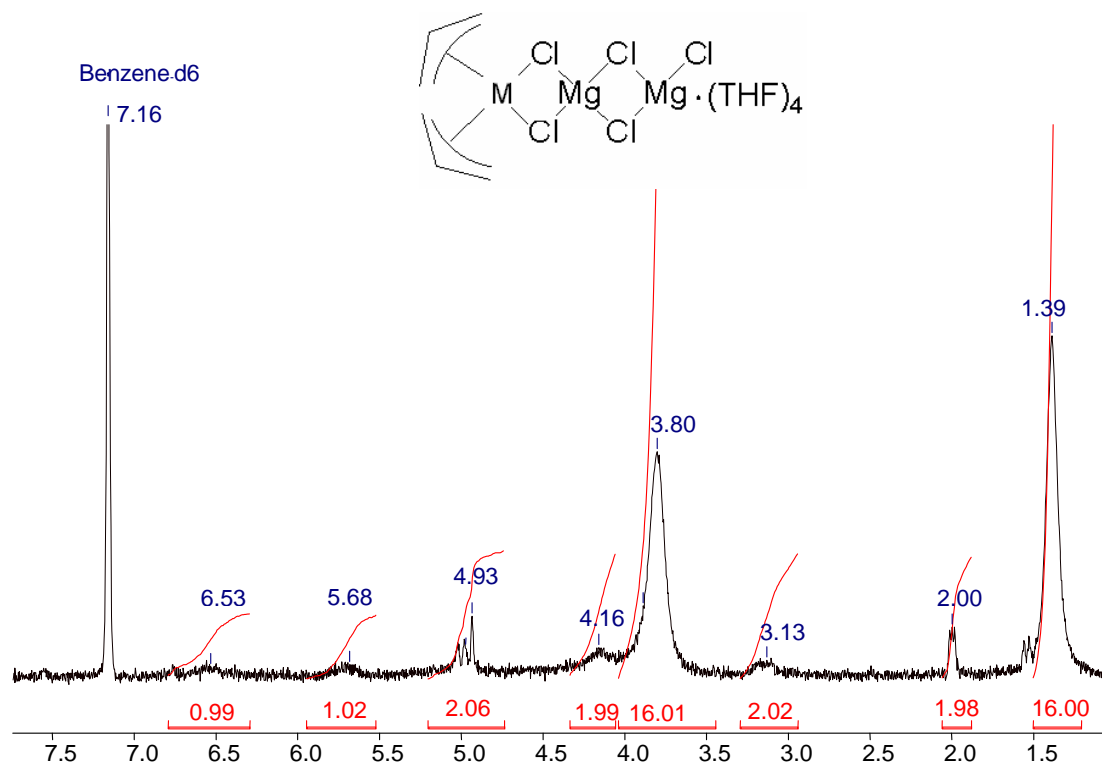


Figure 35. ^1H NMR spectrum (C_6D_6) of $\text{La}(\text{allyl})_2\text{Cl}(\text{MgCl}_2)_2(\text{THF})_4$ catalyst.

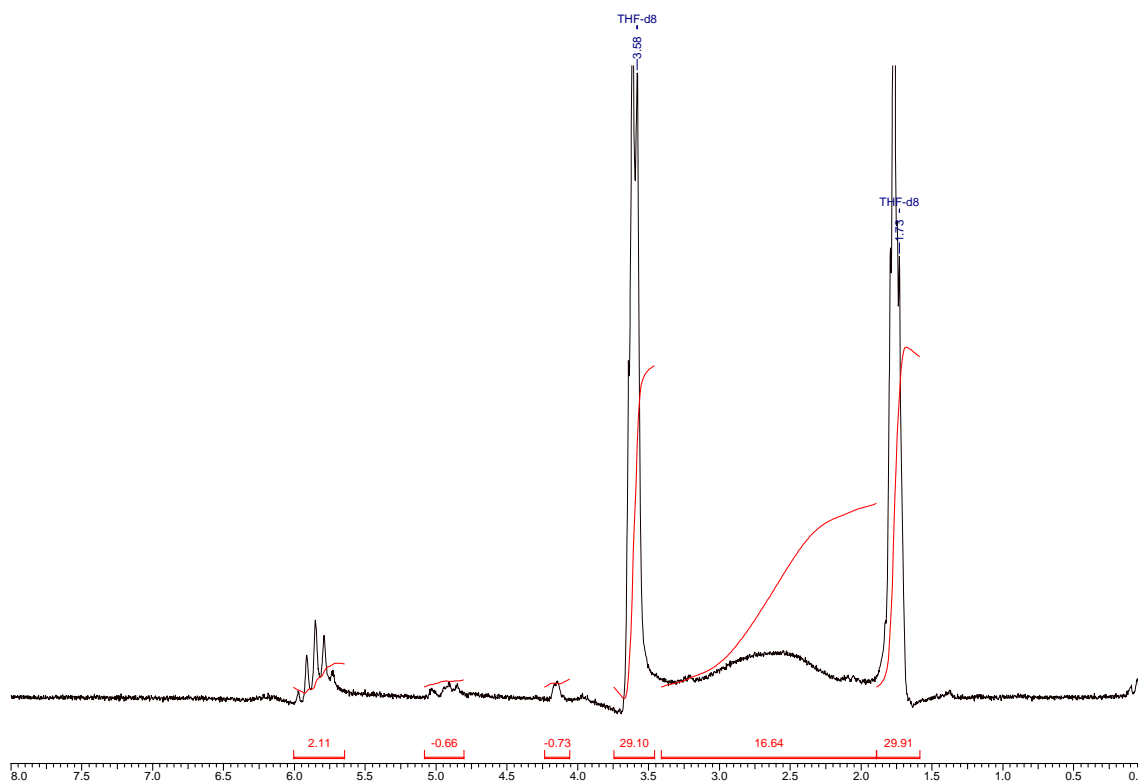


Figure 36. ^1H NMR spectrum (THF-d_8) of $\text{La}(\text{allyl})_2\text{Cl}(\text{MgCl}_2)_2(\text{THF})_4$ catalyst.

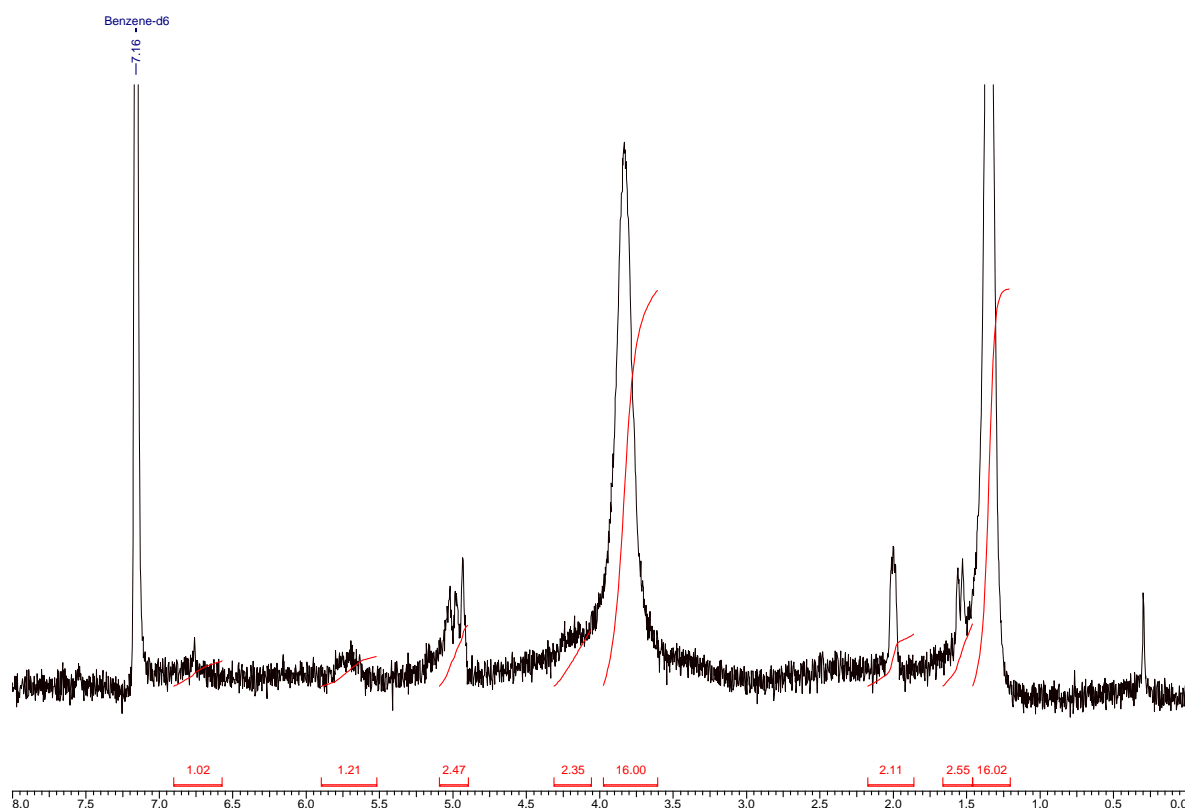


Figure 37. ^1H NMR spectrum (C_6D_6) of $\text{Y}(\text{allyl})_2\text{Cl}(\text{MgCl}_2)_2(\text{THF})_4$ catalyst.

5.3.2. Isoprene polymerization using Lanthanide systems composed by $\text{Nd}(\text{allyl})_2\text{Cl}(\text{MgCl}_2)_2(\text{THF})_4$ / MAO and the effect of polymerization parameters in polyisoprene properties.

Previous studies⁶⁶ showed the synthesis and the application of $\text{Nd}(\text{allyl})_2\text{Cl}(\text{MgCl}_2)_2(\text{THF})_4/\text{MAO}$ as efficient catalysts for isoprene polymerization with high yields (up 90%). In this work, different activation times (time of contact of the Nd precursor and the MAO cocatalyst) and amounts of MAO as cocatalyst were evaluated. The system with an activation time of 10 min showed good properties control, i.e. good agreement of molecular weight theoretical and experimental. Activation times $\geq 60\text{min}$ did not afford good control of properties probably because the active species decompose over this time. The effect of the Al:Nd ratio (Al:Nd = 5-200) showed that the best results are obtained with small

amounts of MAO. A ratio Al:Nd = 5 is insufficient for formation of the active species. High PI yield was obtained by reducing the amount of MAO (Al:Nd = 30). As determined by ^1H NMR, the polyisoprene produced by Nd complex/MAO has a high content of *cis*-1,4 form (96%) at 20 °C using the ratios Al:Nd = 30 and 60. Reduction of the *cis*-selectivity was observed for ratios Al:Nd >200. The GPC results showed molecular weight in order of 65 to 118×10^3 with narrow and monomodal molecular weight distribution (1.38 at 1.73). Based in multiple runs, the activation time of 10 min using Al:Nd = 30 is the best condition for a good polymerization control and results reproduction, although there is a small decrease of the *cis*-selectivity when compared with the reactions using activation time of 60 min. (the 1,4-*cis* content is 99 % (activation time = 60 min) and 96 % (activation time = 10 min)). Based on this preliminary work, it became necessary to investigate thoroughly the effect of different parameters in isoprene polymerization and their consequence on polyisoprene properties.

Isoprene polymerization mediated by the $\text{Nd}(\text{allyl})_2\text{Cl}(\text{MgCl}_2)_2 \cdot (\text{THF})_4$ complex using methylaluminoxane (MAO) was carried out under different reaction conditions. Table 5 shows the effect of different polymerization times (0.25 to 60 min), temperatures (-20 to 60 °C) and amounts of MAO (Al/Nd = 1180 at 7000) on isoprene polymerization. The influence of experimental parameters was evaluated by ^1H NMR spectroscopy and gel permeation chromatography (GPC).

Table 5. Results of Isoprene polymerizations^a using Nd(allyl)₂Cl(MgCl₂)₂·(THF)₄/ MAO

entry	time (min)	T (°C)	IP/Nd	Yeld (%)	Mn (.10 ⁻³) (theo.) ^b	Mn (.10 ⁻³) (exp.) ^c	Mw / Mn
37	0.25	20	1180	9	7.5	26.5	2.39
38	0.5	20	1180	14	11.7	31.1	2.27
39	1	20	1180	68	57.0	65.0	1.90
40	2	20	1180	79	66.0	80.0	1.54
41	5	20	1180	99	83.0	90.5	1.51
42	60	-20	1180	34	27.3	52.8	2.41
43	60	0	1180	84	67.4	96.0	1.63
44	60	20	1180	99	83.0	86.0	1.51
45	60	40	1180	94	75.4	63.5	1.83
46	60	60	1180	85	68.2	87.1	2.72
47	60	20	2350	94	150.2	152.7	1.55
48	60	20	4700	96	306.8	262.6	1.61
49	60	20	7000	56	466.5	210.0	1.70

(a) Polymerization conditions: [Nd]= 17,0 μmols; solvents: toluene and hexane (5:3 mL); Al/Nd = 30 (MAO solution, 30% in toluene); Activation time = 10 min; (b): Theoretical molecular weight = Yeld x Ip/Nd x molar mass of Isoprene; (c): Determined by GPC in THF calibrated vs. PSt standards

The reactions performed with the Nd complex employing different polymerizations times (entries 37-41 and 44) showed that the yields and molecular weights of the polymers are affected by the reaction time, i.e. the yields increase with the polymerization time. For the polymerization reaction accomplished in 0.25 min (entry 37), a low yield was observed (9%), but the yield reached 68% only after 1min of polymerization (entry 39) and the isoprene is 99% converted after 5 min of reaction (entry 41). As a consequence, polymerization times longer than 5 min do not bring significant changes in the yield as it can be seen comparing the result obtained at 60 min of reaction (99%, entry 44). The variation of the yield in function of the polymerization time can be seen in the figure 38.

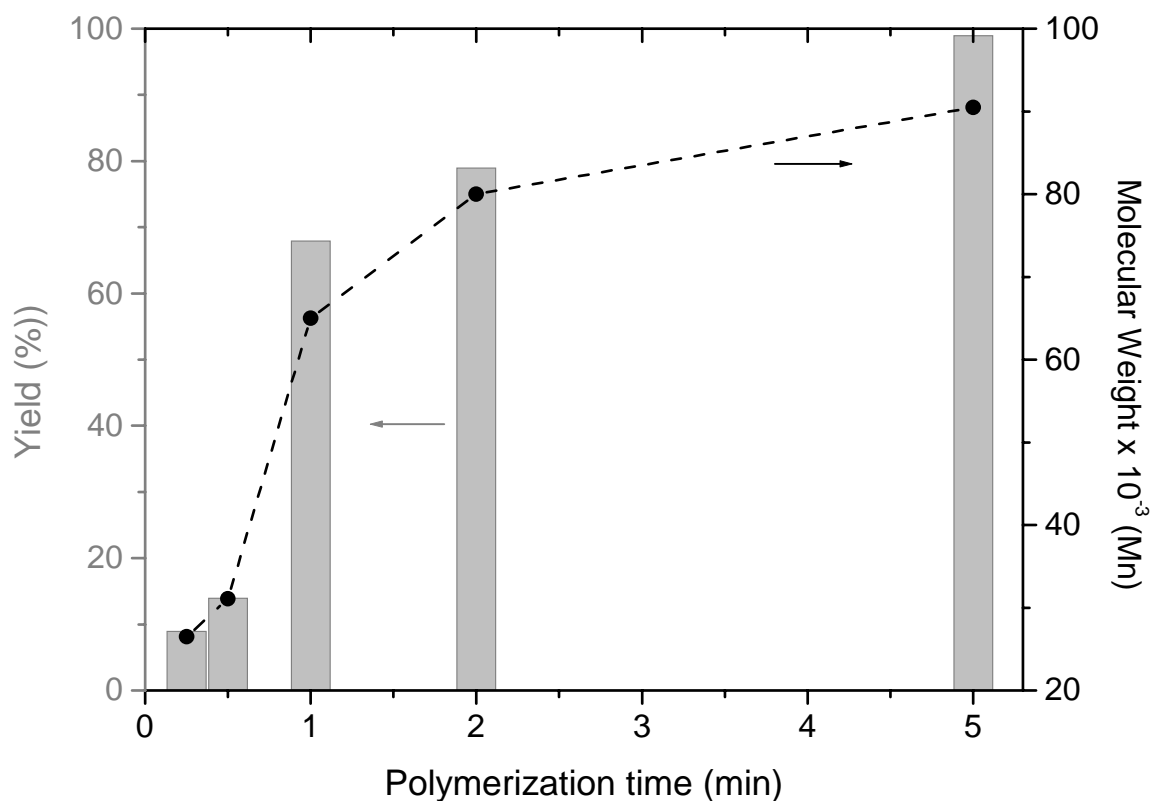


Figure 38. Influence of polymerization time in the Yield and molecular weight (Mn) on isoprene polymerization using $\text{Nd}(\text{allyl})_2\text{Cl}(\text{MgCl}_2)_2 \cdot (\text{THF})_4 / \text{MAO}$.

Analyzed by GPC (Figure 39), the molecular weight of the polyisoprene increase with the polymerization time. It is important to note that the molecular weight increases 3.0 fold (varying from 26,5 to 80,0 $\times 10^3 \text{ g}\cdot\text{mol}^{-1}$) when the polymerization time increases of 0.25 to 2 min (entries 37 and 40). On the other hand, the differences among the Mn experimental and theoretical are larger at polymerizations times lower than 1min, indicating slow propagation of the chains in the beginning of the polymerization. Reactions times higher than 2 min do not have significant effect on the molecular weight.

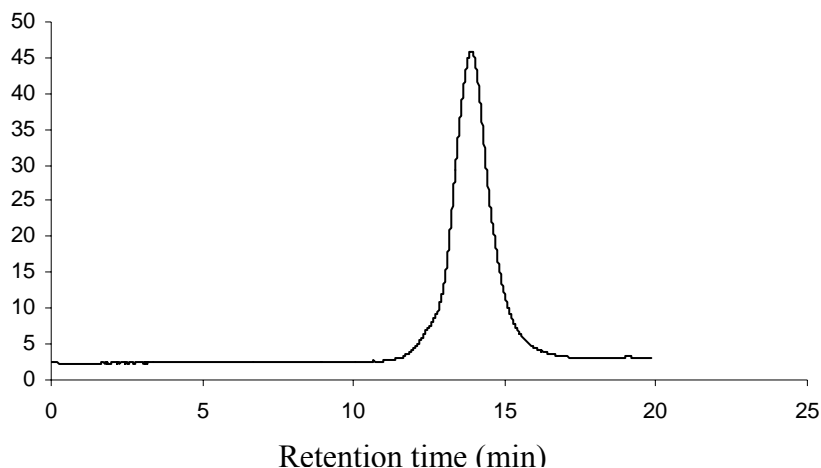


Figure 39. Typical GPC chromatogram (THF, 25 °C) of PI produced by $\text{Nd}(\text{allyl})_2\text{Cl}(\text{MgCl}_2)_2(\text{THF})_4/\text{MAO}$.

The performance of the $\text{Nd}(\text{allyl})_2\text{Cl}(\text{MgCl}_2)_2(\text{THF})_4/\text{MAO}$ system at different polymerization temperatures, in the range 0-60°C (entries 43-46) showed high yields (84-94%). In these cases, the system is relatively well controlled because the molecular weights present a good agreement between the theoretical and the experimental values, varying of 63,5 to 87,1 x 10³ g.mol⁻¹. However, for the reaction performed at -20°C (entry 42), low yield (34%) is observed and molecular weight experimental lower than theoretical values. In this case, the low polymerization temperature reduce the propagation of the chains.

The influence of the isoprene-to-catalyst ratio in the yield and polyisoprene properties showed high yields in the reactions with molar ratio IP/Nd between 1180 and 4700 (entries 44, 47 and 48). The experimental molecular weight presents a good agreement with the theoretical values (between 86.6 and 262.6 x 10³ g.mol⁻¹). On the other hand, high concentrations of Isoprene (ratio IP/Nd = 7000) result in a decrease of the yield (56%) and a difference between the theoretical and experimental molecular weight in ≈ 2 fold, indicating that the molecular weights present a limited growth, not surpassing 262 x 10³ g.mol⁻¹, probably attributed to increase of chain transfer reactions by factors as the increase of the

viscosity of the system and/or the sensibility of Nd species with high amounts of isoprene. Figure 40 show a non lineal relationship between the molecular weight and the ratio IP/Nd, presenting a maximum of molecular weight in IP/Nd = 4700.

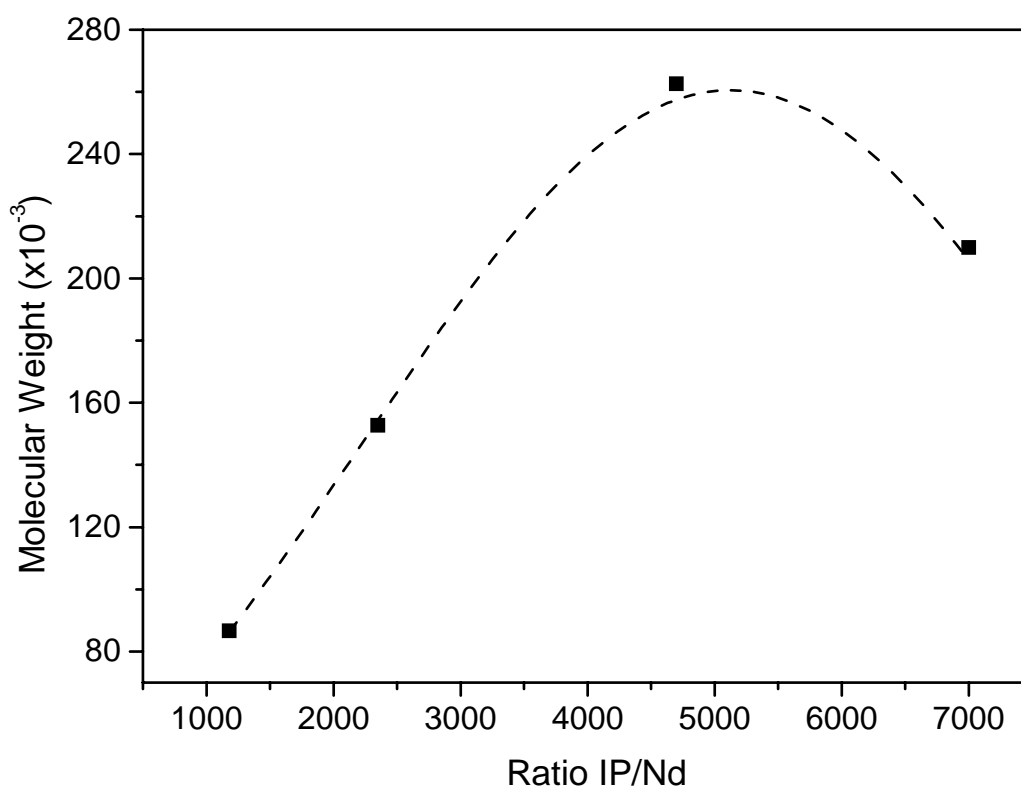


Figure 40. Influence of Ratio Ip/Nd on the molecular weight (Mn) in isoprene polymerization using $\text{Nd}(\text{allyl})_2\text{Cl}(\text{MgCl}_2)_2 \cdot (\text{THF})_4 / \text{MAO}$.

The GPC results (similar of Figure 39) of $\text{Nd}(\text{allyl})_2\text{Cl}(\text{MgCl}_2)_2 \cdot (\text{THF})_4 / \text{MAO}$ system showed PI with monomodal and narrow molecular weight distribution ($M_w/M_n = 1.51$ at 1.72), characteristic of single site catalysts.

The ^1H NMR analysis of the polyisoprene microstructure (Figure 41) using the system $\text{Nd}(\text{allyl})_2\text{Cl}(\text{MgCl}_2)_2(\text{THF})_4 / \text{MAO}$ indicates a quite high selectivity for *cis*-1,4 (up 96%), as shown by the presence of an intense signal at 1.67 ppm and small contributions of *trans*-1,4-PI (at 1.59 ppm) referring of 3 hydrogen of C_5 . Very small contributions were observed by 3,4-PI form (at 4.70 ppm).

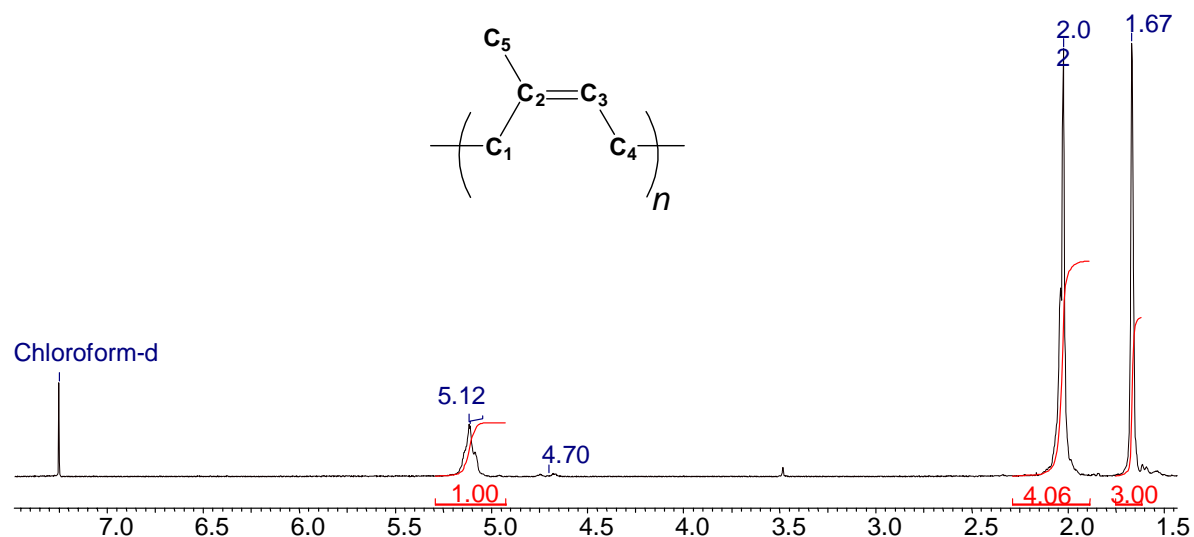


Figure 41. Typical ^1H NMR spectrum (CDCl_3) of polyisoprene produced by $\text{Nd}(\text{allyl})_2\text{Cl}(\text{MgCl}_2)_2(\text{THF})_4/\text{MAO}$; Indications of hidrogens of *cis*-1,4-form (1,67ppm), *trans*-1,4-form (1.57ppm) and 3,4-form (4.70 ppm).

The ^{13}C NMR analysis of the polyisoprene microstructure using the system Nd / MAO shows *cis*-1,4- structure composed by signals of C₂ (135.2 ppm), C₃ (125.0 ppm), C₁ (32.19 ppm), C₅ (26.37 ppm) and C₄ (23.42 pm) in Figure 42.

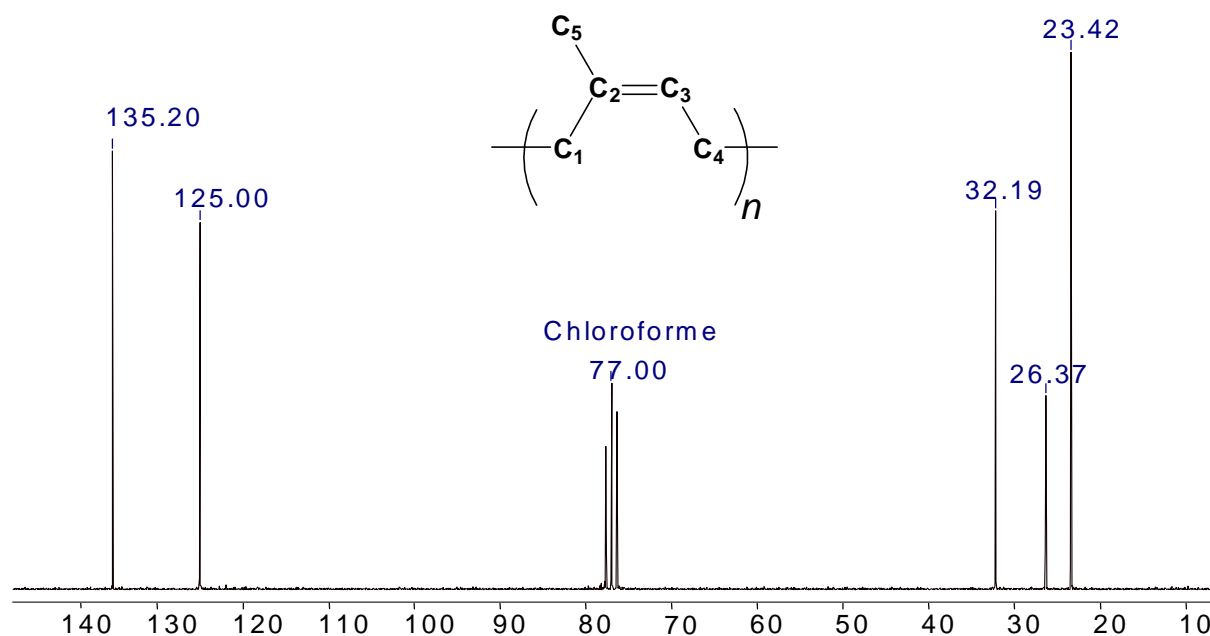


Figure 42. Typical ^{13}C NMR spectrum (CDCl_3) of PI produced by $\text{Nd}(\text{allyl})_2\text{Cl}(\text{MgCl}_2)_2(\text{THF})_4/\text{MAO}$; Indications of C₂ (135.2 ppm), C₃ (125.0 ppm), C₁ (32.19 ppm), C₅ (26.37 ppm) and C₄ (23.42 pm).

5.3.3. Influence of cocatalyst using group 3 metals complexes $\text{M}(\text{allyl})_2\text{Cl}(\text{MgCl}_2)_2(\text{THF})_4$ (M = Nd, Y and La) in isoprene polymerization and their effect on polyisoprene properties.

Isoprene polymerizations were carried with group 3 metal complexes $\text{M}(\text{allyl})_2\text{Cl}(\text{MgCl}_2)_2(\text{THF})_4$ (M = Nd, Y and La) using different cocatalysts systems (MAO, Dry-MAO, TMA, TEA and TiBA). Table 6 shows the effect of these different cocatalysts in isoprene polymerization reactions.

Table 6. Results of Isoprene polymerizations^a using $M(\text{allyl})_2\text{Cl}(\text{MgCl}_2)_2(\text{THF})_4$ complexes with different alkylaluminum cocatalysts.

Entry	M ^a	Cocat	Yield (%)	Mn (x10 ⁻³) (theo) ^b	Mn (x10 ⁻³) (exp.) ^c	Mw/Mn	1,4-Cis ^d (%)	1,4-Trans ^d (%)	3,4 (%)	Tm ^e (°C)	χ ^e (%)
44	Nd	MAO	88	70.6	67.3	1.58	96	2	2	- ^f	- ^f
45	Nd	Dry MAO	90	72.2	56.3	1.55	96	2	2	- ^f	- ^f
46	Nd	TMA	45	36.1	36.4	4.09	84	14	2	nd ^g	nd
47	Nd	TEA	37	29.7	29.9	3.40	80	17	3	nd	nd
48	Nd	TIBA	75	60.2	32.1	6.24	84	12	4	nd	nd
49	Y	MAO	54	43.3	33.4	6.55	75	23	2	51	12
50	Y	Dry MAO	22	17.7	30.3	6.31	65	35	0	52	11
51	Y	TMA	8	6.4	10.1	5.89	33	64	3	51	20
52	Y	TEA	58	46.5	11.6	8.59	8	91	1	51	39
53	Y	TIBA	57	45.7	12.4	6.71	9	90	1	52	48
54	La	MAO	46	36.9	46.2	2.22	70	30	1	nd	nd
55	La	Dry MAO	63	50.6	49.6	2.45	91	7	2	- ^f	- ^f
56	La	TMA	28	22.5	20.7	5.19	86	13	1	nd	nd
57	La	TEA	38	30.5	24.5	3.17	81	18	2	nd	nd
58	La	TIBA	44	35.3	21.2	8.82	92	7	1	nd	nd

(a) Conditions : [Ln]= 17,0 μmols; solvents: toluene and hexane (5:3 mL); Activation time= 10 min; Polymerization temperature= 20 °C; Al/Ln=30; IP/Ln= 1180; M = group 3 metal catalysts: Nd = Nd (Allyl)₂Cl (MgCl₂)₂.(THF)₄; Y = Y (Allyl)₂Cl (MgCl₂)₂.(THF)₄; La = La (Allyl)₂Cl (MgCl₂)₂.(THF)₄; (b): Theoretical molecular weight = Yield x Ip/Nd x molar mass of Isoprene; (c) Determined by GPC in THF at 20°C (Nd and La catalysts); For the PI produced by Y catalyst (insoluble in THF), in 1,2,4-trichlorobenzene at 140 °C (d): determined by NMR ¹H; (e): determined by DSC, χ = Crystallinity (f) Amorphous PI (g) nd = not determined.

The results show that the yields and polymer properties are affected by the nature of the cocatalyst and metal type. The three complexes $M(\text{allyl})_2\text{Cl}(\text{MgCl}_2)_2(\text{THF})_4$ (M = Nd, Y and La) were active with all the aluminum cocatalysts studied (MAO, Dry-MAO, TMA, TEA and TiBA).

In the polymerization reactions promoted by $\text{Nd}(\text{allyl})_2\text{Cl}(\text{MgCl}_2)_2(\text{THF})_4$ (entries 44-48), high activities were obtained when MAO was utilized (88-99%). In this case, the presence of dry-MAO doesn't induce significant changes in the yields as well as polymer properties. Low yields were observed when TMA and TEA were used (37 and 45%, respectively, entries 46-47). The GPC analysis of polymers showed high molecular weights using MAO (entries 44 and 45) and narrow molecular weight distribution, between 1.55 and 1.58. In addition, MAO determines a good agreement among the theoretical and experimental molecular weight values. The use of TiBA (entry 48) generates polyisoprene with low molecular weight ($32.1 \times 10^3 \text{ g}\cdot\text{mol}^{-1}$), broad molecular weight distribution ($M_w/M_n = 6.24$) and the experimental molecular weight smaller than the theoretical. In this context, the reactions using TiBA did not allow a good control of the polymer properties. On the other hand, although the polyisoprene produced using TMA and TEA (entries 46 and 47) present low molecular weights (36.1 and $29.7 \times 10^3 \text{ g}\cdot\text{mol}^{-1}$, respectively), there is a good agreement with the theoretical values. However, broad MwDs are observed ($M_w/M_n = 3,40$ for TEA and $4,09$ for TMA). The analyses of the polymeric materials using ^1H NMR shows influence of the cocatalyst type on the microstructure of the polyisoprene produced by Nd catalyst, with high content of *cis*-1,4-polyisoprene formation (96%) in MAO solution. For the other activators (TMA, TEA and TiBA), an increase of the *trans*-1,4 content was observed (12 at 17%).

In the results of reactions using $\text{La}(\text{allyl})_2\text{Cl}(\text{MgCl}_2)_2(\text{THF})_4$ complex (entries 54-58), the substitution of MAO by dry-MAO (entries 49 and 50) increased the yield (46 to 63%, respectively) and the amount of *cis*-1,4 polyisoprene in the microstructure (70 for 91%), attributed by absence of TMA in dry-MAO. The molecular weight and the MwD were not significant affected. Other aluminum cocatalysts (TMA, TEA and TiBA, entries 56-58) provide lower yields (38-44%) and lower molecular weights (22.5 at $35.3 \times 10^3 \text{ g}\cdot\text{mol}^{-1}$).

Although there is proximity between theoretical and experimental molecular weight, TMA and TiBA afford broad MwD (5.19 and 8.82, respectively). The microstructure of the polyisoprene produced by La catalyst presented high *cis*-1,4 content in TiBA (92%) and increase of *trans* content in TMA and TEA (13 and 18%).

Different behaviors in the polymerizations promoted by $Y(\text{allyl})_2\text{Cl}(\text{MgCl}_2)_2\cdot(\text{THF})_4$ were observed according to the nature of the Al activator (entries 49-53). The use of Dry-MAO in substitution of MAO lowered 2.5 folds the yield (54 to 22%) and increased the *trans*-1,4 content (23 for 35%) of polyisoprene. In this case, the presence of residual TMA in MAO increase the polymer properties. Remarkable changes in stereoregularity were obtained in TMA, TEA and TiBA (entries 51-53) by inversion of stereoselectivity with formation of *trans*-1,4 structure in our majority (64-91%), contrary to the polyisoprene obtained by $\text{Nd}(\text{allyl})_2\text{Cl}(\text{MgCl}_2)_2\cdot(\text{THF})_4$ and $\text{La}(\text{allyl})_2\text{Cl}(\text{MgCl}_2)_2\cdot(\text{THF})_4$ complexes. This stereocontrol afforded by cocatalyst changes can be compared to propylene polymerization using $[\text{Me}_2\text{-Si}(\text{Flu})\text{tBuN}]\text{ZrCl}_2$, when activated with MAO (syndiospecific) versus when activated with $\text{Ph}_3\text{C}^+\text{B}(\text{C}_6\text{F}_5)_4^-/\text{TIBA}$ (isospecific)⁶⁷. As evaluated by DSC, the *trans*-polyisoprenes produced by Y complex present melting temperatures (T_m) of ca. 51 °C and a maximal crystallinity of 48% with TiBA. Low molecular weights (maximum of $33.4 \times 10^3 \text{ g}\cdot\text{mol}^{-1}$ in MAO) and broad MwDs (5.89 at 8.59) were observed in the specific case of $Y(\text{allyl})_2\text{Cl}(\text{MgCl}_2)_2\cdot(\text{THF})_4$

Comparing all systems in isoprene polymerization using $M(\text{allyl})_2\text{Cl}(\text{MgCl}_2)_2\cdot(\text{THF})_4$ complexes, the cocatalyst type and the metal type were determinant for the yield and the polymer properties.

Under the same conditions, much higher activities were obtained with the neodymium complex (up 88%)⁴⁴ as compared to Yttrium and Lanthanum complexes, which led to

moderate yields ($\approx 60\%$) (Figure 43). High yields were obtained with MAO. The absence of TMA (dry-MAO) increased the polymer yield⁵⁸ (for Nd and La catalyst).

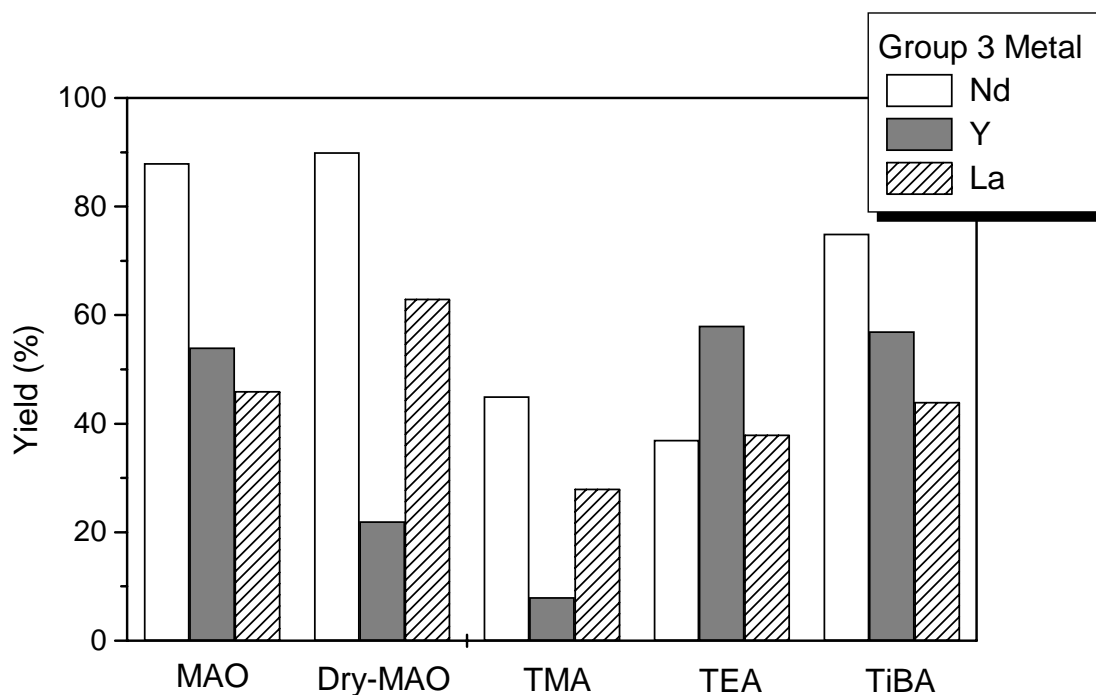


Figure 43. Influence of lanthanide on polymer yield using group 3 metal complexes $M(\text{allyl})_2\text{Cl}(\text{MgCl}_2)_2 \cdot (\text{THF})_4$ ($M = \text{Nd}, \text{Y}$ and La).

The influence of cocatalyst on molecular weight of PI using group 3 metal complexes composed by $M(\text{allyl})_2\text{Cl}(\text{MgCl}_2)_2 \cdot (\text{THF})_4$ ($M = \text{Nd}, \text{Y}$ and La) (Figure 44) showed high molecular weight polyisoprene production using MAO. The metal type is determinant for the molecular weight, in order of $\text{Nd} > \text{La} > \text{Y}$ in all cocatalysts, suggesting that the electronic effect is determinant for the molecular weight. These results are in agreement with the order of metals size ($\text{Nd} > \text{La} > \text{Y}$).

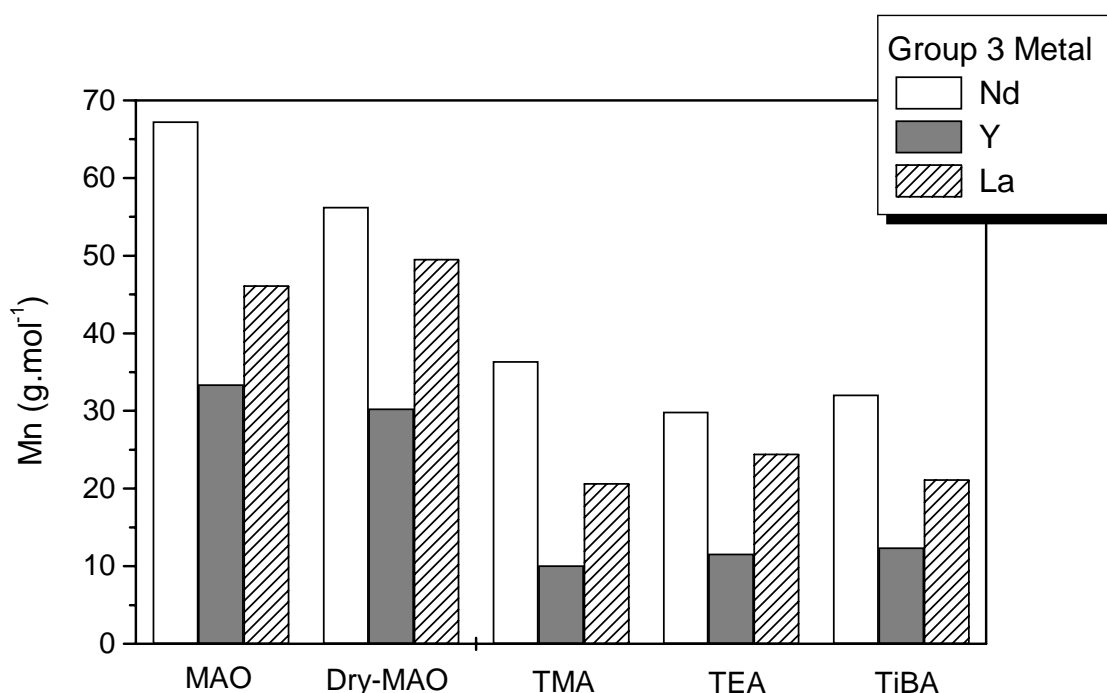


Figure 44. Influence of cocatalyst type on polymer molecular weight using group 3 metal complexes composed by $M(\text{allyl})_2\text{Cl}(\text{MgCl}_2)_2 \cdot (\text{THF})_4$ ($M = \text{Nd}, \text{Y}$ and La).

In all systems, the best performance using MAO as cocatalyst⁶⁸ is probably by your high Lewis acidity than others cocatalysts systems (TMA, TEA or TiBA).

5.3.4. Addition of Borate based cocatalysts in isoprene polymerization using Lanthanide catalysts composed by $\text{Ln}(\text{allyl})_2\text{Cl}(\text{MgCl}_2)_2 \cdot (\text{THF})_4$ ($\text{Ln} = \text{Nd}$ and La) and their effect on polyisoprene properties.

Isoprene polymerization was also carried out by lanthanide complexes $\text{Ln}(\text{allyl})_2\text{Cl}(\text{MgCl}_2)_2 \cdot (\text{THF})_4$ ($\text{Ln} = \text{Nd}$ and La) with different activator compositions. Table 7 shows the effect of $\text{B}(\text{C}_6\text{F}_5)_3$ (B_1) and $[\text{Ph}_3\text{C}][\text{B}(\text{C}_6\text{F}_5)_4]$ (B_2) addition in isoprene polymerisation using lanthanide complexes $\text{Ln}(\text{allyl})_2\text{Cl}(\text{MgCl}_2)_2 \cdot (\text{THF})_4$ ($\text{Ln} = \text{Nd}$ and La).

The influence of cocatalyst system was evaluated by ^1H RMN and gel permeation chromatography (GPC).

Table 7. Effect of Borate addition in isoprene polymerization^a using $\text{Ln}(\text{allyl})_2\text{Cl}(\text{MgCl}_2)_2 \cdot (\text{THF})_4$ complexes ($\text{Ln} = \text{Nd}$ and La).

Entry	Ln^b	Cocatalyst	Borane ^c	Al/Ln/Borate (μmol)	IP/Ln	Yield (%)	Mn ($\cdot 10^3$) (theo) ^d	Mn ($\cdot 10^3$) (exp) ^e	Mw/ Mn ^e
59	Nd	TMA	none	30/1/0	1180	45	36.1	36.4	4.09
60	Nd	TMA	B ₁	30/1/0,15	1180	67	53.8	53.5	2.24
61	Nd	TMA	B ₁	30/1/1	1180	84	67.4	60.7	1.91
62	Nd	TMA	B ₁	30/1/3	1180	88	70.6	58.4	1.39
63	Nd	TMA	B ₁	30/1/5	1180	96	77.8	85.5	1.36
64	Nd	TMA	B ₁	10/1/3	1180	94	75.4	93.3	1.58
65	Nd	TMA	B ₁	30/1/0,15	2350	71	113.5	116.5	1.54
66	Nd	TMA	B ₁	30/1/3	2350	91	145.4	132.3	1.66
67	Nd	TMA	B ₁	30/1/3	4700	44	140.6	129.4	1.57
68	Nd	TMA	B ₁	30/1/3	7000	41	195.2	186.4	1.72
69	Nd	TiBA	none	30/1/0	1180	75	60.2	32.1	6.24
70	Nd	TiBA	B ₂	30/1/0,15	1180	80	64.2	38.5	3.55
71	Nd	TiBA	B ₂	30/1/1	1180	74	59.4	49.8	2.12
72	Nd	TiBA	B ₂	30/1/3	1180	72	57.8	53.6	1.84
73	Nd	TiBA	B ₁	30/1/3	1180	89	71.4	54.8	2.68
74	La	TMA	none	30/1/0	1180	28	22.5	20.7	5.19
75	La	TMA	B ₁	30/1/0,15	1180	19	15.3	20.2	5.81
76	La	TMA	B ₁	30/1/1	1180	26	20.9	30.6	3.14
77	La	TMA	B ₁	30/1/3	1180	20	16.0	21.4	2.37

(a) Conditions: $[\text{Ln}] = 17,0 \mu\text{mol}$; solvents: toluene and hexane (5:3 mL); Activation time = 10 min; Polymerization temperature = 20 °C; Polymerization time = 1h; (b) Nd = Nd (Allyl)₂Cl (MgCl₂)₂·(THF)₄; La = La (Allyl)₂Cl (MgCl₂)₂·(THF)₄ (c) Borane: B₁=B(C₆F₅)₃, B₂=[Ph₃C][B(C₆F₅)₄]; (d) Theoretical molecular weight = Yield x Ip/Nd x molar mass of Isoprene; (e): determined by GPC (f): determined by NMR ^1H ;

Isoprene polymerization performed employing the system Nd(Allyl)₂Cl (MgCl₂)₂·(THF)₄/TMA (entry 59) show that the catalytic system Nd/TMA exhibited moderate yield (45%), PI with low molecular weight ($36.4 \times 10^3 \text{ g}\cdot\text{mol}^{-1}$) and broad MwD

(4.09). However, the absence of aluminium cocatalyst, i.e. using only Nd / B₁ or Nd / B₂, led to inactive systems (B₁ = B(C₆F₅)₃ and B₂ = [Ph₃C][B(C₆F₅)₄]).

For instance, the system Nd(Allyl)₂Cl (MgCl₂)₂.(THF)₄/TMA is very sensitive to different amounts of B₁. The addition of 0.15 μmol of B₁ (entry 60) increases 1.5 folds the yield and the molecular weight and enables reducing significantly the MwD (4.09 for 2.24). The use of 1 μmol of B₁ (entry 61) increases these data (yield, molecular weight and MwD) in ≈ 2 folds. High amounts of B₁ (5 μmol) (Al/Ln/B₁ = 30/1/5, entry 64) afford high yield (96%), molecular weight in order of 85.5x10³ g.mol⁻¹ and considerable reduction of MwD (4.09 to 1.36; broad to narrow MwD). On the other hand, a small Al/B ratio (entries 63 and 64) doesn't significantly change the yield and polymer properties. All polymerizations using the system Nd/Al/B₁ showed good agreement between the theoretical and experimental molecular weight values. Figure 45 shows the good control of MwD in function of B₁ borate addition using TMA/Nd system with considerable reduction of MwD by increase of B₁.

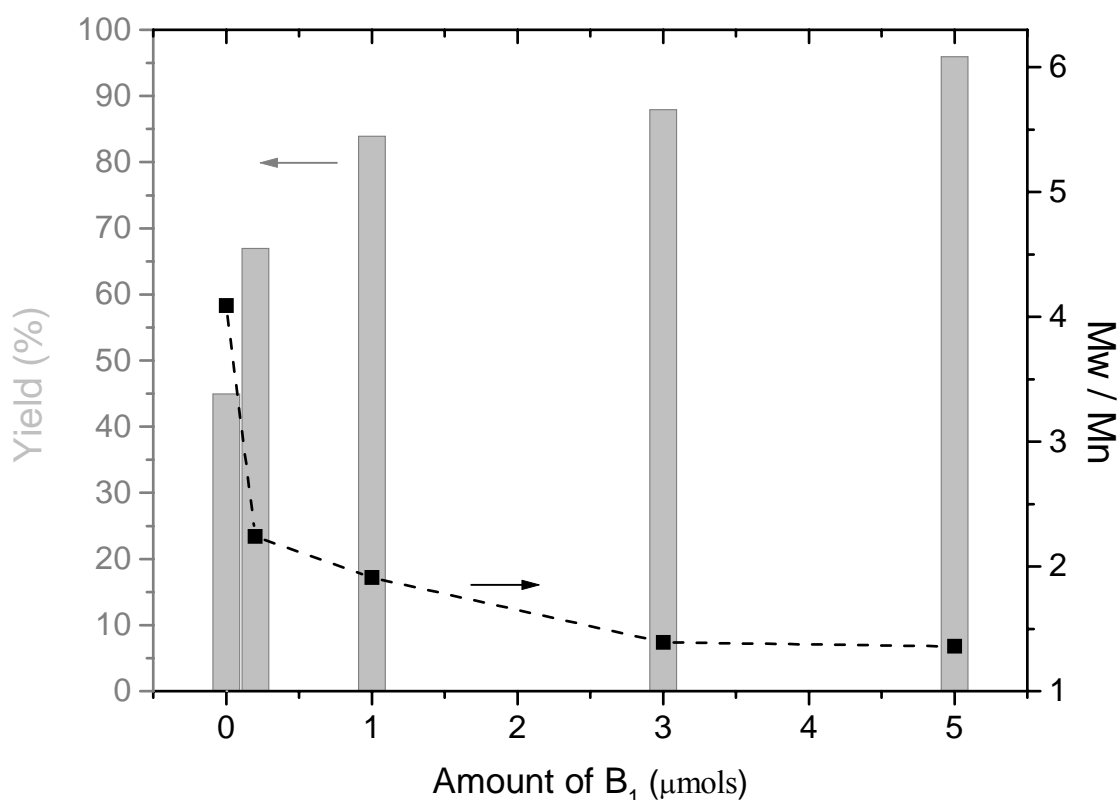


Figure 45. Effect of B₁ addition employing the system TMA/Nd (Allyl)₂Cl (MgCl₂)₂·(THF)₄.

The amount of isoprene determines also changes in the yield and polyisoprene properties using the TMA/Nd (Allyl)₂Cl (MgCl₂)₂·(THF)₄ system, when ratios IP/Nd between 1180 and 7000 were utilized (entries 62 and 65-68). Using 0.15 μmols of B₁ (compare entries 60 and 65) the increase of the IP/Nd ratio in 2 folds (1180 for 2350) increases to the same extent the molecular weight (53.5 for 116.5x10³). At Ip/Nd ≥ 4700, the yield of polymerizations reactions decreased (Figure 46). The molecular weight of polymers increases with the IP/Nd ratio (maximum of 186.4x10³, IP/Nd = 7000, entry 68). It is important to note that the system present a good agreement with the theoretical values and production of polyisoprene with narrow MwD. Figure 46 show a relationship between the yield and molecular weight with the IP/Nd ratio.

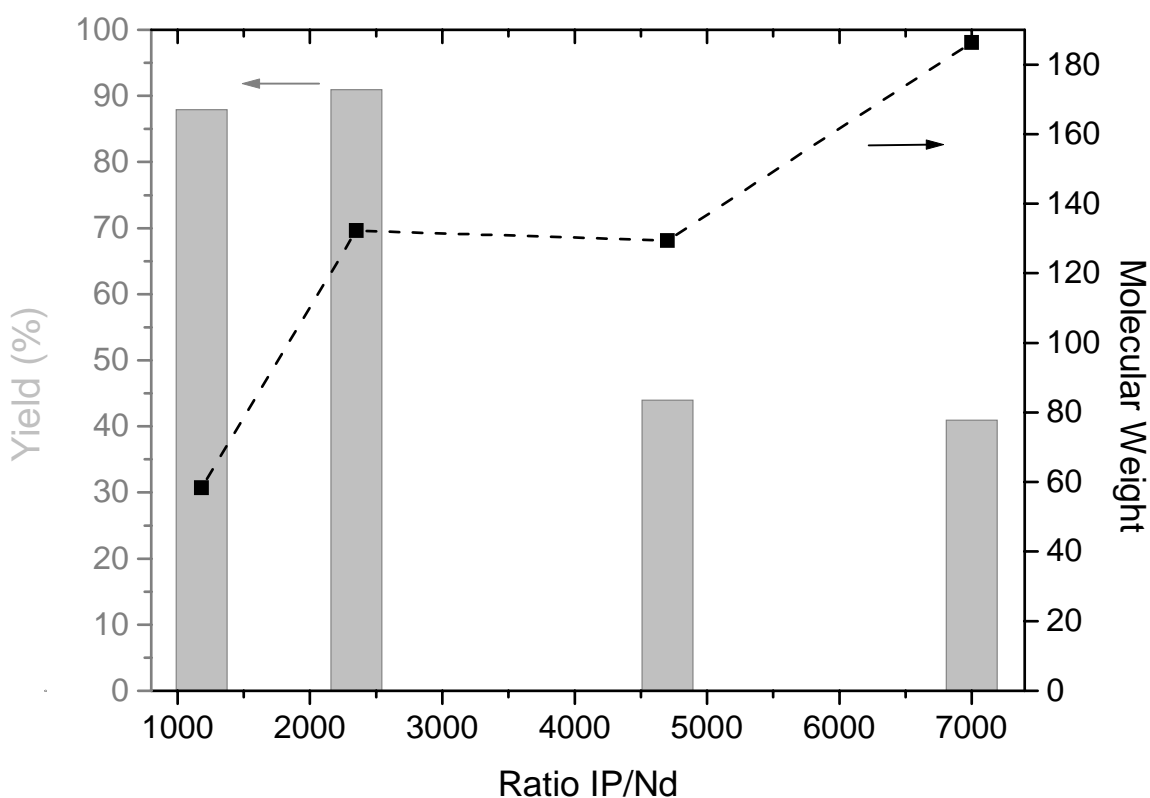


Figure 46. Influence of Ratio Ip/Nd on the Yield and molecular weight (M_n) of polyisoprene produced by TMA/ Nd(allyl)₂Cl(MgCl₂)₂.(THF)₄ / B₁ using Al/Nd/B₁ = 30/1/3.

Reduction of Mw/Mn was observed when the TMA / La(allyl)₂Cl (MgCl₂)₂.(THF)₄ system was used with different amounts of B₁ (entries 74-77). Increase of the amount of B₁ (B₁ ≥ 1 μmol) decreases the MwD (5.81 to 2.37, figure 47). On the other hand, a small amount of B₁ (0.15 μmol, entry 76) does not decrease the molecular weight distribution, contrary as observed for the Nd complex. Analysing the yield and molecular weight of polyisoprene produced by the system TMA / La (Allyl)₂Cl (MgCl₂)₂.(THF)₄, the amount of B₁ is not determinant for changes in this properties.

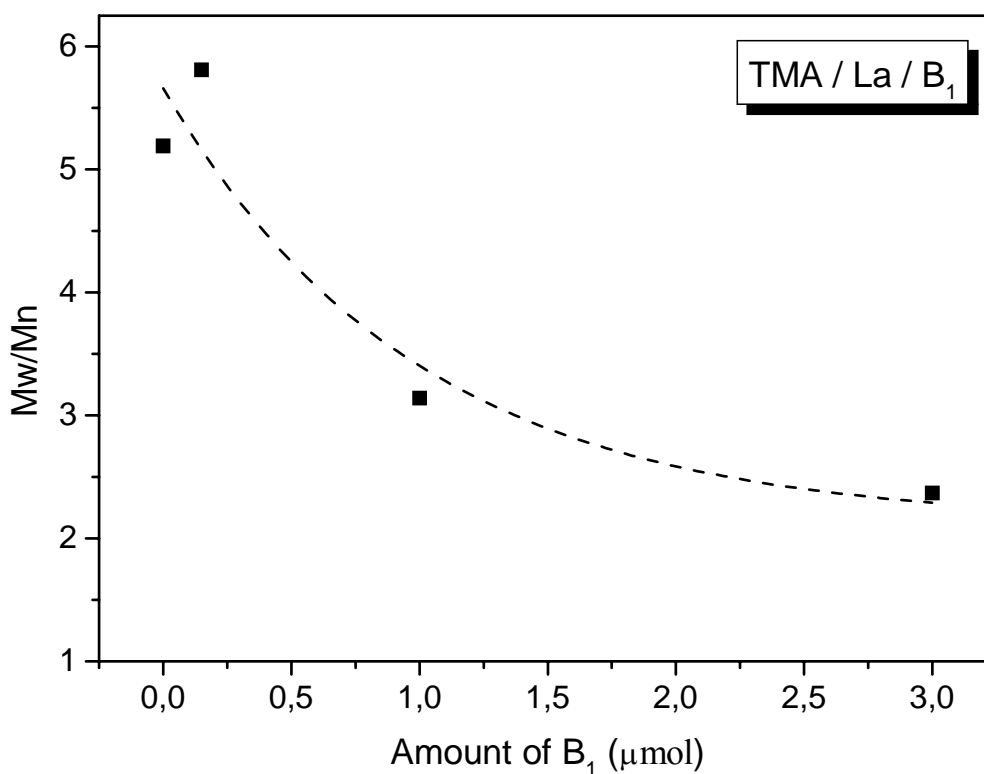


Figure 47. Effect of amount of B₁ in molecular weight distribution employing the system TMA / La (allyl)₂Cl (MgCl₂)₂·(THF)₄ (Al/La = 30/1) in isoprene polymerization.

Substituting TMA by TiBA, the control of MwD is effective using the Nd catalyst (compare entries 62 and 73). Significant reduction in Mw/Mn is observed (6.24 to 2.68) and increase on molecular weight (32.1 to 54.8×10^3) in polymerizations performed in TiBA in presence of B₁.

Varying the borate-based system, by change of B₁ for B₂ in the system composed by TiBA / Nd / B₂ (B₂ = [Ph₃C][B(C₆F₅)₄]) entries 69-72, showed that the increase of B₂ affords considerable decrease in the Mw/Mn (6.24 to 1.84, entries 69 at 72) and increase in the molecular weight of polymers (32.1 to 53.6×10^3). Figure 48 show the effect of B₂ addition on the MwD in the system composed by TiBA / Nd / B₂.

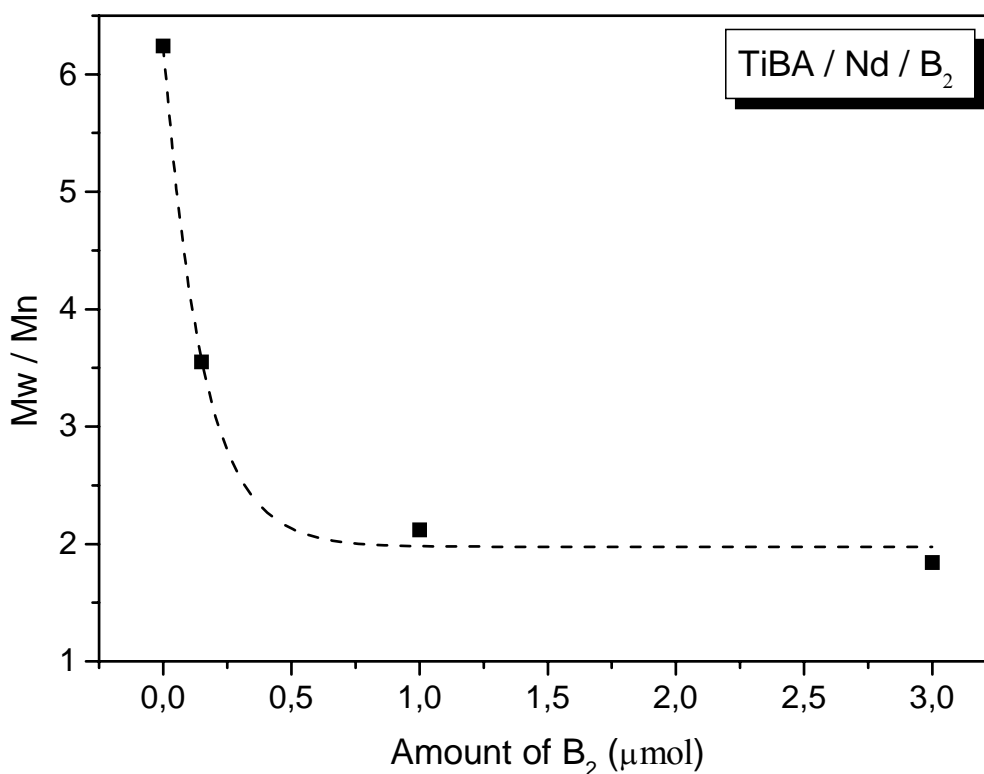


Figure 48. Effect of B₂ content in molecular weight distribution employing the system TIBA / Nd (Allyl)₂Cl (MgCl₂)₂·(THF)₄ /B₂ (Al/Nd =30/1) in isoprene polymerisation.

These results show that the modern chemistry of borane-based cocatalysts⁶⁹ allows effective isoprene polymerization using lanthanide catalysts, probably thanks to the formation of a high Lewis acid by Alkylaluminum / borate mixtures^{70,54}. In association with the catalyst precursor Nd(Allyl)₂Cl(MgCl₂)₂·(THF)₄, strongly improved catalytic activity and molecular weight were observed. Considerable reduction and control of MwD, with addition of small amounts of borate based cocatalysts, using Nd/Al compositions was possible, with small ratios B:Al.

5.3.5. Production of *Cis/Trans* polyisoprene Blends using combination of group 3 metals composed by $M(\text{allyl})_2\text{Cl}(\text{MgCl}_2)_2\cdot(\text{THF})_4$ ($M = \text{Y}$ and La) activated by TiBA and the effect of Yttrium Molar Fraction (x_Y) on polyisoprene properties.

The isoprene polymerization reactions were carried using $\text{Y}(\text{allyl})_2\text{Cl}(\text{MgCl}_2)_2\cdot(\text{THF})_4$ and $\text{La}(\text{allyl})_2\text{Cl}(\text{MgCl}_2)_2\cdot(\text{THF})_4$ complexes activated by trisobutylaluminum (TiBA) in hexane/toluene solutions. Table 8 shows the results of polymerization runs varying the yttrium loading molar fraction (x_Y) at 20 °C, using $\text{Al/Ln}=30$ (TiBA) and $\text{IP/Ln}= 1180$.

Table 8. Isoprene polymerization reactions using combinations of $\text{Y}(\text{allyl})_2\text{Cl}(\text{MgCl}_2)_2\cdot(\text{THF})_4$ and $\text{La}(\text{allyl})_2\text{Cl}(\text{MgCl}_2)_2\cdot(\text{THF})_4$ activated by TiBA.

Entry	x_Y ^b	Yield (%)	Mn ($\times 10^{-3}$) (theo) ^c	Mn ($\times 10^{-3}$) (exp) ^d	Mw/Mn	<i>Cis</i> -1,4 ^e (%)	<i>Trans</i> -1,4 ^e (%)	3,4 ^e (%)
78	0	44	35.3	21.2	8.82	93	7	1
79	0.05	32	nd ^f	nd	nd	89	11	0
80	0.1	55	nd	nd	nd	84	14	2
81	0.25	54	43,3	11.5	4.90	82	16	1
82	0.50	56	44,9	12.8	7.33	53	46	1
83	0.75	39	31,3	14.3	5.20	26	73	1
84	0.90	42	nd	nd	nd	26	74	0
85	1.00	57	45.7	12.4	6.71	9	90	1

(a) Conditions : $[\text{Ln}]$ total= 17,0 μmol s; (b) Yttrium molar fraction, $x_Y = [\text{Y}] / [\text{Y}] + [\text{La}]$; solvents: toluene and hexane (5:3 mL); Activation time= 10 min; Polymerization time = 1h; Polymerization temperature= 20 °C; $\text{Al/Ln}=30$ (TiBA); $\text{IP/Ln}= 1180$; (c) Theoretical molecular weight = $\text{Yield} \times \text{IP}/\text{Nd} \times \text{molar mass of Isoprene}$; (d) determined by NMR ¹H (e) determined by ¹H NMR (f) nd = not determined.

The isoprene polymerization reactions performed employing $\text{Y}(\text{allyl})_2\text{Cl}(\text{MgCl}_2)_2\cdot(\text{THF})_4$ and $\text{La}(\text{allyl})_2\text{Cl}(\text{MgCl}_2)_2\cdot(\text{THF})_4$ catalysts separately (entries 78 and 85) showed that the catalytic system La/TiBA and Y/TiBA exhibits moderate Yields (44

and 57%, respectively), low molecular weight PI (21.2 and $12.4 \times 10^3 \text{ g.mol}^{-1}$) with broad MwDs (8.82 and 6.71 , respectively).

Because of similar properties (M_n and MwD) of PI produced by Y and La catalysts, with constant amount of TiBA, no significant changes were obtained when different Yttrium molar fractions x_Y were utilized ($x_Y = 0.05$ - 0.90 , entries 79-84). It's observed the maintenance of the molecular weight in the order of 10 at $20 \times 10^3 \text{ g.mol}^{-1}$ and broad MwDs (4.90 - 7.33). These results showed that the catalysts works separately in the polymerizations reactions.

However, the microstructure of polyisoprenes, evaluated by ^1H NMR, was strong affected by the yttrium molar fraction x_Y . Separately, the La catalyst generates polyisoprene with high *cis*-1,4 content and the Y catalyst affords high *trans*-1,4 forms (entries 78 and 85). Thus, the increase of x_Y increases the *trans*-1,4 configuration in $x_Y = 0.05$ at 0.90 (increase of signal at $1,58$ ppm and decrease of signal at $1,67$ ppm). This behavior is due to difference of PI microstructure generated by La and Y complexes separately, indicating that catalysts work independently. Figure 49 shows the dependence of the *cis/trans* content with x_Y , where is possible the control of microstructure with generation of *cis/trans* polyisoprene blends *in situ*⁴⁸ by simple combination of group 3 metal catalysts composed by $\text{Y(allyl)}_2\text{Cl(MgCl}_2)_2\text{(THF)}_4$ and $\text{La(allyl)}_2\text{Cl(MgCl}_2)_2\text{(THF)}_4$ actived by TiBA.

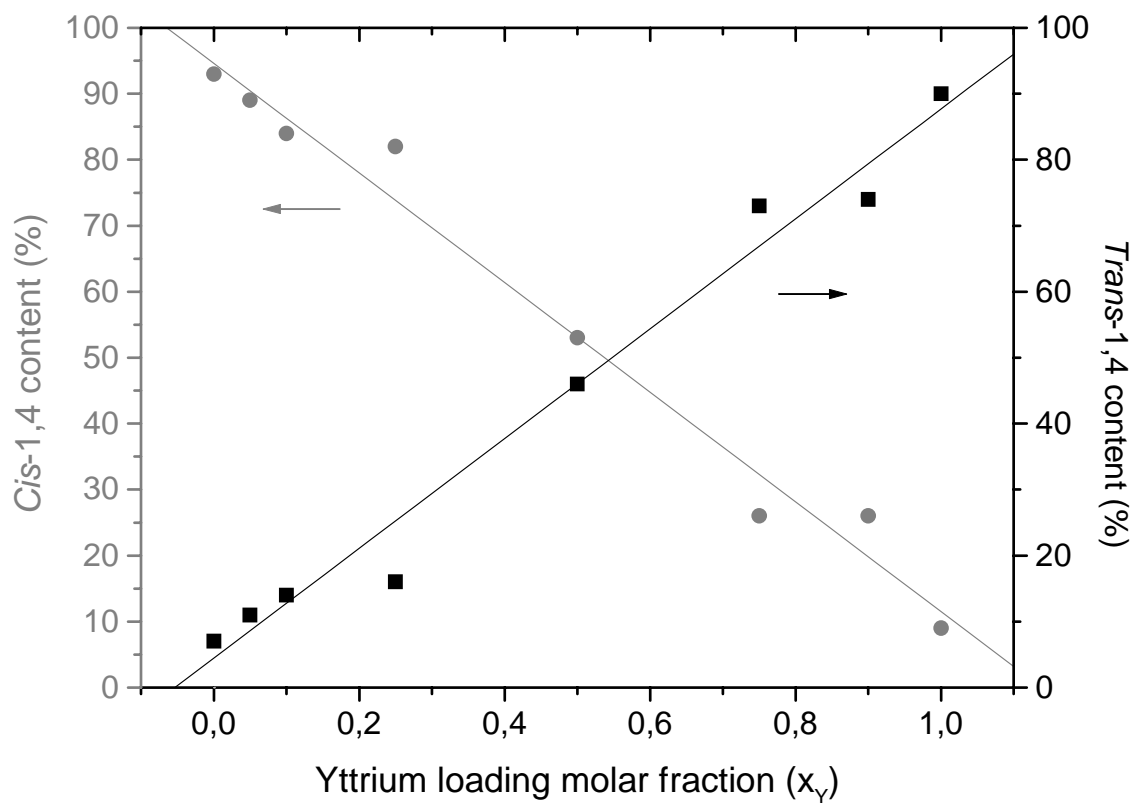


Figure 49. Influence of Yttrium Molar Fraction (x_Y) in stereoregularity of polyisoprene produced by $M(\text{allyl})_2\text{Cl}(\text{MgCl}_2)_2 \cdot (\text{THF})_4 / \text{TiBA}$ ($M = \text{Y}$ and La) combinations.

6. CONCLUSIONS

First, we have shown that combining $\text{Ni}(\alpha\text{-diimine})\text{Cl}_2$ and $\{\text{TpMs}^*\}\text{V}(\text{Ntbu})\text{Cl}_2$ catalysts precursors allows production polymers with different and controlled properties in a single reactor. In the presence of MAO as cocatalyst, generates an effective binary catalyst system for ethylene polymerization and *in situ* reactor blends generation. Different types of polyethylene blends are produced, depending on the polymerization temperature, solvent and x_{Ni} . Higher activities have been found using toluene as solvent at 0°C thanks to the better stability of $\text{Ni}(\alpha\text{-diimine})\text{Cl}_2$ precursor at this polymerization conditions. The surface morphology of the blends revealed very low miscibility between the PE phases, resulting in the formation of big holes and defects distributed on the HDPE matrix. This behavior is associated mainly to the large difference of the PE properties produced by $\text{Ni}(\alpha\text{-diimine})\text{Cl}_2$ and $\{\text{TpMs}^*\}\text{V}(\text{Ntbu})\text{Cl}_2$ that has been determined a spontaneous separation of phase for ethylene polymerization carried out in hexane at 50°C.

In second, the combination of a novel homogeneous binary catalyst system, composed by $\{\text{Tp}^{\text{Ms}}\}\text{NiCl}$ and Cp_2ZrCl_2 activated with MAO/TMA, is able to produce linear low density polyethylene (LLDPE) using only ethylene, by Tandem process. The turnover frequencies as well as the polymer properties are dependent on x_{Ni} . The control of molecular weight and branched content is possible with only the adjusting of proportion of catalysts precursors. Higher activities were reached using high x_{Ni} . The melting points of the copolymers and the branching contents show a linear correlation with respect to x_{Ni} .

Finally, the use of group 3 metal complexes, $\text{M}(\text{allyl})_2\text{Cl}(\text{MgCl}_2)_2 \cdot 4\text{THF}$ ($\text{M} = \text{Nd}, \text{La}$ and Y), enables to produce polyisoprene with high yield and good and controlled properties. The variation of experimental parameters (Polymerization time, Temperature, cocatalyst and amount of cocatalyst) is determinant for the polymer properties such as molecular weight,

molecular weight distribution and microstructure. High yields and high conversions in *cis*-1,4-polyisoprene were obtained with use of Nd catalyst. The polymerization tests showed that the cocatalyst type is fundamental for determination of polyisoprene properties. The addition of borate-based cocatalysts is able to increase the molecular weight. Remarkable reduction and control of MwD is possible with simple addition of small amounts of borate-based cocatalysts. The combination of Yttrium and Lanthanum catalyst precursors generates effective systems for the *cis/trans*- polyisoprene blends using TiBA as cocatalyst. The microstructure of polymers is dependent of Yttrium molar fraction x_Y and the control of microstructure (*cis-trans*-1,4) is possible only by changes in compositions of precursors.

(3). The application of different experimental parameters using group 3 metals catalysts based, $M(\text{allyl})_2\text{Cl}(\text{MgCl}_2)_2 \cdot 4\text{THF}$ ($M = \text{Nd, La and Y}$), with different experimental conditions, cocatalyst systems and their effect in polyisoprene properties.

7. BIBLIOGRAPHIC REFERENCES

- 1 McKnight, A. L.; Waymouth, R. M. *Chem. Rev.* **1998**, *98*, 2587.
- 2 Brintzinger, H. H.; Fischer, D.; Mulhaupt, R.; Rieger, B.; Waymouth, R. M. *Angew. Chem., Int. Ed. Engl.* **1995**, *34*, 1143.
- 3 Thomson Scientific, *KnowledgeLink newslette*, 2004.
- 4 Gibson, V. C.; Spitzmesser, S. K.; *Chem. Rev.* **2003**, *103*, 283.
- 5 (a) Keim, W.; Kowaldt, F. H.; Goddard, R.; Kruger, C. *Angew. Chem., Int. Ed. Engl.* **1978**, *17*, 466. (b) Starzewski, K. A. O.; Witte, J. *Angew. Chem., Int. Ed. Engl.* **1985**, *24*, 599. (c) Klabunde, U.; Ittel, S. D. *J. Mol. Catal. A: Chem.* **1987**, *41*, 123. (d) Klabunde, U.; Mulhaupt, R.; Herskovitz, T.; Janowicz, A. H.; Calabrese, J.; Ittel, S. D. *J. Polym. Sci. Polym. Chem.* **1987**, *25*, 1989.
- 6 (a) Small, B. L.; Brookhart, M.; Bennett, A. M. A. *J. Am. Chem. Soc.* **1998**, *120*, 4049. (b) Britovsek, G. J. P.; Gibson, V. C.; Kimberley, B. S.; Maddox, P. J.; McTavish, S. J.; Solan, G. A.; White, A. J. P.; Williams, D. J. *Chem. Commun.* **1998**, 849.
- 7 Coates, G. W.; Hustad, P. D.; Reinartz, S. *Angew. Chem., Int. Ed.* **2002**, *41*, 2237.
- 8 (a) Britovsek, G. J. P.; Gibson, V. C.; Wass, D. F. *Angew. Chem., Int. Ed.* **1999**, *38*, 429. (b) Ittel, S. D.; Johnson, L. K.; Brookhart, M. *Chem. Rev.* **2000**, *100*, 1169.
- 9 Ahn, T. O.; Hong, S. C.; Kim, J. H.; Lee, D. *J. of Appl. Polym. Sci.*, **1998**, *67*, 2213.
- 10 Ewen, J. A. *Studies in Surface Science and Catalysis*, Amsterdam: Elsevier 1986, *25*, 271.
- 11 Souza, R. F.; Casagrande, O. L.; *Macromol. Rapid Commun.* **2001**, *22*, 1293.
- 12 Ahlers, A.; Kaminsky, W.; *Makromol. Chem., Rapid Commun.* **1988**, *9*, 457.
- 13 Heiland, K. W.; Kaminsky, W.; *Makromol. Chem.* **1992**, *193*, 601.
- 14 D'agnillo, L.; Soares, J. B. P.; A. Penlidis, A.; *J. Polym. Sci., Part A: Polym. Chem.* **1998**, *36*, 831.

-
- 15 Mecking, S.; *Macromol. Rapid Commun.* **1999**, 20, 139.
- 16 Beigzadeh, D.; Soares, J. B. P.; Duever, T. A.; *Macromol. Rapid Commun.* **1999**, 20, 541.
- 17 Kunrath, F. A., Souza, R. F., Casagrande, O. L.; *Macromol. Rapid Commun.* **2000**, 21, 277.
- 18 (a) Mota, F.F., Santos, R.M., Souza, R. F., Casagrande, O. L, *Macromol. Chem. Phys.* **2001**, 202, 1016. (b) Mota, F.F., Santos, R.M., Souza, R. F., Casagrande, O. L, *Polymer* **2003**, 44, 4127.
- 19 Junges, F.; Souza, R. F.; Santos, J. H. Z.; Casagrande, O. L. *Macromol. Mater. Eng.* **2005**, 290, 72.
- 20 Wasilke, J. C., Obrey, S. J., Baker, R. T., Bazan, G. C. *Chem. Rev.* **2005**.
- 21 (a) Beach, D. L.; Kissin, Y. V. *J. Polym. Sci.: Polym. Chem. Ed.* **1984**, 22, 3027 (b) Beach, D. L.; Kissin, Y. V. *J. Polym. Sci.: Polym. Chem. Ed.* **1986**, 24, 1069.
- 22 Pettijohn, T. M.; Reagan, W. K.; Martin, S. J. (Phillips Petroleum Company, invs.). US 5,331,070, 1994.
- 23 Benham, E. A.; Smith, P. D.; McDaniel, M. P. *Polym. Eng. Sci.* **1988**, 28, 1469.
- 24 (a) Ostoja-Starzewski, A. K.-H.; Witte, J.; Bartl, H.; Reichert, K.-H.; Vasiliou, K. (Bayer AG, invs.). EP 0,250,999, 1992; (b) Ostoja-Starzewski, A. K. H.; Witte, J.; Bartl, H.; Reichert, K.-H.; Vasiliou, G.; Bayer AG, invs.. US Patent 5,616,529, 1997;
- 25 Bennett, A. M. A.; Coughlin, E. B.; Citron, J. D.; Wang, L. (E. I. Du Pont De Nemours and Company, invs.). WO 50,318, 1999.
- 26 Johnson, L. K.; Killian, C. M.; Brookhart, M. *J. Am. Chem. Soc.* **1995**, 117, 6414.
- 27 Quijada, R.; Rojas, R.; Bazan, G.; Komon, Z. J. A.; Mauler, R. S.; Galland, G. S.; *Macromolecules* **2001**, 34, 2411.

-
- 28 Johnson, L. K.; Killian, C. M.; Arthur, S. D.; Feldman, J.; McCord, E. F.; McLain, S. J.; Kreutzer, K. A.; Bennett, A. M. A.; Coughlin, E. B.; Ittel, S. D.; Parthasarathy, A.; Tempel, D. J.; Brookhart, M. S. (E. I. Du Pont De Nemours and Company, invs.). WO 23010, 1996;
- 29 Denger, C.; Haase, U.; Fink, G. *Makromol. Chem., Rapid Commun.* **1991**, *12*, 697.
- 30 Rogers, J. S.; Bazan, G. C.; Sperry, C. K. *J. Am. Chem. Soc.* **1997**, *119*, 9305.
- 31 Barnhart, R. W.; Bazan, G. C.; Mourey, T. *J. Am. Chem. Soc.* **1998**, *120*, 1082.
- 32 Ye, Z.; AlObaidi, F.; Zhu, S. *Macromol. Rapid Commun.* **2004**, *25*, 647.
- 33 Roos, W. D., Dixon, J. T., *Macromolecules*, **2004**, *37*, 9314.
- 34 Musikhbumma, K.; Spaniol, T. P.; Okuda, J. *J. Polym. Sci., A: Polym. Chem.* **2003**, *41*, 528.
- 35 Komon, Z. A., Diamond, G. M., Leclerc, M. K., Murphy, V., Okazaki, M., Bazan, G., *J. Am. Chem. Soc.*, **2002**, *124*, 15280.
- 36 (a) Abramo, G. P.; Li, L.; Marks, T. J. *J. Am. Chem. Soc.* **2002**, *124*, 13966. (b) Li, L.; Metz, M. V.; Li, H.; Chen, M.-C.; Marks, T. J.; Liable-Sands, L.; Rheingold, A. L. *J. Am. Chem. Soc.* **2002**, *124*, 12752.
- 37 Song, J. S.; Huang, B. C.; Yu, D. S. *J. Appl. Polym. Sci.* **2001**, *82*, 81-89.
- 38 Friebe, L.; Nuyken, O.; Windisch, H.; Obrecht, W. *Macromol. Chem. Phys.* **2002**, *203*, 1055.
- 39 Boochathum, P.; Prajudtake, W. *Eur. Polym. J.* **2001**, *37*, 417.
- 40 Edelmann, F. T.; Freckmann, D. M.; Schumann, H.; *Chem. Rev.* **2002**, *102*, 1851.
- 41 Gromada, J.; Carpentier, J. F.; Mortreux, A.; *Coord. Chem. Rev.*, **2004**, *248*, 397.
- 42 Yang, J. H.; Tsutsui, M.; Bergbreiter D. E.; *Macromolecules*. **1982**, *15*, 230-233
- 43 Ricci, G.; Itália, S.; Cabassi, F.; Porri, L.; *Polym. Commun.* **1987**, *28*, 223.
- 44 Jin, Y.; Li, F.; Pei, F.; Wang, F.; Sun, Y. *Macromolecules*. **1994**, *27*, 4391.

-
- 45 Barbier, D. B.; Andre, N.; Dormond, A.; Pardes, C.; Richard, P.; Visseaux, M.; Zhu, C.J. ; *Eur. J. Inorg. Chem.* **1998**, 1721.
- 46 Dong W, Masuda T. *J Polym Sci, Part A: Polym Chem* **2002**, 40, 1838.
- 47 Evans, William J.; Giarikos, Dimitrios G.; Allen, Nathan T.; *Macromolecules* **2003**, 36, 4256.
- 48 Evans, William J.; Giarikos, Dimitrios G.; *Macromolecules* **2004**, 37, 5130.
- 49 Fischbach, A.; Perdih, F.; Sirsch, P.; Scherer, W.; Anwander, R.; *Organometallics* **2002**, 21, 4569.
- 50 Bonnet, F.; Visseaux, M.; Pereira, A.; Baudry, D.; *Macromolecules* **2005**, 38, 3162.
- 51 Ricci, G.; Rotunno, D.; Italia, S.; Porri, L.; Italian Patent 1228442, **1991**.
- 52 Wu, W.; Chen, M.; Zhou, P. *Organometallics*. **1991**, 10, 98.
- 53 Porri, L.; Ricci, G.; Giarusso, A.; Shubin, N.; Lu, Z.; *ACS Symp. Ser.* **2000**, 749, 15.
- 54 Biagini, P.; Lugli, G.; Abis, L.; Andreussi, P. U.S. Pat. 5,602,-269, 1997 (Enichem).
- 55 Hair, G. S.; Cowley, A. H.; Jones, R. A.; Mcburnett, B. G.; Voigt, A. *J. Am. Chem. Soc.* **1999**, 121, 4922.
- 56 (a) Chien, J. C. W.; Tsai, W.-M.; Rausch, M. D. *J. Am. Chem. Soc.* **1991**, 113, 8570. (b) Ewen, J. A.; Elder, M. J. Eur. Pat. Appl. 0,426,637, 1991.
- 57 Elder, M. J.; Ewen, J. A. Eur. Pat. Appl. 0,573,403, 1993.
- 58 Chen, E. Y.X.; Marks, T. J.; *Chem. Rev.* **2000**, 100, No. 4
- 59 Van Koten, G.; Vrieze, K.; In *Adv. Organomet. Chem.*; F. G, A Stone and R West editors, New York, 1982, 169.
- 60 Casagrande, A. C. A.; Ph.D thesis, UFRGS, Porto Alegre, RS, Brazil, 2005.
- 61 Kunrath, F. A.;Souza, R. F.; Casagrande, O. L.; Brooks, N. R.; Young, V. G.; Jr. *Organometallics* **2003**, 22, 4739.

-
- 62 (a) Simon, L. C.; Mauler, R. S.; De Souza, R. F.; *J. Polym. Sci. A: Polym. Chem.* **1999**, *37*, 4656; (b) Mota, F. F.; Kunrath, F. A.; De Souza, R. F.; Mauler, R. S.; Casagrande Jr., O. L.; *Macromol. Chem Phys.* **2002**, *203*, 2407.
- 63 (a) Gates, D. P.; Svejda, S. A.; Onate, E.; Killian, C. M.; Johnson, L. K.; White, P. S.; Brookhart, M., *Macromol.* **2000**, *33*, 2320.
- 64 (a) Kaminsky, W.; Arndt, M.; *Adv. Polym. Sci.* **1997**, *127*, 143; (b) Brintzinger, H.H.; Fischer, D.; Mülhaupt, R.; Rieger, B.; Waymouth, R.M.; *Angew. Chem., Int. Ed. Engl.* **1995**, *34*, 1143.
- 65 (a) Komon, Z.J.A.; Bu, X.; Bazan, G.C.; *J. Am. Chem. Soc.* **2000**, *122*, 1830; (b) Galland, G.B.; Souza, R.F.; Mauler, R.S.; Nunes, F.F.; *Macromolecules* **1999**, *32*, 1620.
- 66 Ajellal, N.; DEA Thesis, University of Rennes, Rennes, France, 2003.
- 67 Shiomura, T.; Asanuma, T.; Inoue, N. *Macromol. Rapid Commun.* **1996**, *17*, 9.
- 68 Kaminsky, W.; Steiger, R. *Polyhedron* **1988**, *7*, 2375-2381
- 69 Yang, X.; Stern, C. L.; Marks, T. J. *J. Am. Chem. Soc.* **1994**, *116*, 10015.
- 70 (a) Lee, C. H.; Lee, S. J.; Park, J. W.; Kim, K. H.; Lee, B. Y.; Oh, J. S.; *J. Mol. Catal., A: Chem.* **1998**, *132*, 231-239. (b) Carnahan, E. M.; Chen, E. Y.-X.; Jacobsen, G. B.; Stevens, J. C. PCT Int. Appl. WO 99/15534; U.S. Pat. Appl. 59572, 1997.